वायुः अन्तरिक्षे दीप्यते। जैमिनि ब्राह्मण १।१९२।

THE AIR GLOWS IN SPACE.

— Jaimini Brahmana 1, 192.

The Jaimini Brahmana (research on Vedas) written by Jaimini Rishi the author of Mimansa Darshana is as old as seven thousand years.

INTRODUCTION

A good deal of work on night airglow and its dependence on other phenomena has been carried out in middle and high latitudes, but systematic studies of this phenomenon in low and equatorial latitudes have been few. Besides, there are some special features in the airglow of low latitudes.

The present work on night airglow was started in November 1964 at Mt.Abu (India) in the quiet phase of solar activity with improved equipment and due attention to regular calibration.

After a general discussion on the seasonal and nocturnal variations of 5577 A, 5893 A and 6300 A emissions, the special features observed in the course of the present work are presented and discussed in this thesis.

A reason for the maximum in 5577 A emission around midnight has been suggested. A regular feature over and above the post-midnight enhancement of 6300 A has been observed and it has been interpreted on the basis of the dynamics of the night-time ionosphere. Employing recent atmospheric models, the seasonal variation observed in post-twilight decay of 6300 A emission has been discussed.

The vertical luminosity profile of 6300 A emission has been discussed from a theoretical point of view and the latitude distribution of intensity has been derived. The results are compared with the latitude distribution observed on board the Altanin ship.

There have been a few occasions when peak-to-peak covariation in 6300 Å and 5577 Å emissions has been observed along with enhancements in their intensities. A chapter has been devoted to discuss this.

Some peculiarities of the nocturnal variation of sodium glow in the upper atmosphere, have been found.

Towards the end of the thesis, isophote-maps of the three radiations in night airglow over the dome of the sky at Mt. Abu have been presented for a number of days showing the progress of nightglow activity in time and space.

Author

Countersigned

K R Ramanathan
23/11/68
P. V. Kulkarni

ACKNOWLEDGMENTS

I wish to express my deep gratitude to Professor K.R.Ramanathan for all-round guidance. I am indebted to him for his keen interest in the work and the time he has spared for discussions.

Dr.P.V.Kulkarni who acted as the leader of the project, guided me in the techniques of accurate observation and analysis. I am also very grateful to him for his critical examination of the manuscript and help in its preparation.

I am very thankful to Dr.J.S.Shirke for his kind help in the early stages of the work. I express my thanks to my colleague Shri V.Ramachandra Rao who has helped me in observations and analysis.

Thanks are due, to Mrs.Antony for typing the manuscript and to Shri R.T.Patel and Shri S.S.Deshikachar for assistance in scaling the photometric records. I am thankful to Mr.S.R. Thakore, the Chief of the Computing Section and to Sarva Shri Rathod, Shah and Vayeda for help in running the computer programmes.

The airglow work at Mt.Abu has been assisted by a generous Grant (No.62-399) from the Airforce Cambridge Laboratory, U.S.A. to Professor K.R.Ramanathan.

(S.R.Pal)

CONTENTS

SECTION B

CHAPTER V

CHAPTER VI

CHAPTER VII

STUDIES OF 5890-96 Å EMISSION IN NIGHTGLOW

CHAPTER VIII

RESULTS FROM THE ISOPHOTE-STUDIES OF THE NIGHT-SKY

CHAPTER I

BRIEF REVIEW OF NIGHT AIRGLOW WORK
EXPERIMENTAL SET-UP AT MT.ABU

1.1 Introduction

1.11 Distinction between auroral light and night airglow

Aurorae and their spectra have long been studied (Angstrom, 1867). The main lines in the visible region of the auroral spectrum are 5577 A, 6300-64 A, 4278 A and 3914 A. The studies of Slipher and Rayleigh of the green auroral line, 5577 A, led them to conclude that there was a component of the night sky which was qualitatively different from the light of the aurora. Rayleigh called the latter 'nonpolar aurora'. Though it is difficult to have a clear-cut distinction between the two, aurora and airglow can be distinguished from the regions of their occurrence, spectra and source of excitation. The characteristic feature of the auroral spectrum is the presence of strong N_2^+ bands (excitation energy 19 ev) which are absent in night airglow and that of the night airglow is the presence of OH bands (excitation energy 3.23 ev) which are absent in the auroral spectrum. Another point of distinction between the two phenomena has been suggested by Barbier (1958a). He found there was a high correlation between 5577 A and the

O_2-Herzberg bands in nonpolar airglow and a lack of correlation of these in aurora.

1.12 Airglow spectrum and its identification

That there was an emission of light from the earth's atmosphere at night was recognised by Yntema as early as 1909. The phenomenon has been investigated by many scientists since then. Using spectrographs of great light gathering power, sensitive plates and long exposures, Slipher (1919) at the Lowell Observatory discovered the green line 5577 Å in the spectrum of the night sky. This was confirmed by Lord Rayleigh (1922) in England. The precise determination of its wavelength at 5577.350 Å by Babcock (1923) with a Fabry-Perot interferometer led to the identification of the line with the forbidden line of atomic oxygen ($^1D_2$-$^1S_0$). The line was produced in the laboratory by McLennan and Shrum (1924). Rayleigh in England and Dufay in France (1922-23) found other features of the night sky spectrum. Similar spectra with many other lines and bands were recorded by Sommer (1929), Dufay (1931) and by Ramanathan (1932).

Frerichs (1930) calculated the values of $^1D_2$ and $^1S_0$ levels on the basis of the ultraviolet spectrum of atomic oxygen. His analysis predicted the oxygen lines (^3P-^1D) near 6300 Å and 6364 Å which Slipher (1929) had discovered as 6315 Å in nightglow. Improved spectroscopy by Sommer (1932,1933), Slipher (1933) and Cabannes (1934, 1935) resolved all these lines and made their identification definite. Dejardin (1936) has reviewed the work done in the early stages of airglow studies and Chamberlain (1961a) has summarised the later work in this subject.

Though some bands were discovered in the red and near infrared their origin was revealed only when Meinel (1950a, 1950b) discovered their rotational structure and identified them as the rotation-vibration bands of OH.

Besides the normal airglow, stable arcs of 6300 Å emission in midlatitudes were observed by Barbier (1958a) and confirmed by Roach and Marovitch (1959) and Duncan (1959). They were named as mid-latitude arcs or M-Arcs. The monochromatic feature of the arc (with the absence of 5577 Å emission) shows that it was excited by energy sufficient for exciting ^1D state only and not ^1S. Such features are observed at geomagnetic latitudes as low as 48^o in both the hemispheres. The arcs are aligned perpendicular to the magnetic field. Arcs as wide as 600-800 km may occur concurrently with visible aurora, but they seem to be independent of the normal visible aurora, both in position and intensity.

The tropical arcs of 6300 Å emission, named and reported by Barbier and Glaume (1962) are located at about 15^o magnetic latitude North and South, and it was suggested that these were connected with the well known equatorial anomaly in F-region electron density enhancement with a dip at the magnetic equator. This phenomenon has about the same height as h'F of the F-layer. Roach and Roach (1963) commented — 'It is not certain whether the word 'arc' is properly used for the tropical phenomenon.' Its occurrence at other low latitude airglow stations has yet to be confirmed.

1.13 Nocturnal variations of airglow emissions

McLennan, McLeod and Ireton (1928), and Rayleigh (1929) reported a maximum in the intensity of 5577 Å near mid-night. Dobrotin, Frank and Cerenkov (1935) and Chvostikov and Lebedev (1935) in Russia observed a rapid increase of green line intensity till a maximum was reached around 1 A.M. and then a decrease till morning. From the observations made during 1957-58 at Mt.Abu (24.6°N), Dandekar, Bhonsle and Ramanathan (1961) reported a midnight maximum in 5577 Å emission. Angreji (1961) pointed out the seasonal variation in the time of occurrence of the midnight maximum. Observations at Huancayo (1961) show a post-twilight decay and post midnight increase in 5577 Å emission. The possibility of a dependence on latitude and on other causes has been explored since then.

Elvey and Farnsworth (1942) studied the nocturnal variation of 5577 Å, 6300 Å and 5893 Å at the McDonald Observatory. They detected a 'post twilight decay' of 6300 Å followed by a 'predawn enhancement'. Dufay and Tcheng (1946) also observed these features and termed them as 'post twilight' and 'predawn effects'. These were later confirmed by other workers. Barbier's (1957a, 1958a, 1959a) observations at Tamanrasset (23°N) showed irregular enhancements of 6300 Å emission. There were large variations of intensity in the post twilight as well as in the predawn values. Now a post twilight decay, steadiness around midnight and a predawn enhancement can be considered to be regular features of this emission in mid latitude night airglow.

The Na D lines do not show a regular pattern of nocturnal intensity variation. Dufay and Tcheng (1946) reported a slight slow increase of intensity during the night.

Infrared sensitive photometers were used by Elvey (1943), Rodionov and Pavlova (1949), Huruhata (1950), Armstrong (1956) and they did not find any regular daily variations in the intensity of OH-bands. The intensity may increase or decrease by 50 % or may fluctuate several times during a night (Chamberlain, 1961b). The localized irregularities may be an important feature of OH emission with patches of emission moving across the sky during the night. The daily variations of O_2-atmospheric bands (Berthier 1955, 1956) and of the ultraviolet part of airglow (Barbier 1953) require to be studied.

1.14 Seasonal variations of airglow emissions

Rayleigh using coloured filters studied the seasonal variation of 5577 Å emission from 1923 to 1927 and found that it had a minimum brightness in December and two weak maxima in March and in October.

Rayleigh and Spencer Jones (1935) made an analysis of the intensity variation of 5577 Å emission at Terling, England (1923-34); Canberra, Australia (1925-34); and Cape Town (1925-33) and found well marked semi-annual variations. The annual variation was found largest at Terling and smallest at the Cape. From the airglow observations of 5577 Å emission made at Mt.Abu (24.6°N) during the IGY-IGC period, Dandekar, Bhonsle and Ramanathan (1961) and Dandekar (1961a) reported a minimum in January-February and a maximum in April. Another minimum and maximum could not be decided due to the impossibility of the observations during the monsoon period, June to September. Angreji (1961) from Srinagar (34°N) observations (1958-60) reported two minima in the solstices and two maxima in the equinoxes, the one in October being conspicuously higher than the other. The strong night to night fluctuations of green line intensity complicate the study of annual variation, but from further investigations by several airglow workers, it appears that the seasonal variations at different latitudes are different.

The seasonal variation of 6300 Å emission remains indecisive because there are large variations in the daily post-twilight decay. The occurrence of a minimum in the red line intensity around midnight shows very little seasonal variation (Barbier 1956).

The sodium D lines show most pronounced seasonal variation with a maximum in winter and a minimum in summer (Dufay and Tcheng 1946). Roach and Pettit (1951) summarized their observations with the conclusion that in the northern hemisphere the sodium intensity shows a minimum in summer and a maximum, 3 to 5 times stronger in winter and that this variation is 6 months out of phase with the annual variation in the southern-hemisphere. They also advocated the movement of excitation patterns from north to south.

Cabannes, Dufay and Dufay (1950); J. and M.Dufay (1951) and Huruhata (1953) studying seasonal variation of OH reported a winter maximum and a summer minimum similar to Na D. Barbier (1959b) also confirmed these results. Krassovsky (1963) also reports a maximum of intensity in winter and minimum in summer.

O_2-Herzberg bands in the UV and blue have been considered to have some seasonal variation, but this remains inconclusive.

The above is a broad description of seasonal variations of night airglow. Systematic patterns of seasonal variation have not been established.

1.15 Variation of airglow emissions with solar and geomagnetic activity

The observations by Rayleigh at Terling and by Spencer

Jones (1939) in Cape Town showed a continuous rise in the intensity of 5577 Å, from 1924 to 1929 followed by a continuous fall till 1933. 1923 and 1933 were years of sunspot minimum and 1928 a sunspot maximum year. Barbier (1959a) covering the observations over the period July 1953 to June 1958 confirmed the covariation of sunspot activity and the intensities of prominent night airglow radiations. Dandekar (1961a) did not find a relation in 5577 Å emission and sunspot number on a day-to-day basis. Angreji (1961) detected that the 5577 Å emission remained steady during 1957 to 1960 as the case of magnetic activity, whereas the sunspot number registered a steady decline all through this period. Hernandez and Silverman (1964) found positive correlation between solar activity and 5577 Å emission. From the data of 1953-64, Barbier (1965) noted that the epoch of maximum of 5577 Å lags behind the sunspot maximum. The observations of 5577 Å emission at Mt.Abu were examined by Dandekar (1961a) to see the effect of solar flares. From this study he reported a substantial increase in intensity on the nights following the solar flares. Dandekar and Silverman (1964) examining the airglow data for Mt.Abu, Tamanrasset and Sacramento Peak also substantiated this earlier finding.

Rayleigh and Spencer Jones (1935) found from the Cape observations that the intensity of 5577 Å emission was greater on magnetically disturbed days. Sandford (1959) reports an increase in 5577 Å emission with increase of magnetic activity.

Dufay and Tcheng Mao-Lin (1947) found negative correlation while Manring and Pettit found no correlation between the two phenomena. An increase in the green line intensity has been observed on magnetically disturbed days and recently this has been supported by Chritophe-Glaume (1963), Weill and Chritophe-Glaume (1965) and Silverman and Bellew (1965). They find an increase in 5577 Å emission after sudden commencements of magnetic storms.

A good correlation between the geomagnetic index C_p and 5577 Å intensity has been reported by Angreji (1967). Angreji has put forward the view that the intensity of 5577 Å is better correlated with magnetic index than with sunspot number or sunspot area.

1.16 Height of airglow layers

The height determination of nightglow radiation from ground-based observations has been made by Van Rhijn and triangulation methods. There are limitations due to variable atmospheric conditions, and the results are varied and inconclusive. Bates and Dalgarno's (1953) theoretical discussion places 5577 Å emission at an altitude of 100 km. In respect of this finding, the observations have been scrutinised taking proper account of atmospheric corrections. The analysis of Roach et al (1958) is important in this connection.

5577 Å

An earlier height determination of 5577 Å emission by Roach and Meinel (1955), using the van Rhijn method placed 5577 Å emission at 62-104 km level. The height determination by Elsasser and Siedentopf (1956) gave 90 $\pm$ 10 km and that by St.Amand et al (1955) by triangulation gave 80-100 km. These lie fairly close to the height determined by rockets. The rocket observations reported by Koomen, Scolnik and Tousey (1956) indicate the height of 5577 Å emission to be at 99 km with emission profile extending from 80 to 115 km. Heppner and Meredith (1958) report the range from 90 to 120 km with maximum at 97 km and Tousey (1958) places this emission in the range of 85 to 105 km with emission maximum at 97 km. A second layer of 5577 Å emission which may make a substantial contribution to the intensity of 5577 Å is expected to be present at F-layer heights (Kulkarni 1965).

6300 Å

An analysis by Seaton (1958) of the deactivation of excited atoms by collision showed an absence of red line emission below 160 km. The rocket observations of Tousey (1958) also indicated the emission to be above 163 km. The strong correlation of 6300 Å emission with the parameters of the ionospheric F-layer and the dissociative recombination of ionisation as a mechanism for excitation, fixes its height in the 250-300 km region. Recent rocket observations by Huruhata et al (1965) show that the red emission maximum is around 270-280 km.

5890-96 A

Packer (1961) reporting the data of two rocket flights, which were least influenced by OH contamination and were duly corrected for background, showed that Na D emission was observed from 70 to 107 km with peak emission at 84 km (December 1955 flight) and from 66 to 118 km with peak emission at 89 km. (March 1957 flight).

OH-Bands

From the two rocket flights Heppner and Meredith (1958) and Packer (1961) have shown that the maximum intensity of OH was around 90 km and 83 km altitude respectively.

Continuum

The height determination from ground observations for the airglow continuum is extremely difficult with the present techniques because of its low intensity and its admixture with the considerably higher intensity of star-light, galactic light etc. The direct observations by rockets as reported by Tousey (1958) show that the airglow continuum at different wavelengths in the green region (5200 A to 5410 A) is generally located between 80 to 110 km.

O_2-Bands

The rocket observations reported by Packer (1961) places UV O_2-bands and (0-0) O_2-atmospheric bands at an altitude around 100 km.

1.17 Correlation between different emissions

The study of the correlation of the different emissions is important for obtaining an idea of the excitation mechanism for the emissions. Barbier's (1954a, 1956) observations with an 8 colour photometer showed that there were two groups of radiations which were well correlated. They are, 5577 and O_2-Herzberg bands, and 5893 sodium doublet and OH bands. 6300-6364 lines of atomic oxygen are unrelated to any of the other prominent emissions. Very recently, Kulkarni and Steiger (1967) confirmed the absence of correlation in 5893/6300, 5577/5893 and 6300/5577 groups of emissions. The development of a second layer of 5577 Å in the night-time F-layer will however require a partial covariance of 6300 Å and 5577 Å.

1.18 Variation of emission in different parts of sky

The night airglow brightness in different parts of the sky is not in general uniform or constant. The presence of moving patches of brightness cause complications in height determination. Variations of the brightness with latitude, with season and with time of night are responsible for making north-south directions unequally bright. The idea that there are zones of maximum intensity of 5577 Å, has been advocated by Roach (1959) and Barbier and Glaume (1959). It is found that the southern sky is brighter at Fritz Peak (39.9°N) and Haute Provence (43.9°N) and the northern is brighter at Sacramento Peak (32.7°N) and Cactus Peak (36°N). The seasonal motion of the zone of maximum intensity studied at Fritz peak by Roach (1959) shows a sinusoidal variation during a year.

1.19 Airglow Observatory at Mt.Abu

The Physical Research Laboratory has maintained an Airglow and Ozone station at Mt.Abu (Lat.24°36' Long.72°43') since 1952.

As is well known, the photometry of night airglow requires a location free from city lights, dust and aerosols, Mt.Abu which is about 200 km north of Ahmedabad was selected as the location for an Airglow Observatory. The Observatory is at an altitude of 1219 m on the eastern outskirts of a small pilgrim hill-station. The photometers are placed on the roof of the building, and power and recording systems are in the room below. There are hills all round the Observatory. They are below 10° in altitude from the horizon. At Mt.Abu, the nights remain generally clear between October and May. Observations have to be closed down for about three months during the monsoon owing to cloud and rain.

1.2 Instrumental set-up at Mt.Abu

The photoelectric photometers utilised for the present study of nightglow are described in the following sections.

1.21 Pole photometer

One of the photometers was continuously directed towards the celestial pole so that the stars included in the angular aperture of the photometer remained the same. The angle of the photometer is 7.5°. The photometer uses an EMI 6095 photomultiplier with head-on cathode and S-10 response. The high voltage D.C. of 1600 volts (negative) applied to the photomultiplier was from a highly regulated D.C. power supply.

The prominent wavelength emissions in the nightglow at 6300 Å, 5893 Å and 5577 Å were isolated with interference filters with their transmission peaks at these wavelengths and half transmission widths 207 Å, 153 Å and 151 Å (Fig.1.1).

A background filter with maximum transmission at 5350 Å (75 Å half width) was used for recording the background intensity; which had to be eliminated in estimating the intensities of light of the wavelengths of interest at the data reduction stage. A precalibration of the filters was done with the help of a Beckman Spectrophotometer at the Ahmedabad Textile Industry's Research Association. The calibration was repeated after one year and no difference was found in the transmission characteristics of the filters.

The filters are symmetrically mounted on a circular disc which could be rotated with a synchronous motor. A geneva movement is so arranged that each filter in turn stays for one minute against the cathode of the photomultiplier to allow its

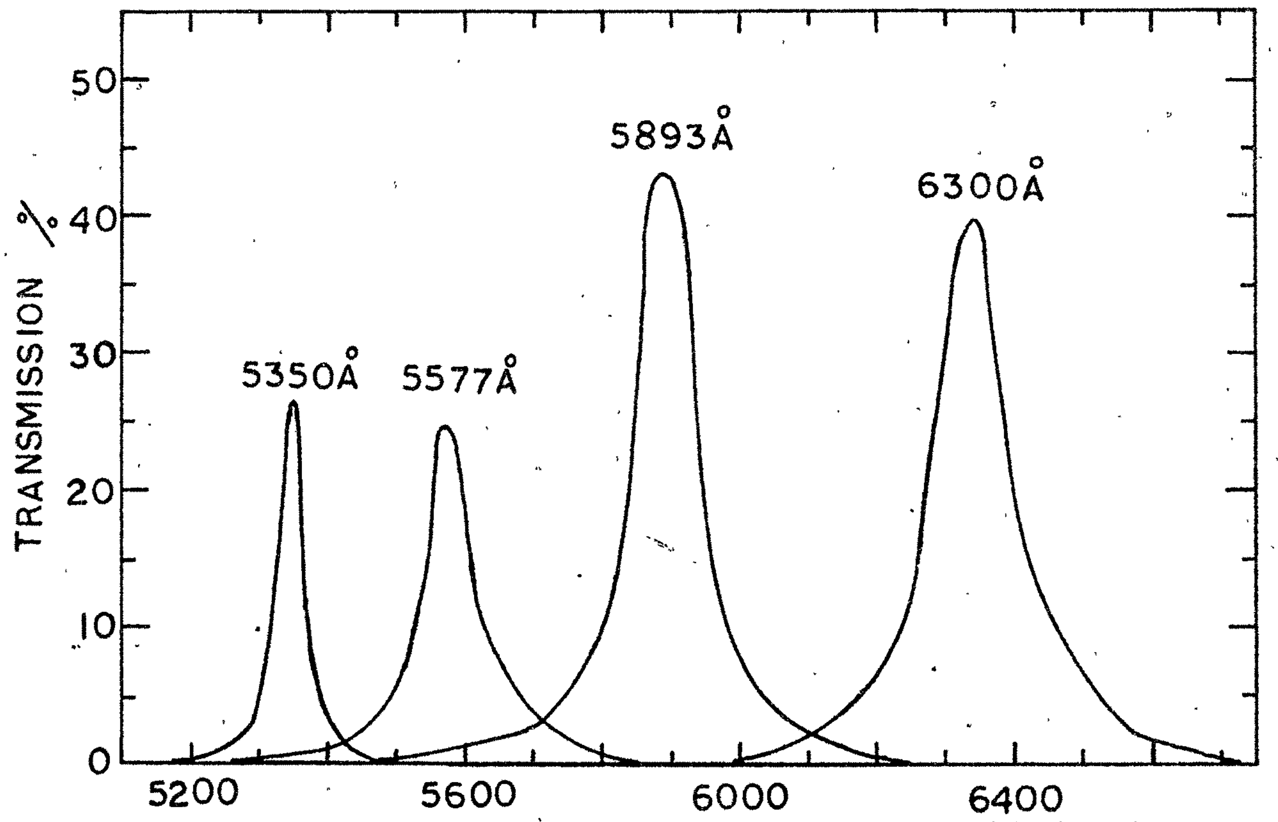

FIG.1.1. Transmission of filters used in Pole Photometer.

characteristic light intensity to be recorded. The zero level when there is no light falling on the photomultiplier is also recorded for one minute. Thus in five minutes, one complete set of the intensities of four wavelengths are recorded. The whole system is made light-tight. The photometer is exposed only when the shutter of the light-gathering cone is uncovered.

The output of the photomultiplier is fed to a D.C. Kipp and Zonen 'Micrograph' pen recorder. The recorder itself is of the balanced bridge type, with transistorized low drift d.c. amplifier. Its sensitivity is 10^{-9} amp/division. The chart is 21 cm wide and linearly divided into 100 divisions. The sensitivity ranges for full scale deflection are listed below :

Current Range	Voltage Range
0.1 μA	0.05 mV
0.25	0.1
0.5	0.25
1.0	1.0
2.5	2.5

With the help of a single rotary switch, any of the ranges can be utilised.

For pole-photometry, no inter-stage D.C. amplifier was needed, because the 1600 VDC applied to the tube was sufficient to record the nightglow signals on 0.1 μA and 0.25 μA ranges of the recorder in all seasons of the year. The A.C. mains supply to all the units was regulated by a constant voltage transformer.

1.22 Zenith photometer

This photometer uses a high-gain, S-20 response EMI 9558B photomultiplier tube. Other constructional details are the same as those of the pole photometer. The signal was recorded on an Evershed Vignoles milli-ammeter. As the output of the photomultiplier was insufficient to be recorded directly on the 0-0.1 mA range of the recorder, a tube D.C. amplifier was used to amplify the signals.

With the high sensitivity of the S-20 tube it was possible to record OH(7, 2) and OH(8, 3) bands on the zenith photometer. The other two filters transmitted 6300 A with half transmission width 100 A and a background filter centred around 6080 A with half transmission width 45 A. The OH(7, 2) and OH(8, 3) filters have half transmission widths 105 A and 90 A respectively (Fig.1.2). The angle of the photometer is about 4.5°.

1.23 All-sky scanning photometer

An RCA 7265, S-20 photomultiplier is used in this photometer, and interference filters (Type B10, BAIRD ATOMIC INC.) centred at 6300 A, 5893 A, 5577 A and 5750 A (background), having half widths of about 40 A (Fig.1.3) are mounted on a circular disc enclosed in a rectangular box. One complete rotation of the disc, recording the intensities of light of the four wavelengths and of the zero level, takes 22.5 sec. The angle of the photometer is about 5°. The photomultiplier is

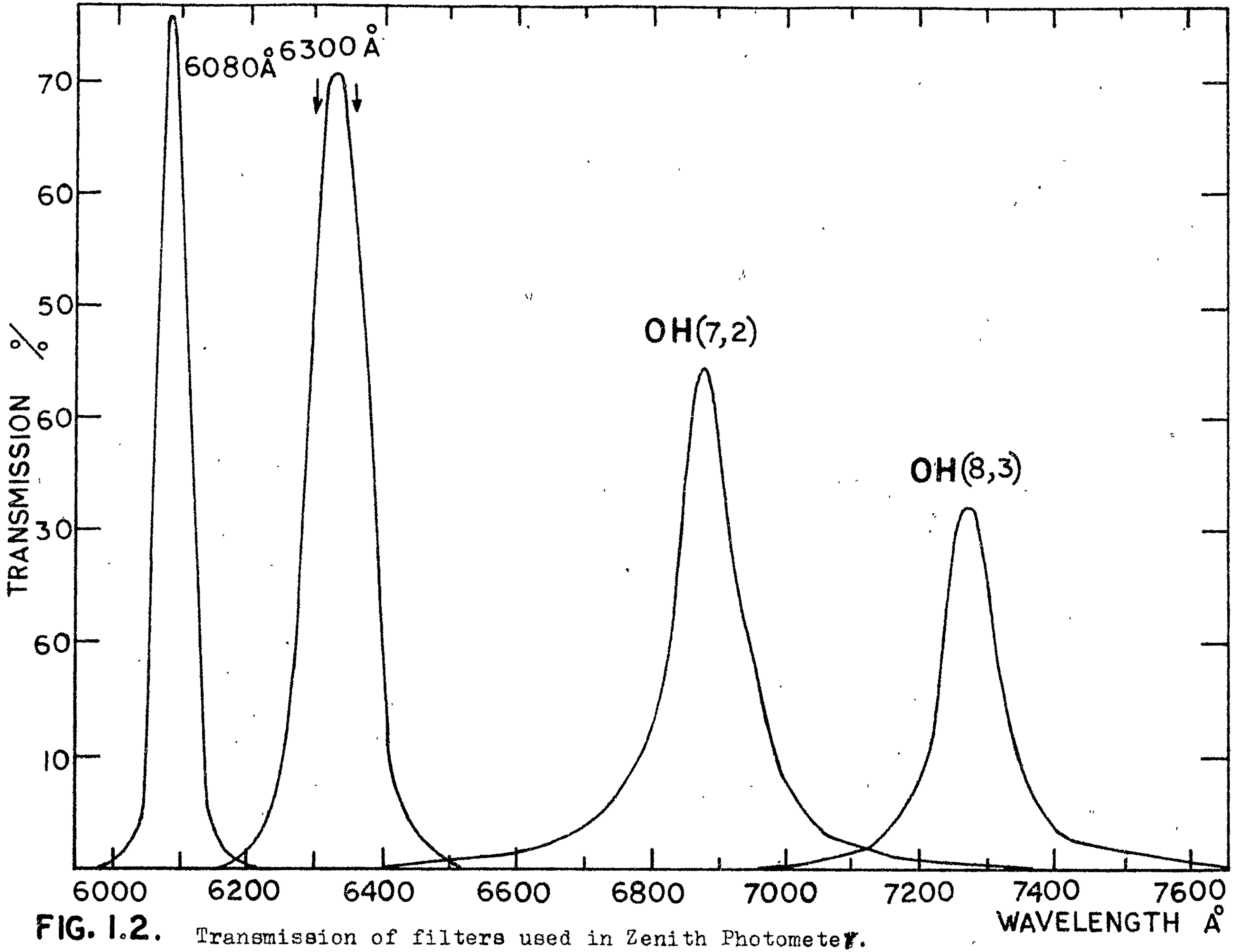

FIG. 1.2. Transmission of filters used in Zenith Photometer.

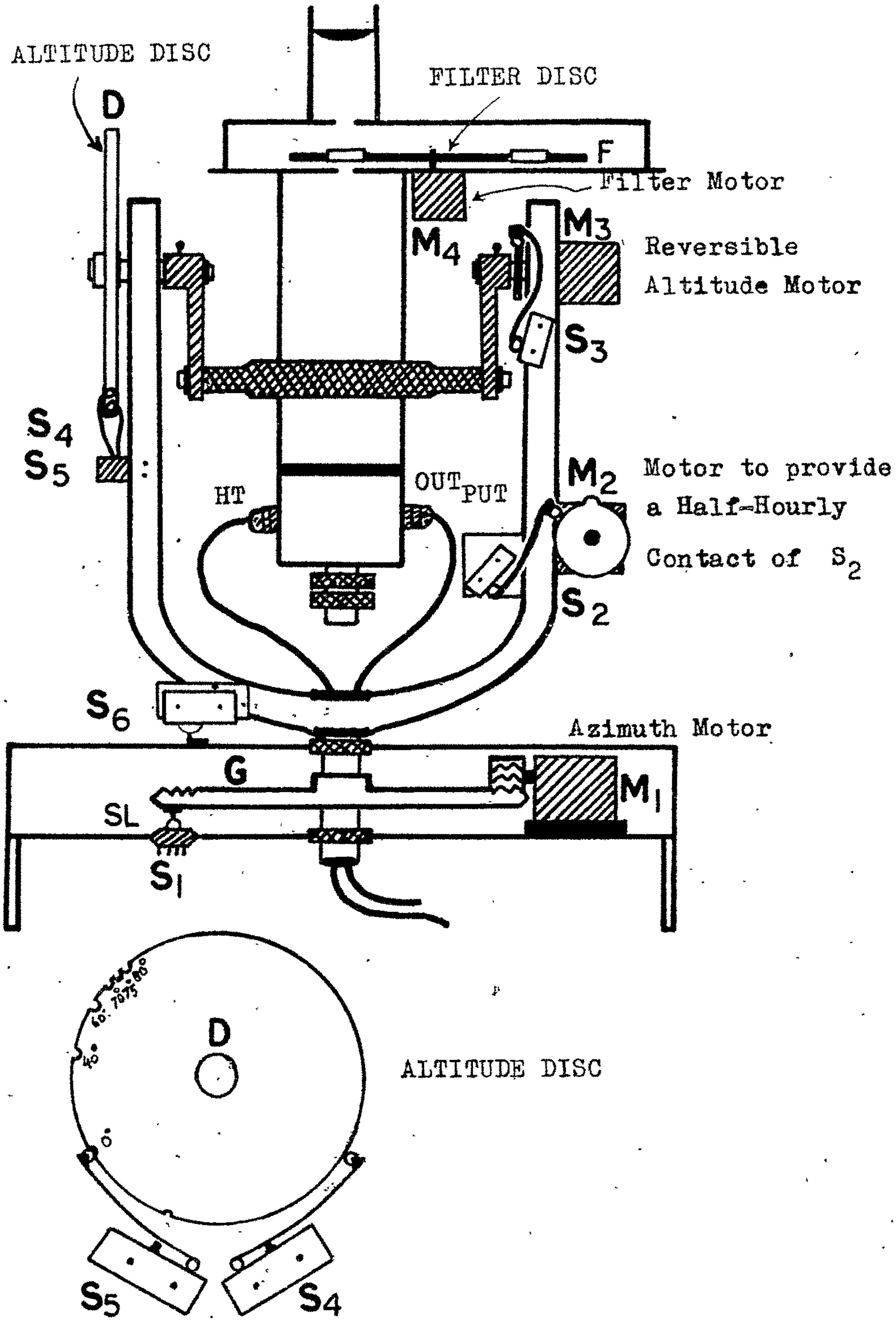

FIG.1.4. ALL-SKY SCANNING PHOTOMETER.

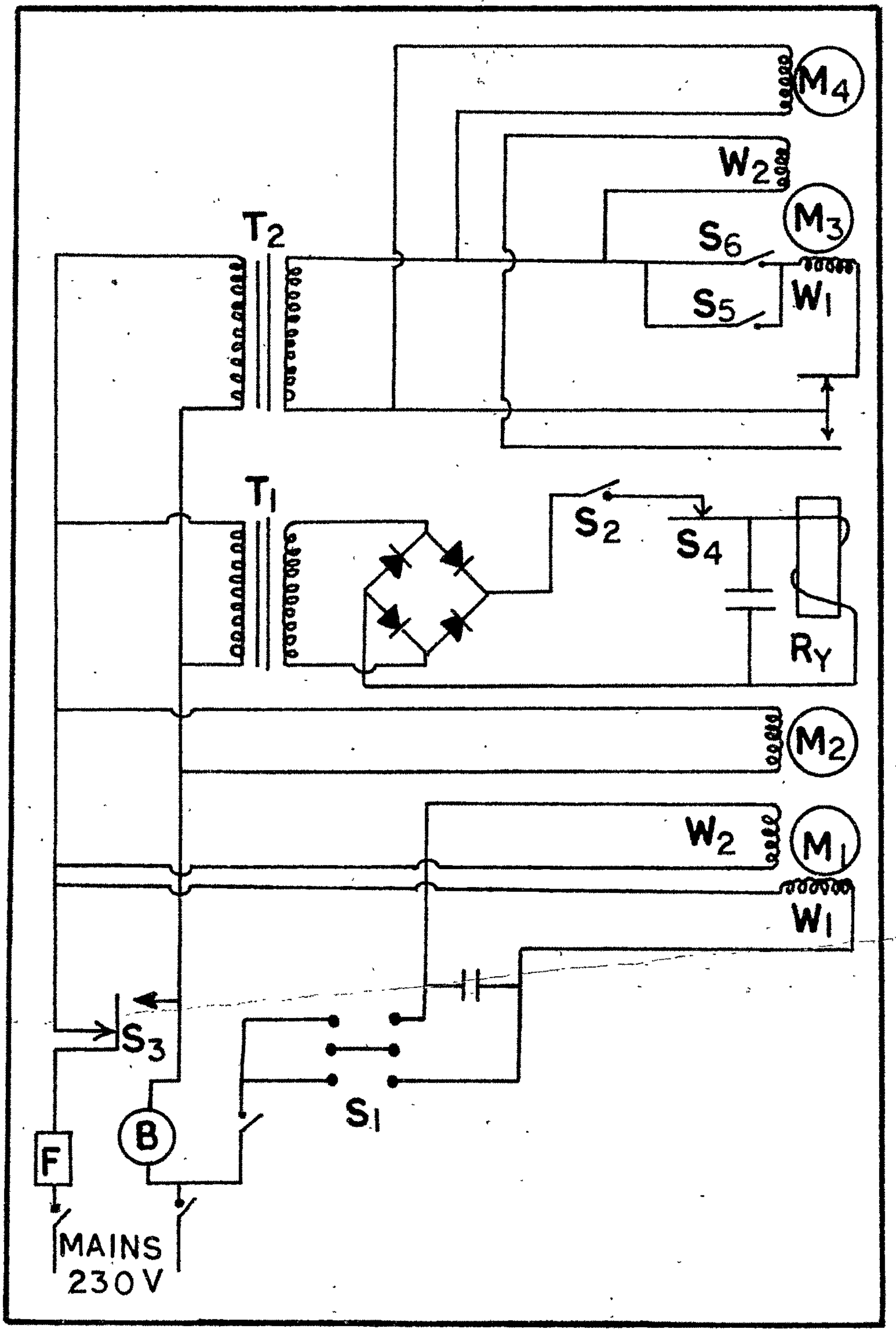

FIG. 1.5. Electrical programming circuit of Scanner.

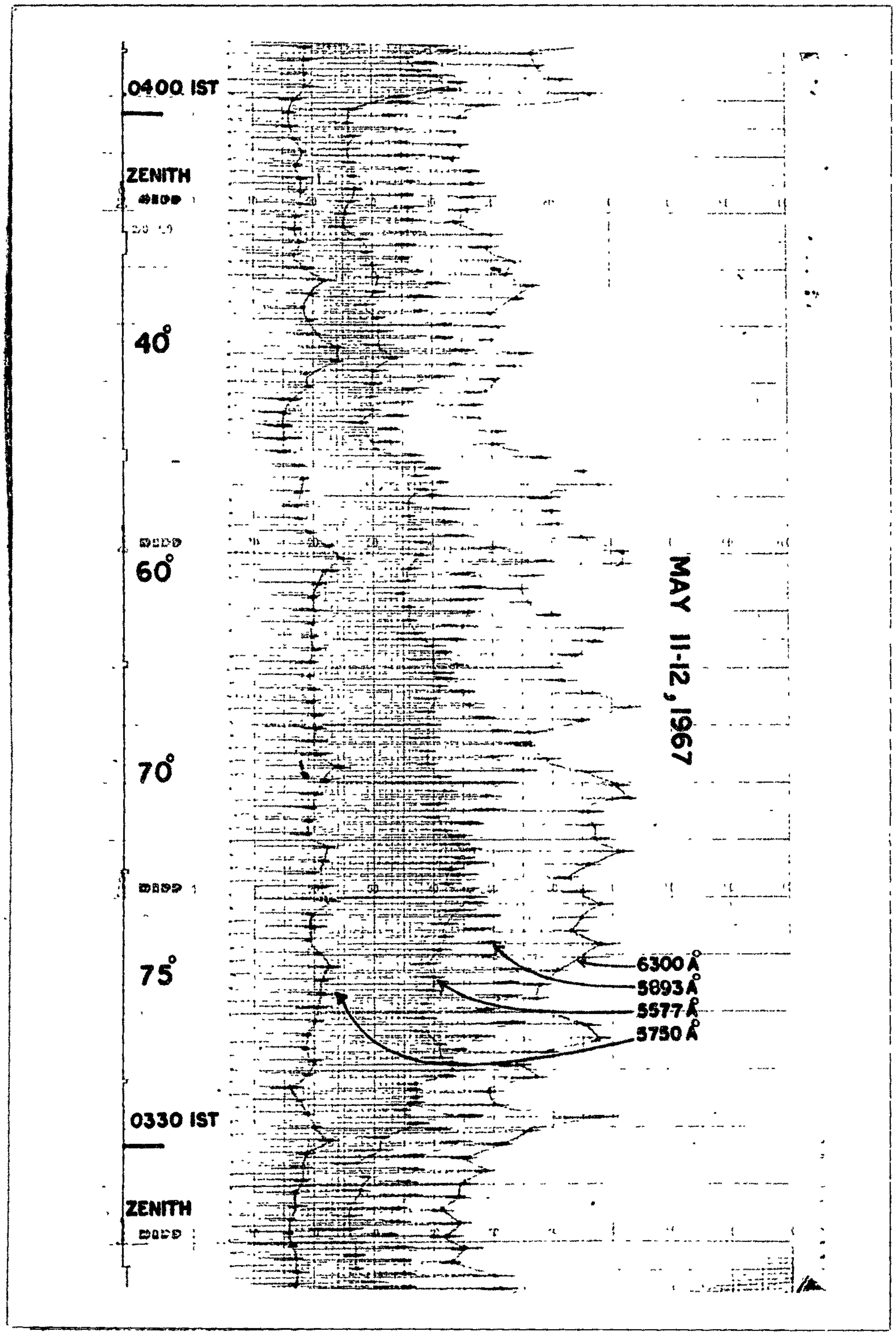

FIG.1.6. A sample record of scanning photometer.

Component	Function	Position
Motors		
M_3-Brass Motor 55V, 60 c/s, 1 RPM reduced to 1^o/sec, two windings W_1 and W_2	When winding 1 is connected, the altitude changes from horizon to zenith. When winding 2 is connected by a relay it goes from zenith to horizon.	On the fork near the axis of P.M. tube.
M_4-Brass motor 55 V, 60 c/s. 1 RPM reduced to 1 Rev/22 sec.	Rotates filter wheel continuously.	On the filter box.
Switches		
S_1-Toggle switch DPDT 5 amp.	When pushed mechanically by a bump on the 6 minute wheel in the base box, the opposite windings W_1 and W_2 of M_1 are connected in turn. Thus the scanning is done alternately in clockwise and anti-clockwise directions.	Inside the base box.
S_2-Microswitch 5 amp.	Normally Open is closed by a bump on a wheel rotating at 1R/30m by M_2; remains closed for about 45 sec.	On the fork near M_2.
S_3-Microswitch 5 amp.	If the altitude wheel turns beyond 80^o and 0^o this switch disconnects the mains. At that time it will ring a bell.	On a wheel opposite to altitude wheel.

Component	Function	Position
Switches		
S_4-Microswitch 5 amp.	Normally closed is opened when the photometer looks at 80^o zenith distance by falling into a notch. This is done when the altitude motor brings the photometer from zenith to the horizon by connecting W_2 of M_3.	On the altitude wheel (only one notch comes into its path).
S_5-Microswitch 5 amp.	Normally open takes over from S_6 when S_5 is pulled out of the notch. It rotates the altitude wheel till S_5 falls in the other notch.	On the altitude wheel.
S_6-Microswitch 10 amp.	Normally Open is closed for about 2 sec. every 6 minutes by a bump on the base box. It activates W_1 of M_3 and starts changing altitude.	On the fork (bump on the base box).
SL-Brass knob sliding in a brass cavity	Turns the toggle switch to change the azimuthal rotation. The slide length can be adjusted by a tangent screw to make the 360^o azimuthal rotation exact.	Attached to the azimuth gear G.

Component	Function	Position
R -Full wave bridge of 4 1N207 diodes.	Provides D.C. voltage for operating the relay Ry.	On the fork.
Ry-Relay 12 VDC carrying capacity 5 amp. (of contacts).	Energises when S_2 and S_4 are closed; connects W_2 and disconnects W_1 of two-way motor M_3.	On the fork.

CHAPTER II

STUDIES OF 5577 A EMISSION :
SEASONAL AND DIURNAL VARIATION
INTERPRETATION OF MIDNIGHT HUMP

CHAPTER II

STUDIES OF 5577 A EMISSION :
SEASONAL AND DIURNAL VARIATION
INTERPRETATION OF MIDNIGHT HUMP

The observations at Mt.Abu reported and discussed in this chapter were obtained with the "Pole Photometer" (explained in Chapter I).

2.1 Seasonal variation of 5577 A emission

To study the seasonal variation of 5577 A emission, the intensities in rayleighs, for the dark hours of the nights were averaged for each complete lunation. The averages relate to the half-hourly data of each lunation centred round each New-Moon. The averaged data from November 1964 to June 1967 are plotted in Fig.2.1. Observations were not possible in July, August and September due to clouds and rain. The observations were also scanty in the month of June in each of the years 1965, 1966, 1967 due to clouding. The continuous curve of Fig.2.1 gives a picture of the seasonal variation of 5577 A.

We can draw the following conclusions regarding the seasonal variation of 5577 A emission :

(1) The minimum intensity is observed in January. This was repeated in each of the years 1965, 1966 and 1967.

(2) There is a second minor minimum of intensity somewhere in June or July. As observations could not be made in July, August, September, the exact month or the intensity of the second minimum cannot be determined from the Abu observations. The trend of intensity in the months of May and June however indicates the existance of a summer minimum.

(3) The first maximum of intensity appears in April in each of the years of observation.

(4) A second maximum occurs in October. The October maximum could not be confirmed in 1966 as data were insufficient in September 1966.

The January-February minimum has been noted by Dandekar (1961b) in Mt.Abu as well as in Tamanrasset (22.8^{o}N) data for IGY-IGC period. The maximum in April in the data of Abu and Tamanrasset noted by Dandekar is also found in the quiet period of the sun (1964-67). Therefore it appears that the months of minima and maxima in the seasonal variation of 5577 Å emission are not affected by solar activity.

We have plotted in Fig.2.2 the Haleakala (20^{o}N) (Hawaii) data of 1964-65. The January-minimum and April maximum and October-maximum are clearly present at Haleakala also. The secondary minimum which we suspected to be present in June-July at Abu is observed in the Haleakala data in July-August.

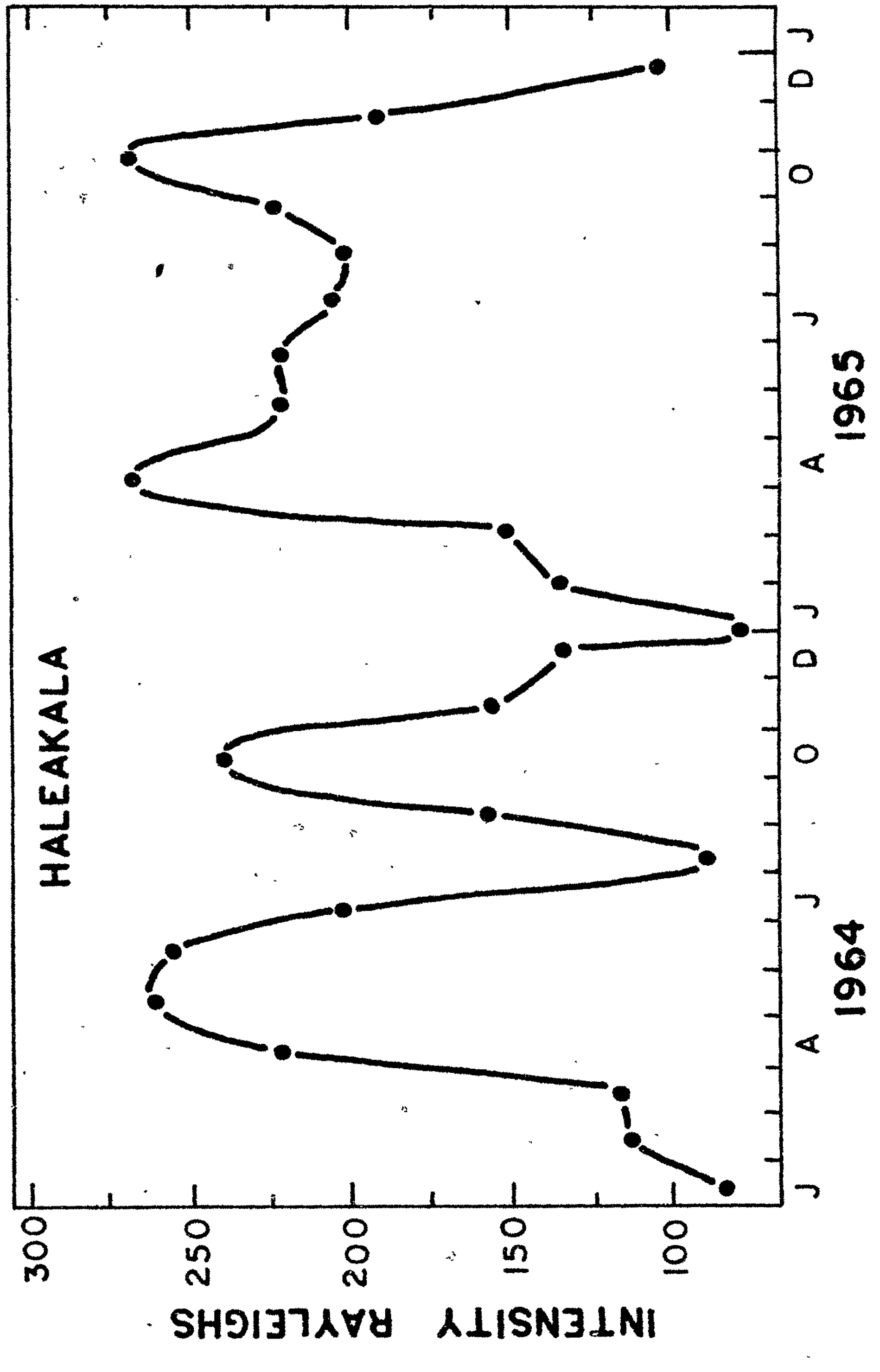

FIG. 2.2. SEASONAL VARIATION OF 5577Å

(5) The intensity of the major minimum in January appears to remain practically constant over the period of the three years of the present observations. The intensity of the April maximum appears to have increased from 1965 to 1967. This continued-increase in 5577 Å emission in the increasing solar activity may indicate the effect of solar activity on the intensity of 5577 Å.

(6) The seasonal occurrence of the minima and maxima are apparently related to the '<u>Solstices</u>' and '<u>Equinoxes</u>' respectively. The minimum of January appears 3 to 4 weeks after the winter solstice (December 22). The maximum of April appears also 3 to 4 weeks after the vernal equinox (March 21). The positions of the second minimum of June-July-August and of the second maximum of the autumn period are not definite to say that they also appear similarly after the summer solstice (June 22) and the autumnal equinox (September 23) respectively. This lag of minima and maxima with respect to the solstices and equinoxes is somewhat like the lag of seasons by several weeks from the actual position of solstices and equinoxes.

To compare the seasonal variation of 5577 Å emission for these years with a solar activity parameter, namely the solar radio flux on λ = 10.7 cm has also been plotted in Fig.2.1.

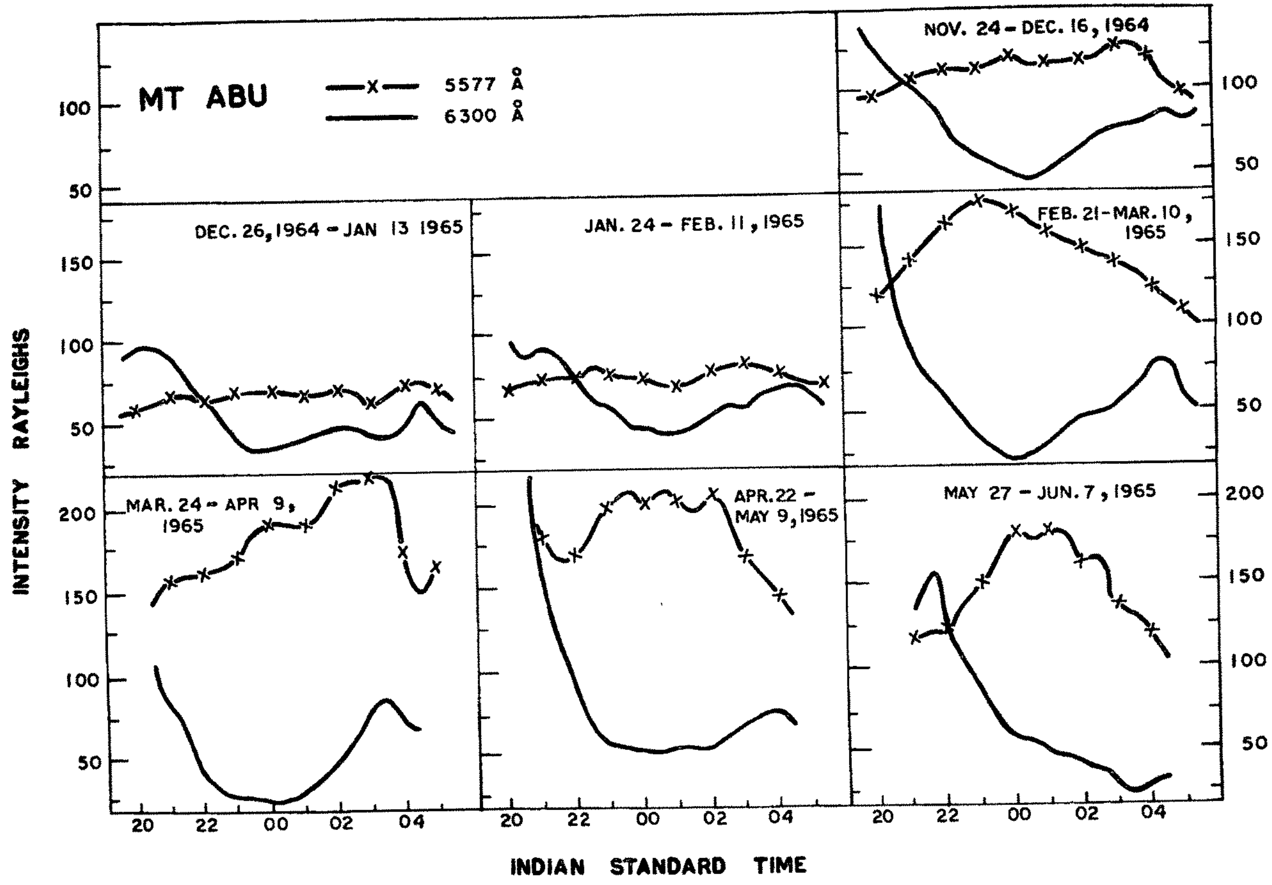

FIG. 2.3. NOCTURNAL VARIATION OF 5577 Å AND 6300 Å INTENSITY NOV. 1964 TO JUN. 1965

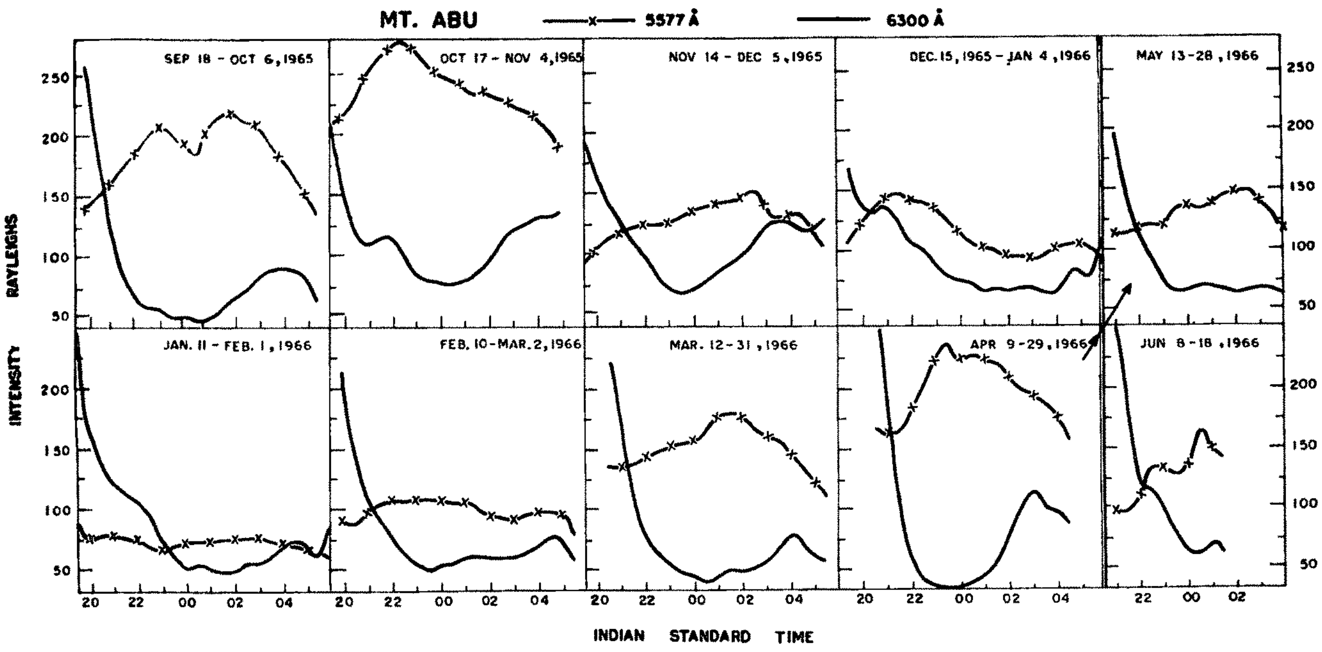

FIG. 2.4. NOCTURNAL VARIATION OF 5577Å AND 6300Å INTENSITY SEP. 1965 JUN. 1966

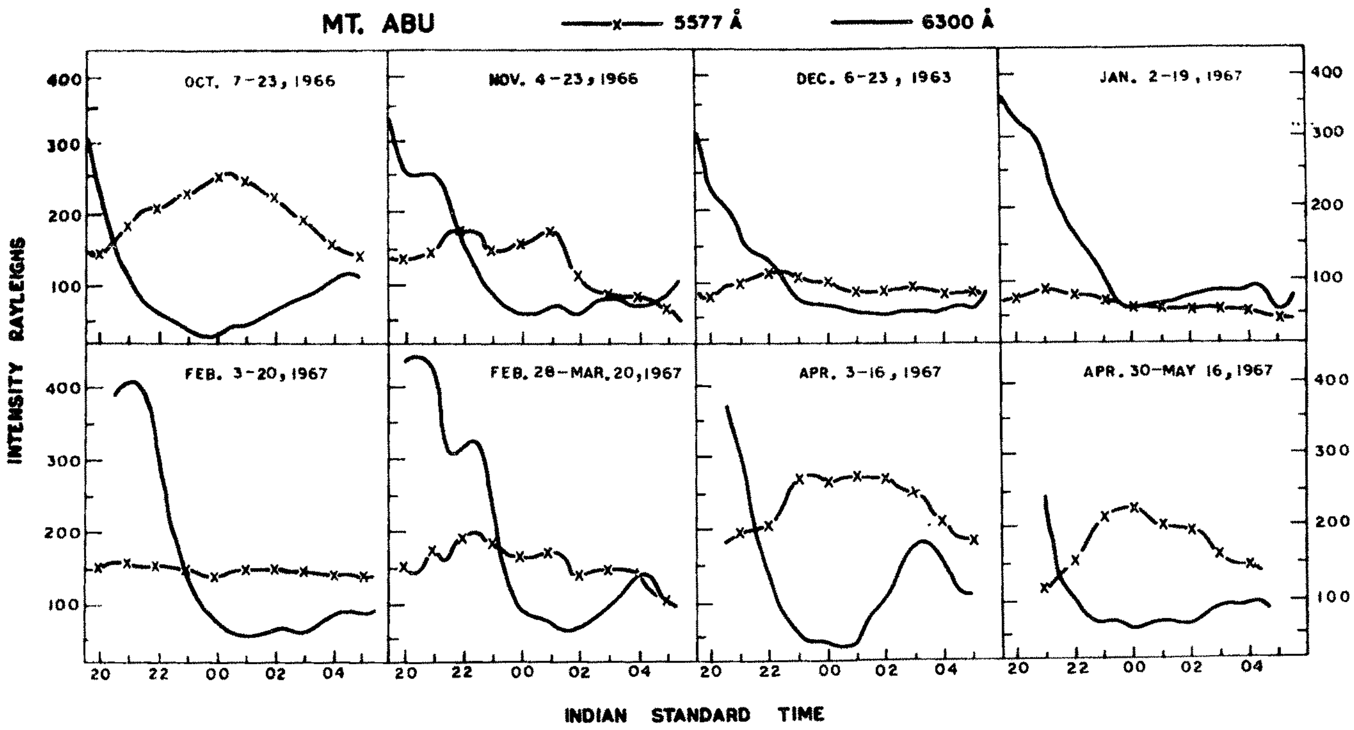

FIG. 2.5. NOCTURNAL VARIATION OF 5577 Å AND 6300 Å INTENSITY OCT. 1966 TO MAY 1967

Similar was the case in 1966 and 1967. In the periods November-December 1965, February-March 1966, December 1966 and February 1967, the intensity variation was of the order of 20 Rayleighs. Thus in the lunations mentioned above, there was not much intensity variation. As far as patterns of variation in these months go, we see that there were in some months one or two (in some cases three) small peaks. The peaks were mostly flat.

In the lunations,

February-March 1965
March-April 1965
May-June 1965
September-October 1965
April 1966, 1967, October 1966

and May 1967, the intensity variations were quite large. Variations of 80-100 R were present in this group of lunations.

2.22 Occurrence of midnight maximum

In the periods of

February-March 1965
May-June 1965
October-November 1965
April 1966
and April-May 1967,

a single pronounced maximum of intensity was present one to three hours before midnight. In March-April 1965, November-December 1965, March 1966, May 1966 and October 1966 a maximum after midnight was present. Peculiarly in September-October 1965, two maxima appeared at 2300 and 0200 IST. In December-January 1966, the maxima separated such that the first maximum appeared at 2130 IST and the other at 0430 IST. In November 1966 two pronounced maxima appeared at about 2200 and 0100 IST and a third one, though small, appeared at 0400 IST. In April-May 1965, May-June 1965 and April 1967 a flat maximum around midnight was observed. It appears that the flat maxima of the said months contained a few minor peaks in them. To study the occurrence of 5577 Å maximum in premidnight, around midnight and postmidnight periods in different seasons, histograms have been prepared from the observations in October 1965 to June 1967 (Fig.2.6). In Fig.2.6, B stands for premidnight hours (20, 21, 22 hrs), M stands for around midnight hours (23, 00, 01 hrs) and A stands for after-midnight hours (02, 03, 04 hrs).

It is found that in the equinoctial months (October, November and April, May) the 5577 Å maximum was most frequent around midnight, with pronounced high frequency in April and May. In the months of December, January, February and March the occurrence of 5577 Å maximum is less frequent about midnight than in the pre-midnight or post-midnight periods.

From these curves, it may be concluded that broadly speaking, the intensity increases from the end of evening twilight with a decrease towards dawn. Maxima are observed near the middle of the night, either before or after midnight, in all the seasons, but they do not occur at the same time in all the lunations.

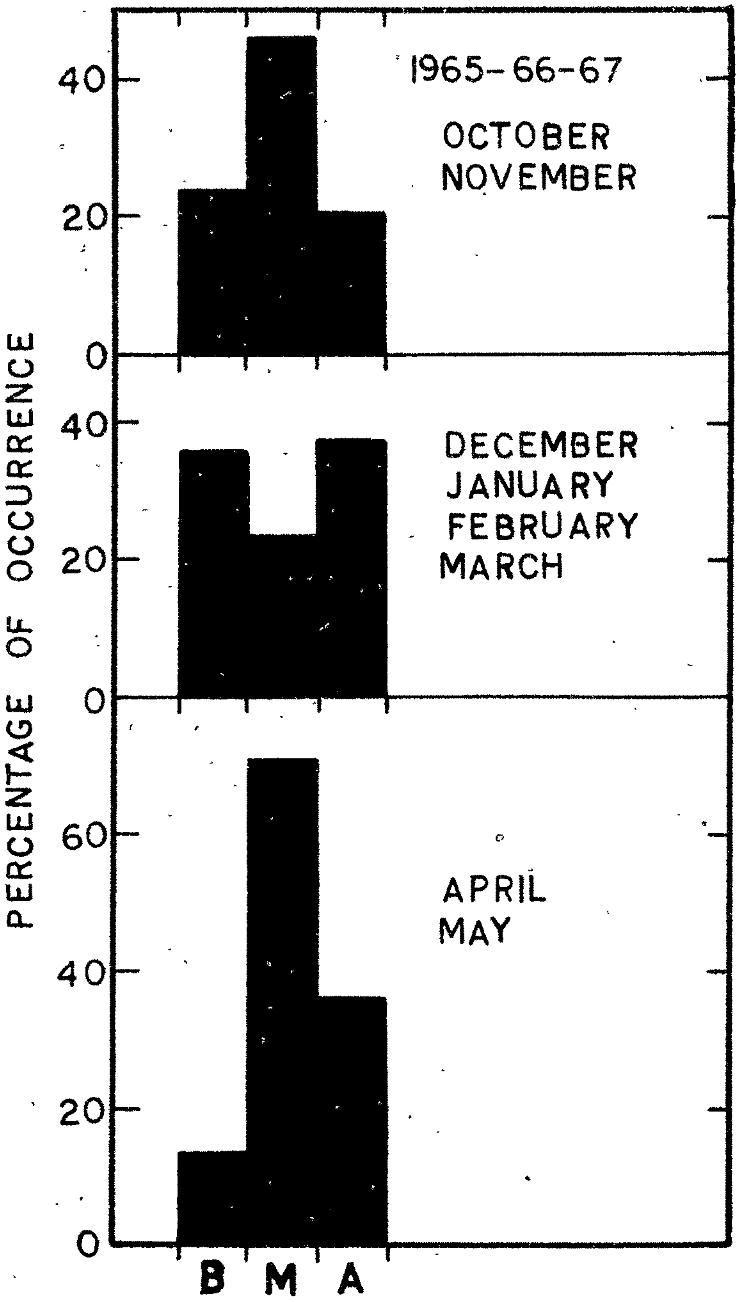

FIG. 2.6. Occurrence of 5577 Å maximum before, around and after midnight hours (B, M, A).

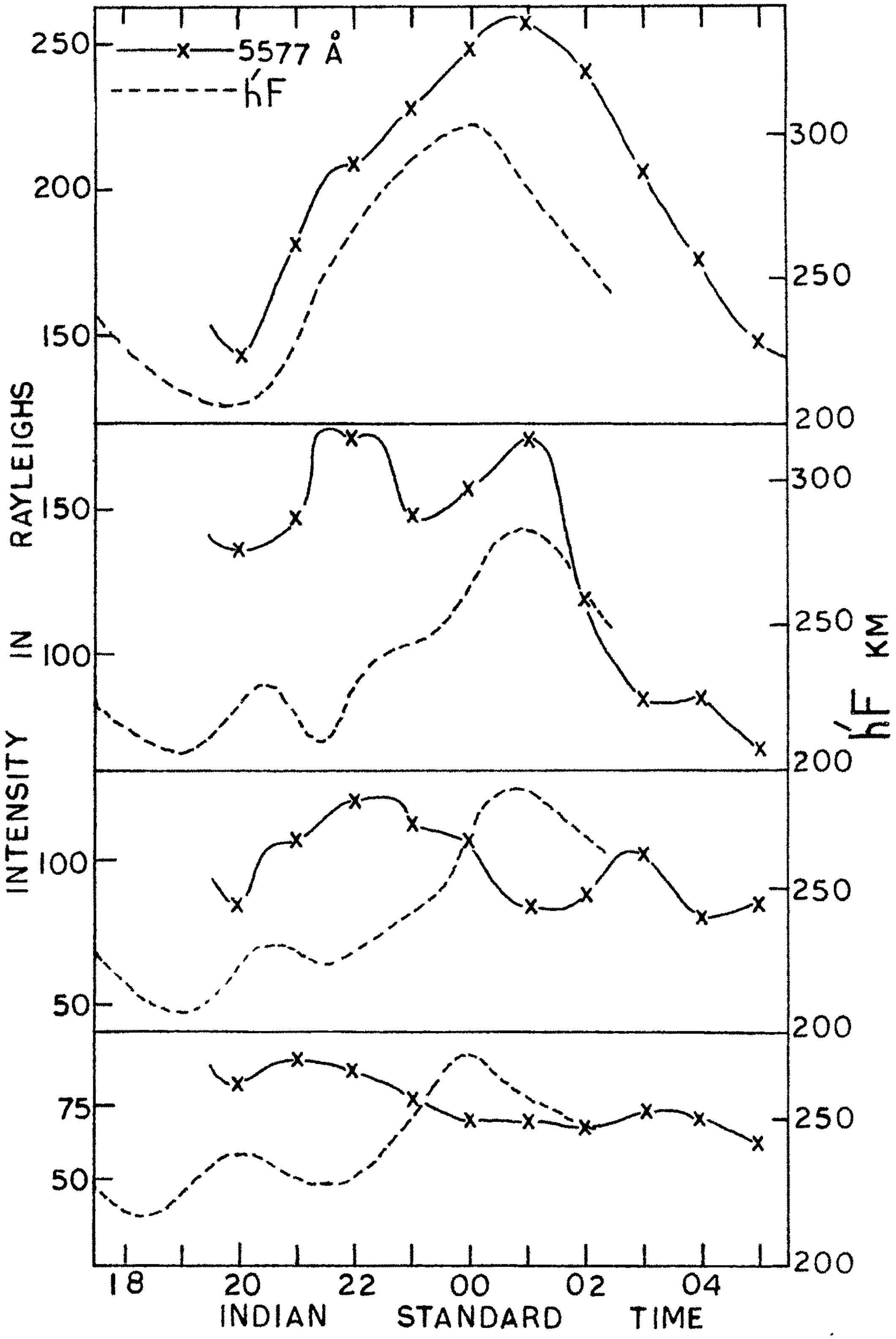

FIG.2.7. Showing the corresponding minima of h'F before 22 hours and the maxima in 5577 A around midnight.

It is possible that a lowering of h'F (around 210 km) corresponds to a pushing down of more oxygen atoms at the top side of the level of maximum 5577 A emission. A rise in intensity of 5577 may follow a lowering of h'F; the delay depending on many factors.

It may be pointed out that atomic oxygen concentration contributing to I_{5577} can be added to the upper part of the atomic oxygen profile, because

1) Rocket observations (Tousey 1958, and Heppner and Meredith 1958) show that the luminosity profile shows a sharp fall at the lower boundary around 90 km while it fades-out rather slowly in the upper part of the profile. The upper part of the luminosity profile may increase in intensity by addition of atomic oxygen.

2) Any additional concentration of atomic oxygen in the lower part of the profile (90 km and below) cannot contribute to the intensity of 5577 A, as most of the excited oxygen atoms will be deactivated due to collisions in the atmosphere of higher density.

CHAPTER III

SECTION A 6300 A EMISSION AND ITS VARIATIONS

SECTION B EXCITATION MECHANISM FOR 6300 A EMISSION

CHAPTER III

SECTION A

6300 Å EMISSION AND ITS VARIATIONS

The observations at Mt.Abu reported and discussed in this chapter were obtained with the "Pole Photometer" (explained in Chapter I).

3.1 Seasonal variation of OI red lines

The seasonal variation of the red line emission of atomic oxygen towards the pole at Mt.Abu is represented by the continuous curve in Fig.3.1; it includes the data from November 1964 to June 1967. The following general conclusions can be drawn.

The seasonal variation of red line emission is less regular than that of the 5577 Å line. From the observations taken at Mt.Abu during the years of high solar activity 1957-58-59, Dandekar (1961a) concluded that there was a minimum of emission in January. From the present observations, it appears that while maxima were found in May and October-November 1965 and a prominent maximum in March 1967 in 1966, a minimum was found in March. The seasonal variations at Mt.Abu appear therefore to be not quite regular.

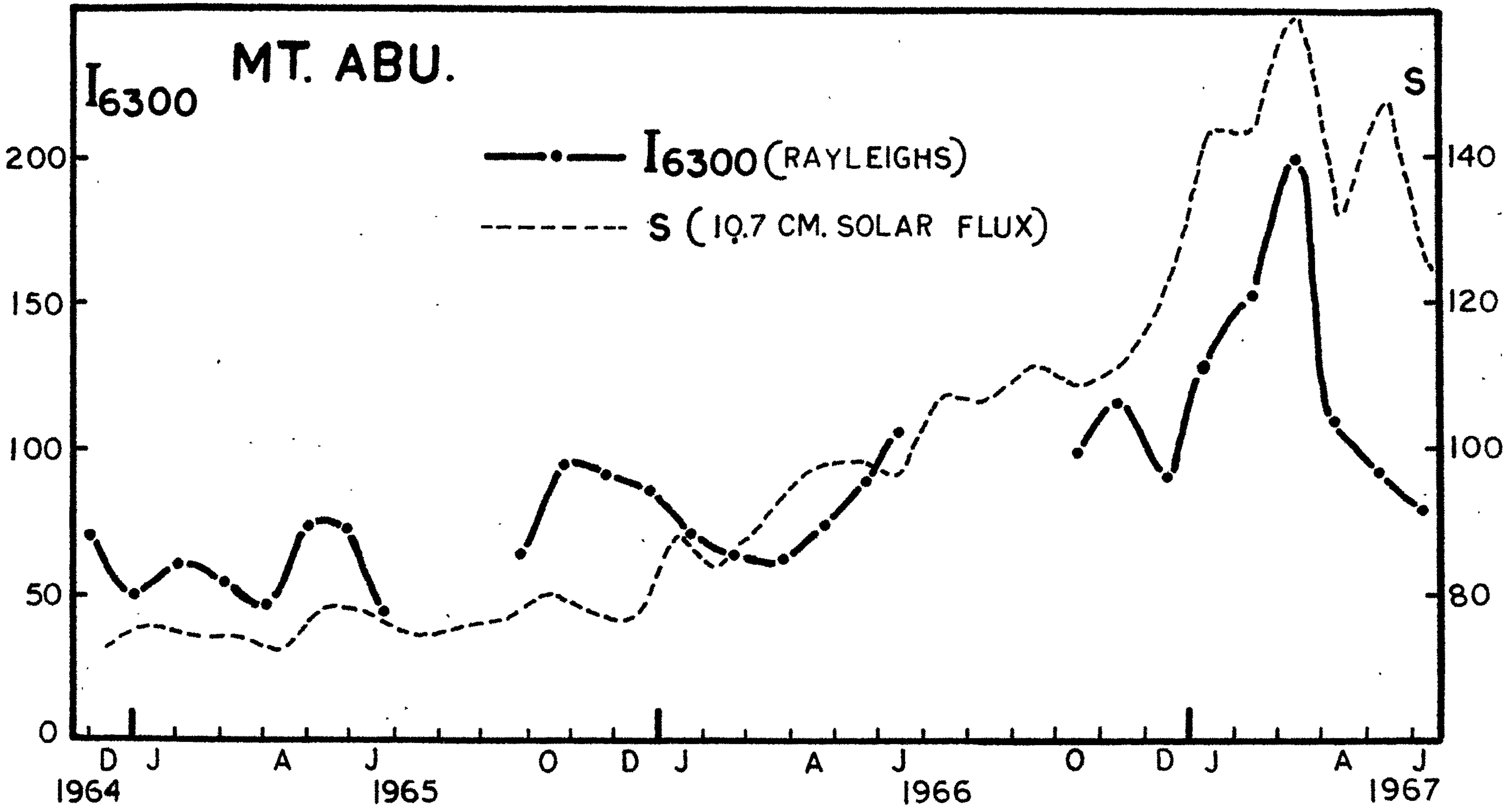

FIG. 3.1. SEASONAL VARIATION OF 6300 Å AND 10.7 CM SOLAR RADIO FLUX

From 1964 to 1967, there was a continuous increase in the level of the red line intensity running somewhat parallel to the increase in solar activity. In the same figure is plotted the curve of 10.7 cm wavelength solar radio flux (broken curve). The general increase in red emission runs nearly parallel to the increase in the solar flux of 10.7 cm radiation.

The occurrence of the sharp peak in the red line emission in March 1967 was associated with a similar increase in solar radio flux and in the midnight electron density in the F -layer.

3.2 Nocturnal variation of OI red lines

The nocturnal variation of red line emission of atomic oxygen is of special interest as it links with the variation in the parameters of the night time ionospheric F-layer.

Observations in middle latitudes show that the intensity of the red oxygen lines undergoes a 'post-twilight decay' and reaches a nearly steady value around midnight. This is followed by a 'pre-dawn enhancement' of intensity. A more or less similar night time variation (Fig.2.3, 2.4, 2.5) is observed at Mt.Abu. However, there are additional features superposed on this general variation.

Additional features

3.21 '6300 Å hump'

A 'hump' of intensity at about 0430 IST is found to be superposed on post-midnight enhancement on almost all the nights of observations. An explanation of the 'pre-dawn enhancement' and of the post-midnight '6300 Å hump' is offered in Chapter IV.

3.22 Post-twilight decay

Throughout the period under investigation (November 1964 to June 1967) the rapid fall of intensity after evening twilight upto about midnight was generally seen.

In some months, an increase in intensity for an hour or so around 2100 IST was found superposed on the post-twilight decay. In 1964-65, the 21 hour peak appeared in the lunations of December-January 1964-65, January-February 1965 and May-June 1965 (in the last lunation however, the data were scanty). The peak occurred at 2200 IST in October- November 1965 and in December-January 1965-66, but only a small flattening of the falling curve was observed in January-February 1966. The peaks were quite pronounced in the lunations of November 1966, and of January, February and March 1967. In other months, the peaks are not discernible.

3.23 Pre-dawn enhancement

In the months of November and February, pre-dawn enhancement is conspicuous at Mt.Abu. In the lunations of December 1964-January 1965, December 1965-January 1966, December 1966 and January 1967 the pre-dawn enhancement was rather small, as compared to that in the months of autumn and spring. In mid-latitudes, the pre-dawn enhamcement is most conspicuous (Barbier 1956, 1957) in the long nights of winter.

It may be mentioned that in the earlier observations made at Mt.Abu by Dandekar (1961b) in the high solar activity years 1957-58-59, he found that the post-twilight decay which continued till midnight was followed by a steady uniform intensity. In the present observations, however, in all the months except May and June, the intensity showed an increase after midnight.

SECTION B

3.3 Excitation mechanism for 6300 A emission

In the following chapters we are concerned with the mechanism of production of 6300 A emission. Therefore, this is considered in brief at this place.

There has been recently some controversy on the proposed mechanism of this emission in airglow. We indicate this point here and draw our conclusions; which we wish to adopt throughout the thesis.

The dissociative recombination of the ionization in the night time F-layer of ionosphere, is admittedly the source of red $(OI)_{21}$ lines at 6300-64 A. The dissociative recombination processes considered important in this regard are mainly the following two (Norton et al 1963)

$$NO^{+} + e = N^{*} + O^{*} + 2.76 \text{ ev} \qquad (1)$$

$$O_2^{+} + e = O^{*} + O^{*} + 6.96 \text{ ev} \qquad (2)$$

The asterisk (*) is used to denote an atom or molecule in excited state. The energy available in the reaction (2) is 6.96 ev which on the examination of the energy level diagram of the atomic oxygen, can be distributed to the atomic oxygen fragments to emerge in the following pair of terms :

$$({}^3P, {}^3P), ({}^3P, {}^1S), ({}^1D, {}^1D) \text{ or } ({}^1D, {}^1S).$$

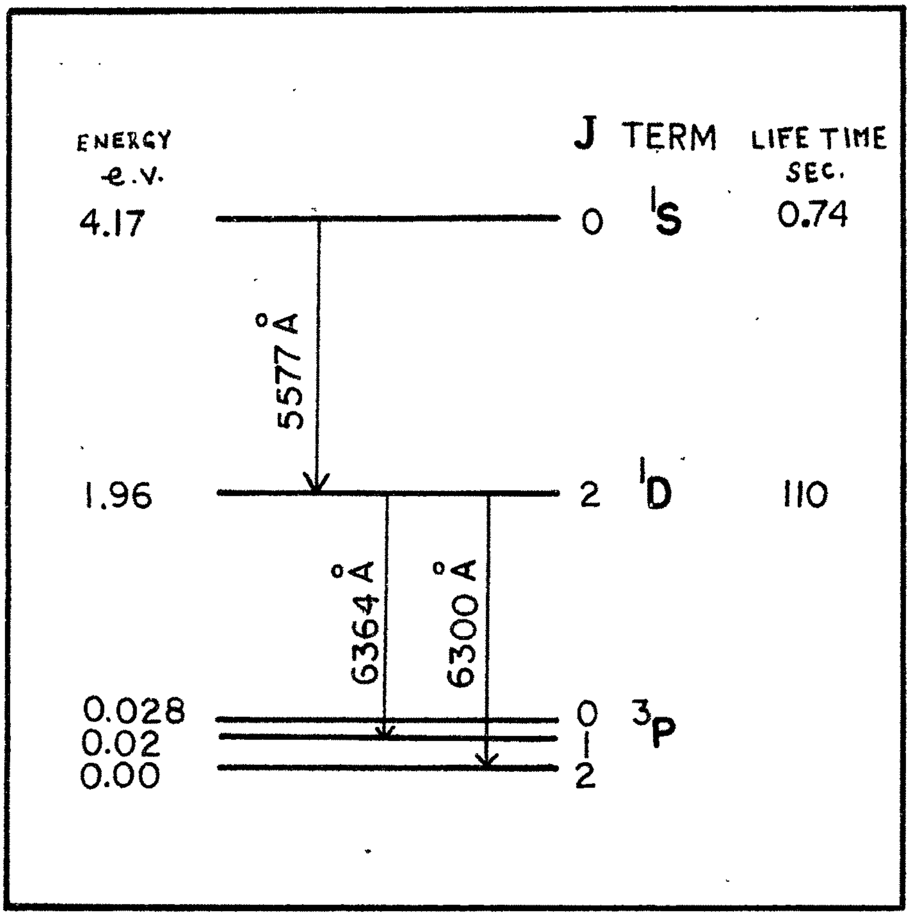

ENERGY LEVEL DIAGRAM OF [OI] LINES.

Similarly the N and O produced in reaction (1) can be in either $N(^4S)$ and $O(^1D)$ terms, or the $N(^2D)$ and $O(^3P)$ terms.

The molecular ions, O_2^+ and NO^+ are provided by O^+ the atomic oxygen ions which are predominantly present in the night time F-region of ionosphere. The processes through which this happens are

$$O^+ + N_2 = NO^+ + N \qquad (3)$$

$$O^+ + O_2 = O_2^+ + O \qquad (4)$$

Dalgarno and Walker (1964) have pointed out that the excitation of the O atom to ^1D level in reaction (1) violates conservation of spin. According to these authors the reaction (1) is incapable of producing ^1D term. On the other hand, very recently Peterson et al (1966) have advocated that the possibility of the immediate excitation of ^1D level as a result of reaction (1) cannot be excluded, and they include reaction (1) in their theory of 6300 emission. It has been suggested by Peterson et al (1966) that O (^1D) can be formed by the deactivation of N (^2D) in collision with O (^3P). It is also possible to prove, on the basis of diffusion mechanism, that O (^1D) can be formed in such collisions and then the effect of reaction (1) would be almost equivalent to the direct excitation of O (^1D) in the reaction. This is the justification for including reaction (1) in the mechanism of red line emission.

Rocket measurements by Johnson et al (1958) and Hertzberg (1958) show NO^{+} to be the dominant molecular ion in the night time F-region of ionosphere. Therefore we conclude that reaction (1) is also important for the red line emission.

Considering the two reactions, (1) and (2) mentioned above we shall try to explain several dynamic features of 6300 Å emission.

CHAPTER IV

SECTION A BEHAVIOUR OF OXYGEN 6300 A EMISSION IN THE NIGHT AIRGLOW AND THE DYNAMICS OF IONOSPHERE IN LOW LATITUDES

SECTION B SEASONAL VARIATION OF THE POST-TWILIGHT DECAY OF OXYGEN 6300 A EMISSION

Extrait des

Annales de Géophysique

Tome 24, 1968

CHAPTER IV

SEC. A

4.1 BEHAVIOUR OF OXYGEN 6300 A EMISSION IN THE NIGHT AIRGLOW AND THE DYNAMICS OF IONOSPHERE IN LOW LATITUDES.

ÉDITIONS DU CENTRE NATIONAL DE LA RECHERCHE SCIENTIFIQUE

Behaviour of oxygen 6300 Å emission in the night airglow and the dynamics of ionosphere in low latitudes*

by S. R. PAL and P. V. KULKARNI,

Physical Research Laboratory,
Ahmedabad-9 (India).

RÉSUMÉ. — *La variation nocturne de l'émission de la raie 6300 du ciel nocturne montre fréquemment un maximum d'intensité au cours de la seconde partie de la nuit. Ce maximum est distinct du renforcement progressif de l'intensité après minuit, renforcement que suit la montée rapide pré-crépusculaire. Cette bosse « de l'intensité 6300 Å est en fait surimposée sur le renforcement d'après minuit.*

Les observations photométriques de la raie 6300 à Mt Abu (Inde) et Haleakala (Hawaï) sont en bonne corrélation avec les paramètres de la région ionosphérique F.

Le renforcement d'après minuit et la « bosse » 6300 qui lui est superposée se comprennent bien si l'on tient compte de la dynamique de la région F *nocturne, y compris les dérives verticales d'ionisation.*

ABSTRACT. — *In the nocturnal variation of the 6300 Å airglow emission, during the second half of the night, there is often observed an intensity peak which is quite distinct from the slowly rising post midnight enhancement followed by the rapidly rising predawn enhancement. This "post midnight 6300 Å hump" as a matter of fact is superimposed on the post midnight enhancement. The photometric observations of 6300 Å at Mt. Abu (India) and Haleakala (Hawaii) show good covariance with the* F *region ionospheric parameters. The post midnight enhancement and the superposed 6300 Å hump can be reasonably accounted for by considiring the dynamics of the night time* F *region including vertical drifts during those hours.*

(*) The airglow work at Mt. Abu has been assisted by AFOSR Grant No. 62-399 from Airforce Cambridge Laboratory, U. S. A. to Dr. K. R. Ramanathan. The observations at Mt.Abu were made by Mr. S. R. Pal.

K.R.R.

At Mt. Abu, India, (Geographic Lat. 24°36′ N Long. 72°43′ E, Altitude 1219 M, Geomagnetic Latitude 15°22′ N) a photoelectric photometer, pointing towards the north pole, is being operated. This photometer records, every five minutes, the intensity of nightsky radiations with optical filters with band widths of about 100 Å around 6300 Å, 5893 Å, 5577 Å, and 5350 Å. Using the "two colour method", (Barbier and Roach, 1950) absolute intensities in Rayleighs, of 6300 Å* [0I], 5893 Å (Na), and 5577 Å [0I] lines in the night airglow spectrum are calculated.

In this communication, we shall discuss observations of 6300 Å radiation only, and point to a phenomenon which is observed consistently at this station. It is necessary to give a very short review of 6300 Å airglow radiation.

BARBIER [1959] proposed for the first time that with an empirical formula, intensity of 6300 Å radiation can be calculated from ionospheric parameters and intensity thus calculated, Q_{6300}, shows good correlation with the photometrically observed 6300 Å intensity, I_{6300}.

Generally accepting the fact that the major contribution of the 6300 Å airglow radiation is due to aeronomic reactions in the F region of the ionosphere a number of workers [BARBIER, 1961*b*; BARBIER, ROACH and STEIGER, 1962; CARMAN and KILFOYLE, 1963] have shown that, at low latitude stations, good correlation is obtained between I_{6300} and Q_{6300} by adjusting the constants A and B in Barbier's formula,

$$Q_{6300} = A + Bf_0F_2^2 \exp\left(-\frac{h'F - 200}{H}\right)$$

where f_0F_2 is the critical frequency in MHz of the F layer; $h'F$ is the virtual height of F layer and H is the scale height. H is assumed to be between 38 to 42 km. Attempts have been made to derive and justify this relation theoretically [LAGOS, BELLEW & SILVERMAN, 1963; PETERSON, VAN ZANDT & NORTON, 1966].

It has been reported by BARBIER [1957] that at low latitude 6300 Å radiation level is very active sometimes showing intensity changes of one order of magnitude in a couple of hours. Similar occasional large increases have been reported by DELSEMME [1960] and STEIGER [1967].

The "classical" variation of 6300 Å airglow radiation during a night in middle latitudes has been described by a number of authors [BARBIER, 1961a; BERTHIER & MORIGNAT, 1956]. According to them, at the end of the evening astronomical twilight, the intensity of 6300 Å continues decreasing, and in a few hours reaches a value which remains more or less constant around mid-night. Before the beginning of the morning twilight, the 6300 Å radiation is again enhanced and merges into the beginning of the morning twilight. However, from Huancayo (Geomagnetic Lat. 0°.6 S) data, it has been reported [SILVERMAN & CASAVERDE, 1961] that the nocturnal variation of 6300 Å is very different from what has been described above, namely, there occurs a maximum around mid-night.

During the nocturnal variation a definite rise in intensity *before* the beginning of the morning twilight has been detected at many stations [ELVEY & FARNSWORTH, 1942; ROACH, 1955], and this phenomenon which is named as "predawn enhancement" has been discussed by CHAMBERLAIN [1961a] and recently by COLE [1965], and CARLSON [1967].

The nocturnal variation of 6300 Å at Mt. Abu is very nearly similar to that in the middle latitudes and does show similar predawn enhancement, but a distinct hump in intensity is superimposed around 4 a.m. over and above the predawn enhancement in which intensity increases continuously. Cole and Carlson's photoelectron theory explains the predawn enhancement of 6300 Å at middle latitudes but it does not account the hump structure which we have observed here. The effect of the photoelectrons from the magnetically conjugate points will be such that it will enhance the 6300 Å emission continuously till it merges into the morning twilight. In the 6300 Å hump, the intensity rises to a maximum followed by a fall before morning twilight. This cannot be explained on the basis of the photoelectron theory.

Statistically present, at Mt. Abu this hump we call as the "post midnight 6300 Å hump, or 6300 Å hump" hereafter and try to account for its occurence by considering the dynamics of the F region during those hours. The F region behaviour also apparently explains the predawn enhancement of 6300 Å emission. Similar 6300 Å humps have also been noted by Japanese workers from the data of their stations [HURUHATA, 1967]. However, at these stations the humps are weak compared to those at our station. At Haleakala (Hawaii) (Geog. Lat. 20° 43′N, Long. 156° 16′W. Geom. Lat. 20° 50′N, Long. 88° 27′W, Altitude 3 000 m) prominant post midnight 6300 Å humps were observed in individual nights. Somewhat similar behaviour of 6300 Å emission has been reported by DELSEMME [1960] at Lwiro (Geog. Lat. 02° S; Long. 28° E).

We have considered the 6300 Å airglow data at Mt. Abu for one year, December 1964 to December 1965, for this study. The observations were made using an optical filter with $\frac{\int T_\lambda d\lambda}{T_\wedge} = 138$ Å where T_λ is the transmissions of the filter at wavelength λ and

$$T_\wedge = \frac{T_1 a_1 + T_2 a_2}{a_1 + a_2}$$

(*) In the present communication all references to 6300 Å, in fact, refer to the red doublet 6300 Å and 6364 Å.

where T_1 and T_2 are the transmissions of the filter at 6300 Å and 6364 Å and a_1, a_2 their relative intensities. It is our estimate that OH (9-3) band in this region would contribute to the extent of 1/3 of its total intensity. Background elimination filter is centred at 5350 Å and has half transmission-width equal to 100 Å. Absolute intensities are calculated according to the standard two colour filter reduction method [BARBIER and ROACH, 1950].

We have also analysed Haleakala 6300 Å airglow data for one year namely December 1964 to December 1965. Haleakala airglow photometer looks at the zenith. The 6300 Å filter has $\frac{\int T_\lambda d\lambda}{T_\lambda} = 24$ Å and the 5300 Å filter has half transmission points separated by 30 Å. It may be pointed out that the 6300 Å filter of this photometer admits less than 7 % of the total OH (9-3) band intensity and thus the 6300 Å radiation is almost free from OH contamination. The Haleakala data were also reduced by the two colour method, to find out the intensity in rayleighs of the 6300 Å radiation.

We have plotted 6300 Å intensity in rayleighs vs. time for each of the available nights individually in the above period for the two stations when at least three hours of observation are available before the morning twilight. The following general properties have been noted regarding the post midnight 6300 Å hump.

(1) At Mt. Abu the 6300 Å hump was present on 80 out of 109 nights i.e. on 3/4 of the total nights. At Haleakala the 6300 Å hump was present on 55 nights out of 81, i.e. on 2/3 of the total nights.

(2) We have not yet been able to predict the occurrence of humps. On successive nights such peaks may or may not occur.

(3) When a hump is present, its time of occurrence is after mid-night and we can detect it with definiteness if it occurs before the beginning of the morning twilight.

(4) It may be noted that peaks even if they occur on successive nights may or may not occur at the same time. Considering one year's data, it may be concluded that the hump occurs around 4 a.m. at Mt. Abu while at Haleakala it is earlier by an hour or so.

(5) The width and the amplitude of the humps do not show any order or regularity.

(6) Even after averaging the data for each observing period (about 20 nights around new moon) the predawn hump shows itself; it is however somewhat flattened due to averaging of the data of many nights. This is shown in Fig. 1a *.

* Monthly average diagrams are drawn for all months in year 1965, but we have presented only four months for the sake of brevity. This is also applicable to Figs. 1b, 5a, and 5b.

Of the many reactions that have been proposed for the emission of 6300 Å [OI] radiation, the following two are of interest.

$$NO^+ + e = N^* + O^*(^1D) \tag{1}$$

$$O_2^+ + e = O^* + O^*(^1D) \tag{2}$$

It is widely accepted now that the major contribution of 6300 Å radiation is from the region around 300 km in the F region of the ionosphere. Hence it would be of interest to study the F region simultaneously, for its electron content and its vertical movements to find if they have any relation with changes in intensity of the 6300 Å radiation. We have therefore considered the data from two ionospheric stations.

(1) Delhi, India (ionospheric) for Mt. Abu (photometric) and.

(2) Maui, Hawaii (ionospheric) for Haleakala (photometric).

As the Abu photometer is looking towards the pole star (65.5° zenith angle) it intercepts the ionosphere over Delhi at about 300 km from the ground. The Haleakala photometer looks at the zenith and the ionosonde station at Maui is only a few miles away from airglow observatory. When the $f_0F_2^2$ values are plotted against the hours of nights on which photometric observations were acquired, it was

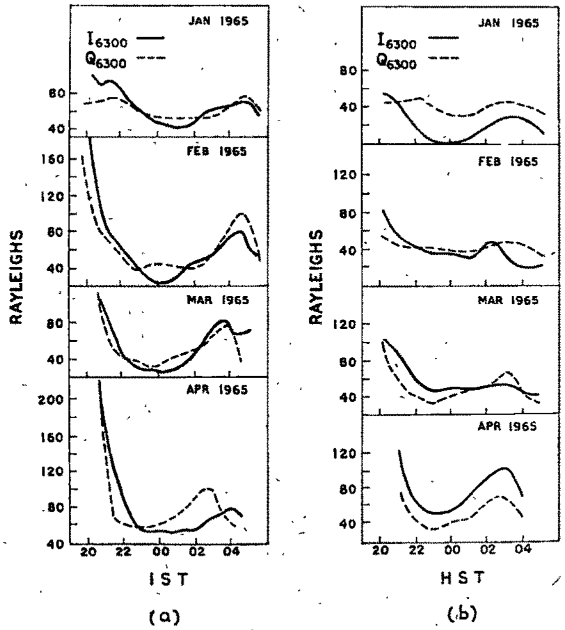

FIG. 1.

Monthly average values of I_{6300} in Rayleighs obtained from airglow observations and Q_{6300} also in Rayleighs obtained from Barbier's formula for (a) Mt-Abu (photometric), and Delhi (ionospheric); and (b) Haleakala (photometric) and Maui (ionospheric) stations.

seen that the curves showed a general similarity of variation, but did not show a good fit with the respective observed I_{6300} photometric curves. It has been pointed out [BARBIER, ROACH & STEIGER, 1962] that $h'F$ appears to be a very important factor in addition to f_0F_2. f_0F_2 with $h'F$ as given in Barbier's formula gives a good fit of the two curves (viz. Q_{6300} as obtained by Barbier's formula and I_{6300} as obtained by photometric observations). Figure 1a shows, for the data under consideration, monthly average values of Q_{6300} and I_{6300} calculated from Delhi ionosphere and Mt. Abu photometric observations. Constants A and B in Barbier's formula are adjusted for every month to get the best fit in the two curves. H was assumed to be 41 km for all these calculations. In Figure 1b similar

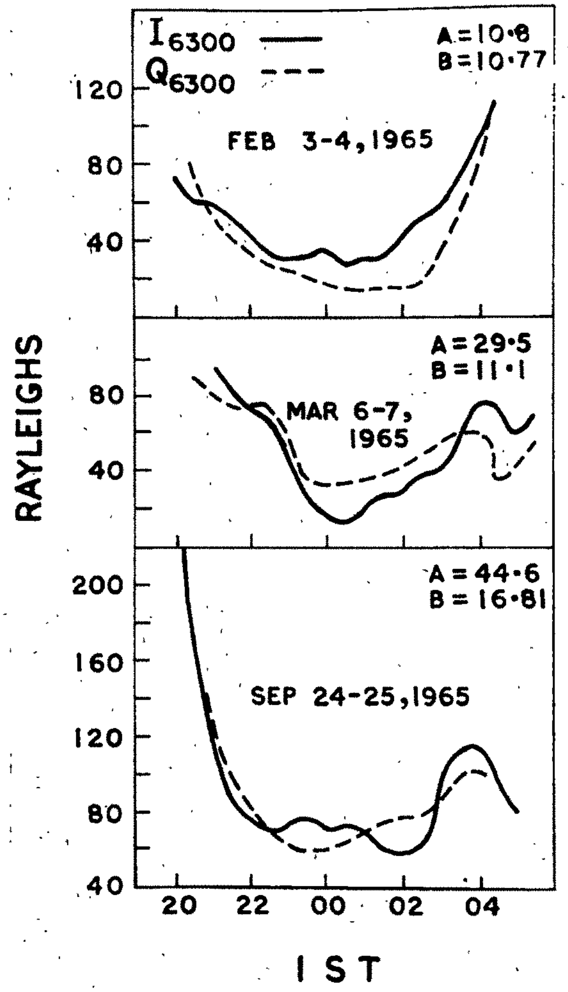

FIG. 2

Three typical nights showing variation of I_{6300} and Q_{6300} for Mt.Abu and Delhi, stations. A and B are constants in Barbier's equation.

monthly average curves of Q_{6300} and I_{6300} are drawn for Maui ionospheric and Haleakala photometric observations. In this case, numerical values of $A = 27$, $B = 4.24$ and $H = 40$ km. have been used for all the months. Figure 2 shows few individual nights on which I_{6300} and Q_{6300} are plotted against Indian Standard Time, for Mt. Abu-Delhi pair of stations. It has been pointed out [CHAMBERLAIN, 1961b] that the rate of dissociative recombination

$$NO^+ + e \rightarrow N^* + O^*(^1D) \quad \text{or} \quad O_2^+ + e \rightarrow O^* + O^*(^1D)$$

is essentially the rate at which the reaction

$$O^+ + N_2 \rightarrow NO^+ + N \quad \text{or} \quad O^+ + O_2 \rightarrow O_2^+ + O$$

of molecular ion-atom interchange proceeds. Both these reactions proceed at the same recombination rate β and depend on the concentration of N_2 or O_2 and e at the height at which the process becomes effective. For the time rate of change of electron density Ferraro has given the equation

$$\frac{\partial N_e}{\partial t} = -\beta N_e + \frac{\partial}{\partial z}\left\{D(z)\left(\frac{\partial N_e}{\partial z} + \frac{N_e}{2H_1}\right)\right\},$$

where N_e is the number of electrons per cc, β the recombination rate, H_1 the scale height of O, and $z = h - h_0$ where h_0 is some reference height. The first term on the right hand side is the loss term due to attachment of electrons while the second term is the diffusion term, which becomes important at great heights. The first term is important at lower heights. β depends on the height according to the relation

$$\beta = \beta_m \exp(-pz/H_1)$$

where $p = 0, 1$, or 2 depending on the assumption about the distribution and mixing of N_2 or O_2 and O; and β_m is the recombination coefficient at the reference height $z = 0$ and given by

$$\beta_m = \alpha N(O_2 \text{ or } N_2) \text{ at } z = 0.$$

The above equation shows that if F layer ionization descends the recombination rate increases and vice versa. From the ionospheric data (see Fig. 3) it will be seen from the values of $h'F$ that in the early hours of morning the F layer ionisation descends to lower levels. Near the lowest levels of $h'F$, the 6300 Å radiation as suggested by reaction (1) and (2) would have maximum enhancement due to enhanced recombination corresponding to high value of β. This recombination of electrons would also cause a raising of $h'F$. As $h'F$ goes up, the values of β become lower. This decreases the emission of 6300 Å radiation and produces a dip in the I_{6300} curve. This whole sequence of phenomena manifests itself as the 6300 Å hump. After this, the predawn enhancement, which had started earlier and on which the 6300 Å hump was superimposed, has a rapid rise in intensity due to the morning twilight.

To examine the behaviour of $h'F$ and its part in contributing to I_{6300}, along with f_0F_2 a study of vertical drifts of levels of maximum ionisation density in the ionosphere was made. Upward drifts will decrease the ionization density at the maximum ionization level and downward drifts will increase the ionization down to certain level below which the ionization will be destroyed by recombination, thus forming a layer at an intermediate level with increased ionization density.

The vertical drift analysis of maximum ionization density shows that during the night, there are upward (positive) as well as downward (negative) vertical drifts. With increasing positive vertical drift the ionization density at h_{max} would go on decreasing. When the positive drift decreases and changes to negative the ionization maximum would move downwards, thus causing an increase in the ionization density at h_{max}.

The descent of h_{max} and increased ionization density would supply more ionization at $h'F$ (the lower boundary of F layer) causing greater recombination of O_2^+ and NO^+ at lower levels. This increased recombination will increase the number of excited oxygen atoms and produce greater emission of the oxygen red lines. It may be seen from the ionospheric observations that $h'F$ actually decreases at this time, thus showing good anticorrelation with I_{6300}. Recently, BARBIER [1964] has made the following remark, "The variability of altitude (of 6300 Å emission layer) in low latitudes is quite real and is in correlation with the altitudes of the base of the F-layer".

Numerical analysis of the vertical drifts from the

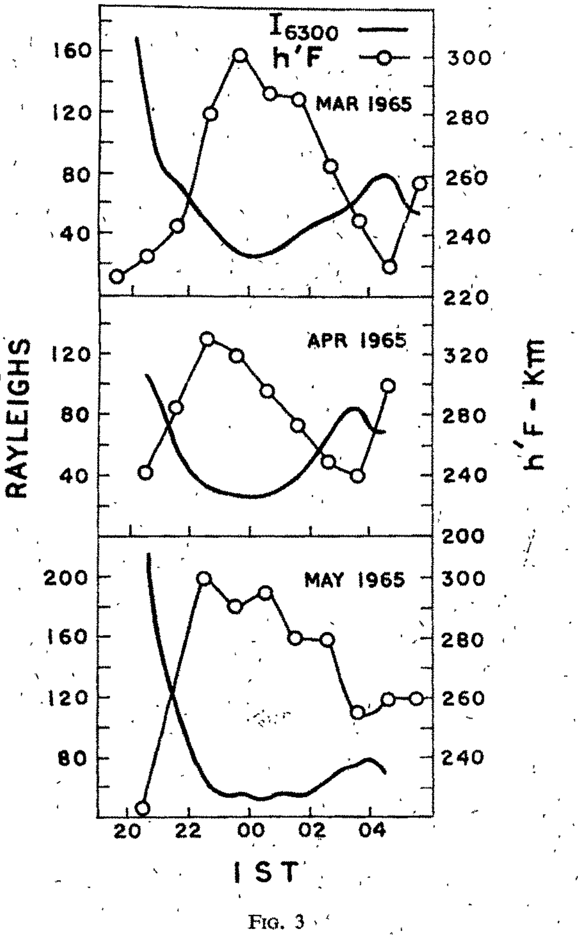

FIG. 3

Monthly average I_{6300} and $h'F$ for three typical months at Mt.Abu-Delhi.

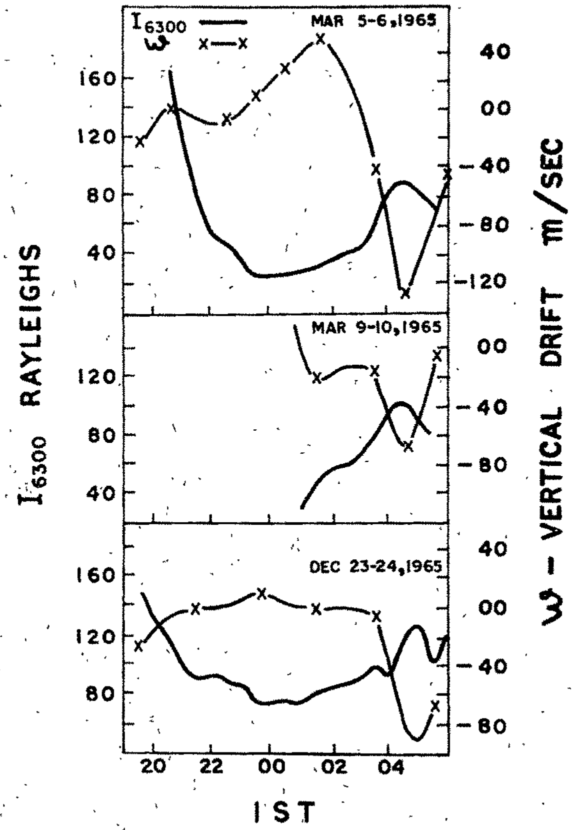

FIG. 4

Nocturnal variation of I_{6300} in Rayleighs and ω the vertical ionospheric drift in m/sec. for three typical nights at Mt.Abu and Delhi.

ionospheric data at Delhi and Maui on a few typical nights and for the monthly averages for one year (1965) was done from the method outlined by HANSON and PATTERSON [1964] and recently used by DEGAONKAR and SANATANI [1966]. Naturally, we have selected the periods when ionospheric as well as photometric data were available. In Fig. 4 are shown the nocturnal variations of I_{6300}, and ω, the vertical ionospheric drift in m/sec for three typical nights. Figures 5a and 5b show the average monthly nocturnal variation of I_{6300}, $f_0F_2^2$, and ω for Mt. Abu-Delhi and Haleakala-Maui during the year under consideration. Figures 6a and 6b show the

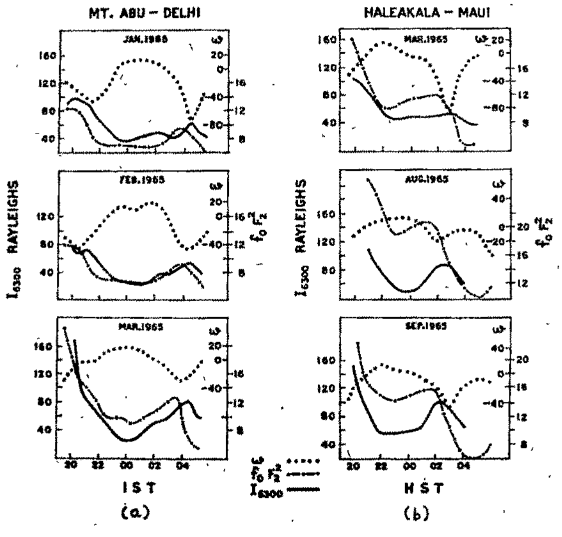

FIG. 5

The average monthly nocturnal variation of I_{6300}, $(f_0F_2)^2$, and ω for (a) Mt.Abu and Delhi; and (b) Haleakala and Maui, stations.

yearly average of the same variables at the two pairs of stations. The $f_0F_2^2$ taken together with ω curves may possibly explain the predawn enhancement and the predawn hump. First we describe the behaviour of the $f_0F_2^2$ and ω curves individually, and then consider them together to explain the predawn enhancement and the 6300 Å hump in the I_{6300} curve.

It will be seen from Figure 6a that:

a) Except during the early hours of night when the vertical drifts are negative they are increasingly positive up to midnight; then they become less positive and change to negative. The maximum negative drift is reached before dawn.

b) The $f_0F_2^2$ decreases before midnight. After midnight it starts gradually increasing, has a broad maximum around 0330 IST then decreases rather fast for an hour or so and then increases rapidly due to the layer sun-rise.

The downward vertical drifts after midnight bring more and more ionisation to lower levels, thus increasing f_0F_2. At this time $h'F$ also lowers. The increase in f_0F_2 which is accompanied by greater negative drifts can not go on indefinitely because below a certain height the loss of electrons by recombination predominates causing a rapid fall in f_0F_2 (shown as point A in Figure 6a). At this time a maximum in $f_0F_2^2$ curve is exhibited. It has already been stated that ω continues to have increasingly negative values causing f_0F_2 to decrease, but this increases recombination of electrons down to $h'F$ and increases the intensity of 6300 Å. This increase of I_{6300} continues to a point where $d\omega/dt = 0$ (shown as point B in Figure 6a). After this point due to the relatively upward direction of the drift (i.e. decreasing negative) the ionization density decreases, correspondingly lowering the rate of recombination and causing a fall in I_{6300} shown by C-D in Figure 6a.

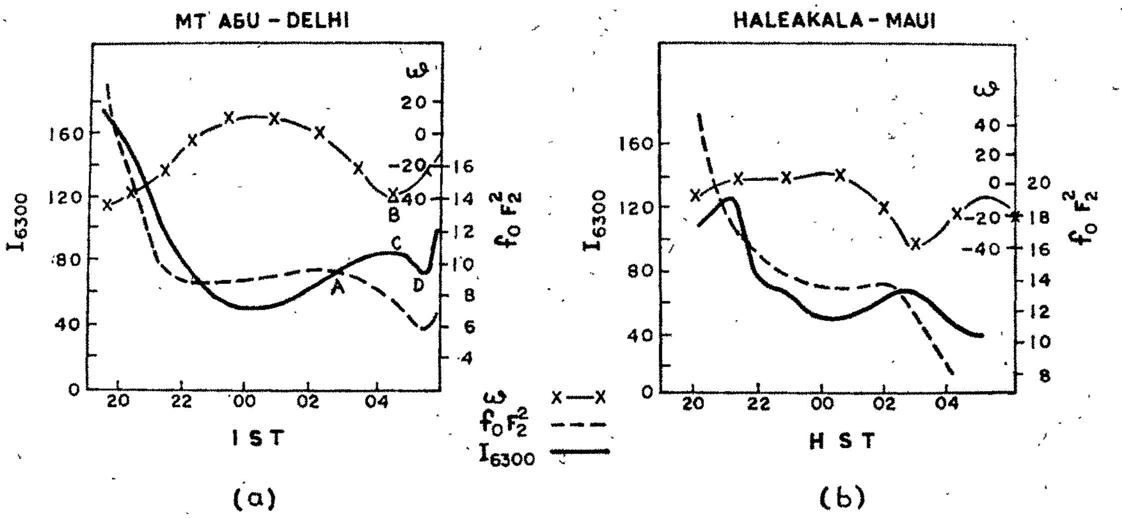

FIG. 6

Yearly nocturnal average of I_{6300}, $(f_0F_2)^2$ and ω at (a) Mt.Abu and Delhi; and (b) Haleakala and Maui Stations.

In this series of events the increase in f_0F_2 after midnight would correspond to the predawn (or post mid-night)enhancement, and the maximum in f_0F_2 to the beginning of 6300 Å hump, while the point $d\omega/dt = 0$ would correspond to the peak of 6300 Å hump.

At two airglow stations, Mt. Abu and Haleakala, the average times of occurrence of the 6300 Å humps are different. Before trying to account for this difference it is necessary to study the 6300 Å hump at more stations.

ACKNOWLEDGMENTS

Our thanks are due to Professor K. R. Ramanathan for making available to us equipment and other facilities for the airglow work at Mt. Abu and for critically going through the manuscript.

We also thank Dr. W. R. Steiger for kindly placing at our disposal 6300 Å airglow data from Haleakala and the authorities of the Maui Station for ionospheric data. One of the authors (PVK) studied the Haleakala-Maui data when he was guest scientist at the Hawaii Institute of Geophysics, University of Hawaii, Honolulu (Hawaii) U.S.A. during September 1966 to January 1967. We also wish to express our thanks to Mr. P. D. Angreji for his assistance during the preparation of this manuscript.

Manuscrit reçu le 26 janvier 1968.

RÉFERENCES

BARBIER D., « La lumière du ciel nocturne en été à Tamanrasset », *C.R. Acad. Sci.*, **254**, 1559-1561, 1957.

BARBIER D., « Recherches sur la raie 6300 de la luminescence atmosphérique nocturne », *Ann. Géophys.*, **15**, 179-217, 1959. (Also, reference above).

BARBIER D., « Les variations d'intensité de la raie 6300 A de la luminescence nocturne », *Ann. Géophys.*, **17**, 3-15, 1961a.

BARBIER D., « L'émission de la raie rouge du ciel nocturne et les propriétés de la couche *F* de l'ionosphère », *C.R. Acad. Sci.*, **252**, 3315-3316, 1961b.

BARBIER D., *Research in Geophysics*, (Ed. H. Odishaw) The M.I.T. Press, Cambridge, U.S.A., **1**, 406, 1964.

BARBIER D., ROACH F. E. and STEIGER W. R., "The summer intensity variation of OI 6300 A in the tropics," *J. Res. Nat. Bur. Std.*, **66D**, 145-152, 1962.

BERTHIER P. and MORIGNAT B., « Variations d'intensité des raies 6300, 5893 et 5577 A et des bandes rouges de **OH** au cours de quelques nuits et rapport des intensités des raies 6300 et 5577 A de [OI] », *Airglow and Aurora* (Ed. E. B. Armstrong and A. Dalgarno) Pergamon Press, London, 60-62, 1956.

CARLSON Jr. H. C., "Preliminary observation of 6300 A predawn enhancement at Arecibo," *Aurora and Airglow* (Ed. Billy M. McCormac) Reinhold Publishing Corporation, New York, 643-647, 1967.

CARMAN E. H. and KILFOYLE B. P., "Relationship between [OI] 6300 A zenith airglow and ionospheric parameters f_0F_2 and $h'F$ at Townsville," *J. Geophys. Res.*, **68**, 5605-5607, 1963.

CHAMBERLAIN J. W., *Physics of Aurora and Airglow*, Academic Press, New York, 385. 1961a.

CHAMBERLAIN J. W., *Physics of Aurora and Airglow*, Academic Press, New York, 524, 1961b.

COLE K. D., "The predawn enhancement of 6300 A Airglow." *Ann. Geophys.*, **21**, 156-158, 1965.

DEGAONKAR S. S. and SANATANI S., "Vertical drifts in the night time ionosphere," *Planet. Space Sci.*, **14**, 459-467, 1966.

DELSEMME A. and D., « La raie rouge du ciel nocturne à l'équateur », *Ann. Géophys.*, **16**, 507-524, 1960.

ELVEY C. T. and FARNSWORTH A. H., "Spectrophotometric observations of the light of night sky," *Astrophys. J.*, **96**, 451-467, 1942.

HANSON W. B. and PATTERSON T. N. L., "The maintenance of the night time F-layer," *Planet. Space Sci.*, **12**, 979-997, 1964.

HURUHATA M., Personal communication, 1967.

LAGOS P., BELLEW W. and SILVERMAN S. M., "The Airglow 6300 A [OI] emission: Theoretical consideration on the luminosity profiles," *J. Atmos. Terr. Phys.*, **25**, 581-587, 1963.

PETERSON V. L., VAN ZANDT T. E. and NORTON R. B., "*F*-region nightglow emissions of Atomic oxygen," *J. Geophys. Res.*, **71**, 2255-2265, 1966.

ROACH F. E., "A review of observational results in airglow photometry," *Ann. Geophys.*, **11**, 214-231, 1955.

ROACH F. E. and BARBIER D., "The height of emission layers in the upper atmosphere," *Trans. Amer Geophys. Union*, **31**, 7-12, 1950.

SILVERMAN S. M. and CASAVERDE M., "Behaviour of the 6300 [OI] line at Huancayo," *J. Geophys. Res.*, **66**, 323-326, 1961.

STEIGER W. R., "Low latitude observations of airglow," *Aurora and Airglow* (Ed. Billy M. McCormac) Reinhold Publishing Corporation, New York, 419-433, 1967.

4.2 Dependence of 6300 Å hump on position of Sun

We have examined the 6300 Å data to see whether the beginning, epoch and the end of the '6300 Å hump' are dependent on the position of Sun below horizon. Our conclusion is negative.

4.3 Latitude effect on 6300 Å hump

We have noted that the 6300 Å emission hump is very intense at Haleakala as compared to that at Mt.Abu. The observations made with the all-sky scanning photometer at Mt.Abu help us to understand this difference in magnitude of the 6300 Å hump at the two places.

The scanning photometer at Mt.Abu scans the sky at 75°, 70°, 60°, 40° and 0° zenith angles. If the layer emitting 6300 Å radiation is considered to be at 300 km altitude, the scans cover the latitude range 7.7° North and South of Mt.Abu (24.6°N). It is therefore possible to make a study of the latitude variation in 6300 Å intensity between approximately 17°N and 32°N latitude at the longitude of Mt.Abu.

The observations of two very clear nights, April 12-13, 1967 and May 10-11, 1967 have been reduced to local zenith intensities in Rayleighs taking due account of extinction and scattering and have been used in this study. The nocturnal variation of 6300 Å intensity for local zenith for latitudes corresponding to Mt.Abu zenith angles 0° to 75° are plotted in Fig.4.7 which show that 6300 Å hump was present at all

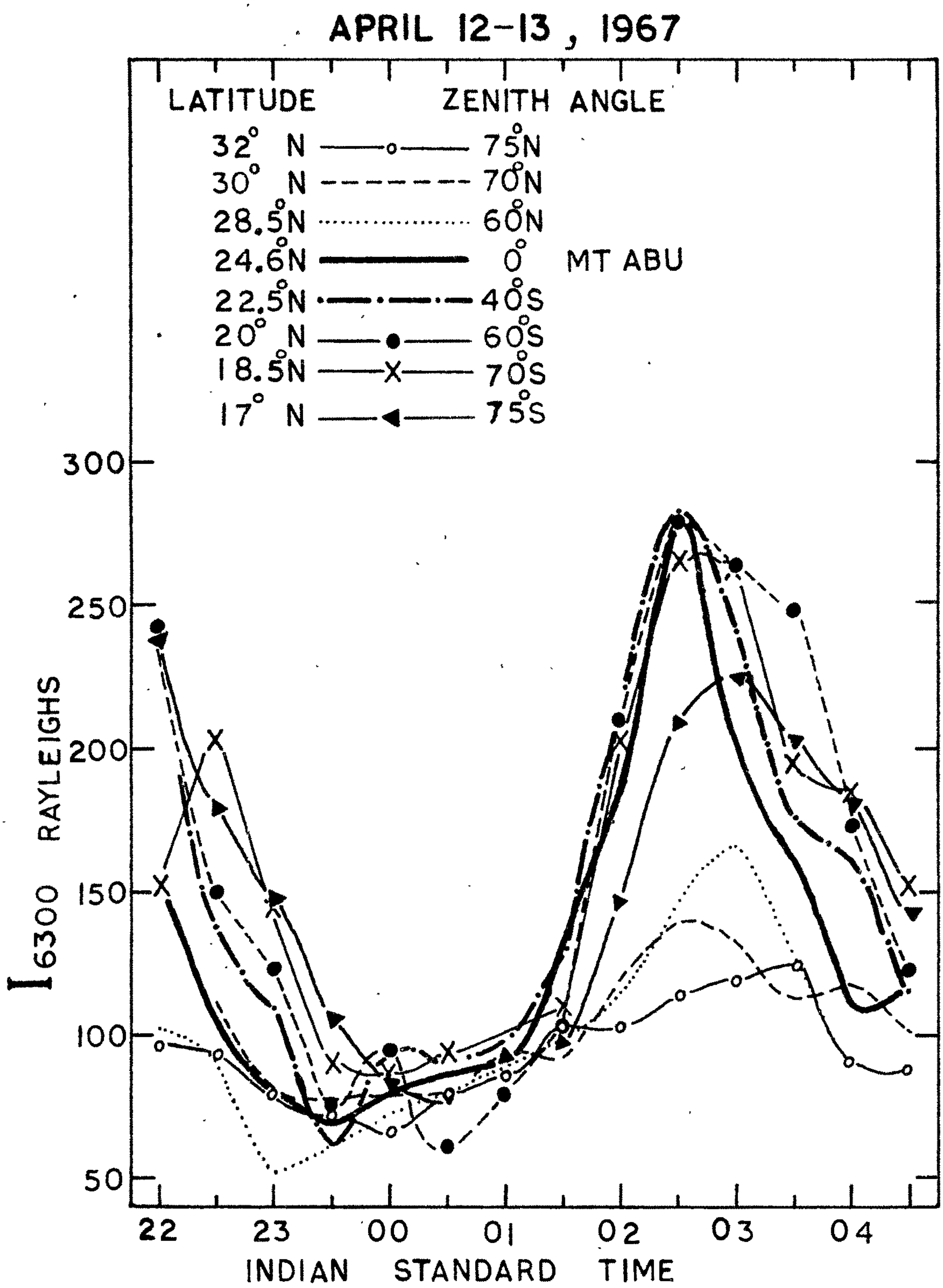

FIG.4.7. Nocturnal Variation of I_{6300} at different Latitudes.

latitudes between $17^{O}N$ to $32^{O}N$ and that it was most pronounced between $20^{O}N$ and $25^{O}N$.

If activity distribution of 6300 A emission is likewise in the zone of Haleakala longitude also, one would expect higher intensity associated with the 6300 A humps observed at Haleakala ($20^{O}N$) as compared to those at $30^{O}N$ latitude. Our observations at Mt.Abu, towards pole star correspond to nearly $30^{O}N$ latitude. Thus, the study of these nights at least gives an indication that difference in activity of 6300 A at different latitudes could be responsible for higher magnitude humps at Haleakala and for lower magnitude humps in our observations. The night of May 10-11, 1967 also shows a similar behaviour as the night of April 12-13, 1967 did.

SECTION B

4.4 Seasonal variation of the post-twilight decay of oxygen 6300 Å emission

4.41 Introduction

The study of the intensity variations of 6300 Å emission in the post-twilight period gives some useful information about the upper atmosphere. In the present section we shall bring out the following points from our observations of 6300 Å emission with the help of pole photometer at Mt.Abu.

(1) The post-twilight intensity variation curves as observed at Mt.Abu, fit reasonably well with Chamberlain's (1958) post-twilight decay theory.

(2) Using appropriate parameters (which are calculated in the present study) the different post-twilight decay rates as observed at Mt.Abu in different periods of the year, can be calculated from Chamberlain's theory.

In the following, a brief out-line of Chamberlain's theory and the parameters involved in the formula employed for the computation, are given.

4.42 Theory

The dissociative recombination processes (1) and (2) in the F-region of ionosphere are perhaps the most important sources for the emission of the red lines of atomic oxygen.

As regards reaction (1), Chamberlain in his book on 'Physics of the Aurora and Airglow' (1961c) expresses the opinion, "it now appears that the reaction with N_2 is generally more important (than with O_2)".

O_2 and N_2 are in diffusive equilibrium in the F-layer, and the variation of these constituents with height would be nearly identical (Chamberlain 1961c).

The theory is based mainly on the following assumptions. (a) The condition of ionization in the layer under consideration is static or changes slowly and (b) at the time of sunset, the distribution of ionization is uniform near the level of 6300 Å emission and the diffusion of ionization can be neglected.

Then the rate of red line emission, per cm^3 per sec. as a result of reaction (1), is integrated over the vertical column and the final relation gives the intensity of 6300 Å emission in Rayleighs. The relation is as follows :

$$Q_{6300} = F_D N_e^o H_2 / t$$

Here N_e^o is the uniform electron density in the F-layer at the time of layer sunset ($t = 0$), H_2 is the scale height of N_2 molecules (or O_2 molecules) and t is the time in seconds after layer sunset. The factor F_D is the efficiency factor of the reaction (1) leading to $O(^1D)$ production. Its value has been assumed here to be 1.

For calculating 6300 Å emission from the above equation, instead of assuming values of N_e^o and H_2, they have been computed in the following way. The assumption of replacing N_e^o by N_{em}^o has been made here.

4.43 Determination of N_{em}^o and H_2

The electron density at the time of sunset is calculated from the following formula :

$$N_{em}^o = 1.24 \times 10^4 \, (f_oF_2)_o^2$$

where $(f_oF_2)_o$ is the critical frequency of the F-layer at layer sunset. The end of evening twilight is taken as the time of the layer sunset.

Our photometer is pointing towards the pole-star. Its line of sight intercepts the atmospheric layer at about 300 km altitude over Delhi (28°38'N, 77°13'E). The ionospheric data of Delhi are therefore taken for the computations in the present study.

The average values of f_oF_2 on the dark nights of observation corresponding to the mean time of the end of astronomical twilight for the geographic latitude 30°N were noted.

To calculate H_2 for the corresponding periods, equation of Harris and Priester (1962), which connects H_2 with the solar radio flux on 10.7 cm and local time was used.

It has been observed that around sunset the values of H_2 do not vary very much within one hour. The H_2 values calculated for the heights corresponding to electron density maximum, at 1900 LMT were used in the present computations. Only a single averaged time corresponding to the end of astronomical twilight was considered for each observing period which is about 18-20 days a month. The values of N_e^o and H_2 and the average time when the astronomical twilight ends are tabulated in Table 4-I.

4.44 Discussion

The calculated and observed curves have been compared for lunations in different seasons. The theory is found to fit well with observations. For the sake of brevity, we represent here the results for four typical lunations in which, relatively fast and slow post-twilight decay rates are associated. Figs.4.8 (a,b) represent the curves from our observations and those calculated from the above mentioned theory; for two lunations in which the mean rates of decay of 6300 Å emission in the post-twilight period were fast (April and September-October) and Figs.4.9(a,b) represent the rates of decay in two lunations when they were small (February-March and March-April).

4.45 General remarks

The sun does not set simultaneously over the whole F-layer and therefore the computed values may not be expected

TABLE 4-I

Lunation	Time of the end of evening twilight as on	at IST	f_oF_2 Mc/S at the end of twilight	N^o_{em} cm^{-3} $x10^5$	H_2 km
Jan.24-Feb.11,1965	Feb. 1	1919	3.67	1.67	19.1
Feb.21-Mar.10,1965	Mar. 3	1941	4.95	3.04	18.3
Mar.24-Apr.11,1965	Apr. 2	1958	4.85	2.92	18.1
Apr.22-May 9,1965	May 1	2022	4.95	3.04	17.5
Jan.11-Feb. 1,1966	Jan.21	1907	3.66	1.66	21.4
Feb.10-Mar. 2,1966	Feb.20	1930	4.67	2.70	20.3
Mar.12-Mar.31,1966	Mar.22	1952	5.82	4.20	21.0
Apr. 9-Apr.29,1966	Apr.20	2012	6.70	5.57	21.0
May 1965	May 15	2056	6.50	5.24	18.1
September 1965	Sep.15	2003	5.00	3.10	18.5
October 1965	Oct.15	1935	3.90	1.89	19.0
November 1965	Nov.15	1907	3.50	1.52	19.0
December 1965	Dec.15	1908	3.47	1.47	19.0

(1) f_oF_2 values for the last five lunations have been calculated from the monthly median values of f_oF_2.

(2) All other f_oF_2 values are average values for the lunations.

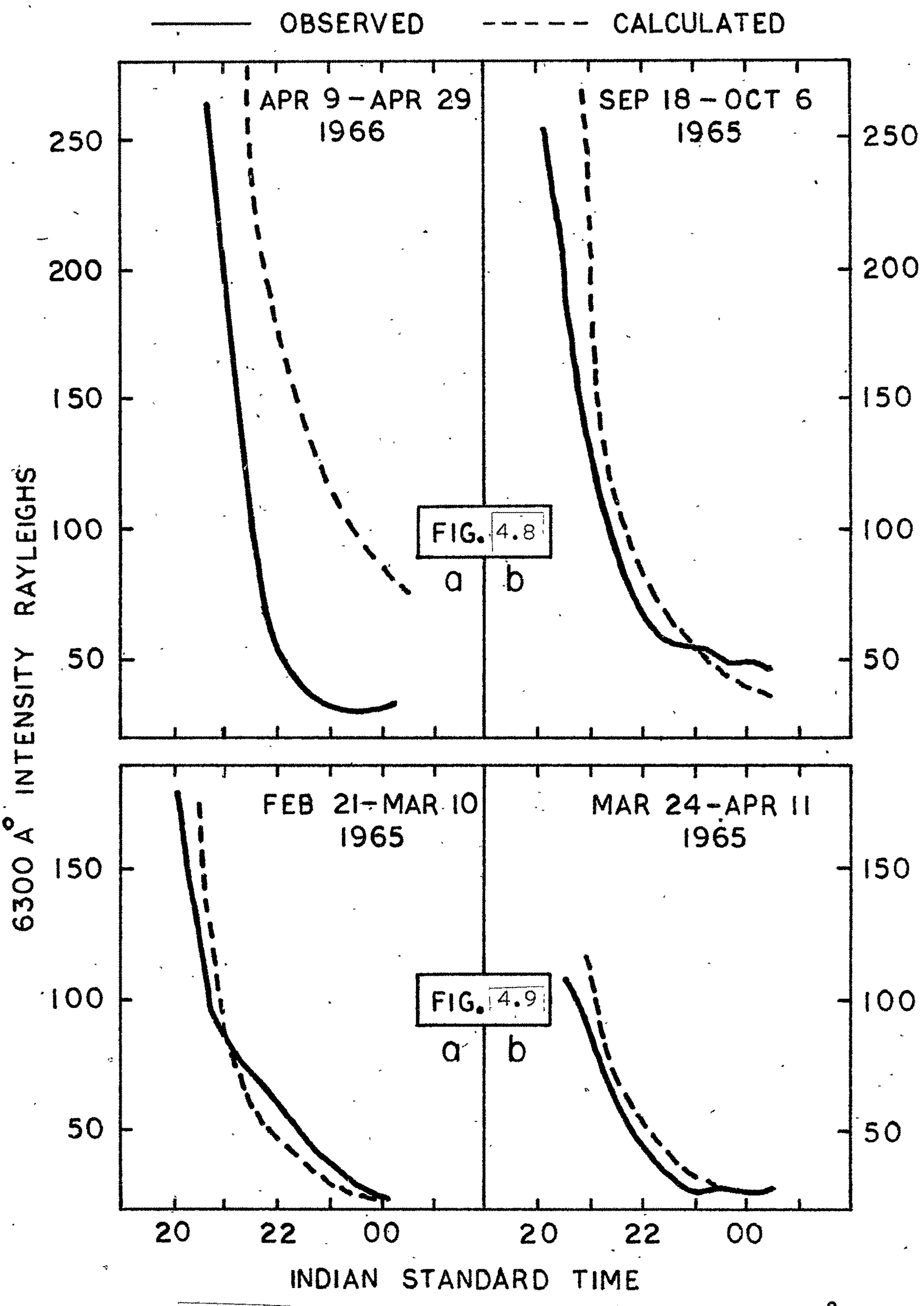

FIG. 4.8 , 4.9. POST TWILIGHT DECAY OF 6300 Å

to agree with observations near t = 0, the assumed time of sun set. It is also not quite correct to assume a uniform distribution of electrons with height over the whole range of the F-layer at the time of sun-set. However, if the assumption of uniformity of ionization is made for the time 10^2 to 10^3 sec. after sun set, for the region below the F-layer peak (from where the main 6300 Å emission is produced), one may not be far from reality. The calculated values at 10^3 sec after layer sunset (as Chamberlain suggested) have been retained in the present study.

Some differences between calculated and observed curves have been found; these may be due to the fact that f_oF_2 values at the time of layer sunset were not available for a few days for which 6300 Å radiation was recorded. In some cases, ionospheric data did not cover exactly the dark period of the month for which airglow data were available. In such cases, the monthly median values of f_oF_2 were accepted. In all cases, however, similar trend of variation in the calculated and observed curves can be seen.

In some months, the observed curve changes its original rate of post twilight decay of intensity. This can be due to a short lived hump structure superposed on the post-twilight decay. This type of perturbation in the smooth post-twilight decay of red line emission is caused either by a sudden rise of electron density or a sudden lowering of F-layer height, causing the F-layer ionization to depart from static conditions. In such a case the initial value of electron density, N_{em}^{o} used in the decay calculations would lose its significance and the assumption of a static condition of the ionosphere would not hold. The present study of post-twilight decay of red emission, has the limitation that dynamic processes leading to a change in the vertical distribution of ions are not taken into account.

4.46 Conclusions

From the analysis of two years data of 6300 A airglow it is apparent that the seasonal variations in the rates of post-twilight decay are caused by seasonal variations in N_e^o and H_2. The seasonal variation of f_oF_2 following the hours of sun-set seem to be responsible for the post-twilight decay rates. The variations in f_oF_2 at sun-set hours can be used to forecast changes in the post-twilight decay curves.

On the whole, the seasonal variation in the post-twilight fall of intensity of red lines of atomic oxygen supports the theory of formation of $O(^1D)$ by dissociative recombination of NO^+ and O_2^+.

CHAPTER V

THE VERTICAL LUMINOSITY PROFILE OF 6300 A AND THE LATITUDE DISTRIBUTION OF 6300 A INTENSITY AT MIDNIGHT

Following is the plan of Chapter V

(a) It was found by Lagos et al (1963) that the vertical luminosity profile of 6300 Å is below the ionization profile and the difference in the levels of profile maxima depends on the scale heights of O and O_2. The relevent equation derived by them for this difference of level is given. If 'ambipolar diffusion' of ionization is considered as an additional factor to be taken into account the difference in the altitudes of the two profile maxima is found to depend not only on the scale heights of O and O_2, but also on β_m the recombination coefficient, and D_m, the diffusion coefficient, both at ionization maximum. Since D_m is a function of the dip angle, the difference in the levels of luminosity maximum and ionization maximum at a place will depend on the dip angle at that place.

(b) Ambipolar diffusion also requires that there should be a latitude shift in luminosity maximum with respect to the ionization maximum, as the movement of ionization is controlled by the lines of magnetic force. The expression for this latitude shift expressed as a change in dip angle dI has been derived.

(c) Using expressions for $\beta(z)$ the recombination coefficient and $N_e(z)$ the electron density distribution, the emission of 6300 Å at one place for its appropriate dip angle was computed theoretically, and by changing the value of the dip angle in D_m the diffusion coefficient, the distribution of total 6300 A emission for 5^o to 85^o magnetic dip latitude was obtained. The results are compared with the latitude distribution of 6300 A emission observed on board the Altanin (1962).

(d) The effect due to a variation of h_m on the latitude distribution of 6300 A, has also been examined.

CHAPTER V

THE VERTICAL LUMINOSITY PROFILE OF 6300 A AND THE LATITUDE DISTRIBUTION OF 6300 A INTENSITY AT MIDNIGHT

5.1 Introduction

The association of the intensity of the forbidden lines of atomic oxygen at 6300-6364 A with the parameters of the ionospheric F-layer is now well-known (Barbier 1959a, Packer 1961). A mechanism of excitation of these lines through dissociative recombination of NO^{+} and O_2^{+} ions and electrons was suggested by several authors (Nicolet 1954, Chamberlain 1958, Lagos et al 1963). Recently, a refined theory was given by Peterson et al (1966). It is now evident that the emission depends mainly on the concentration of ions, and hence also on electrons in the F-layer, and it is important to know how the ionization is distributed with height and how it changes with time.

Lagos et al (1963) have derived an expression for the volume emission rate ϵ of 6300 A radiation. They have assumed an α-Chapman distribution of electrons in the ionosphere, that is,

$$N_e = N_{em} \exp \tfrac{1}{2}\left[1 - z/H_1 - \exp(-z/H_1)\right] \qquad (1)$$

where $\quad z = h - h_m \qquad (2)$

H_1 = scale height of atomic oxygen.

h_m = height of the maximum electron density.

N_{em} = maximum electron density.

For the concentration of the diatomic molecules $N(X_2)$, (X_2 may be O_2 or N_2) the exponential function

$$N(X_2) = N_m (X_2) \exp(-z/H_2) \qquad (3)$$

is used, where

$N_m(X_2) = N(X_2)$ at h_m.

and H_2 = scale height of the molecule X_2.

Equations (1) and (3) were used for finding the volume emission rate of 6300 A, from which they derived an expression for the difference between the levels of N_{em} and ϵ_m, the maximum volume emission rate of red line emission. The relation is

$$h_m - h_{m\epsilon} = H_1 \ln (1 + 2H_1/H_2) \qquad (4)$$

The right hand side of equation (4) gives the depth of luminosity maximum below the electron density maximum. The difference in levels depends on H_1 and H_2, the scale heights of O and of O_2 or N_2.

5.2 Ambipolar diffusion of ionization

In the above treatment, the effect of ambipolar diffusion of ionization has not been considered. The red line luminosity is affected not only by recombination of ionization but also by ambipolar diffusion and other motions of ions and electrons. We shall now examine the problem of finding ϵ and the depth of the level of luminosity maximum below that of ionization maximum.

Ferraro's equation for electron density in the F-region (Chamberlain 1961d) is

$$\partial N_e / \partial t = -\beta(z) N_e + \partial / \partial z \left[D(z) (\partial N_e / \partial z + N_e / 2H_1) \right] \tag{5}$$

Here $\beta(z)$, the recombination rate is given by

$$\beta(z) = k N_m (O_2 \text{ or } N_2) \exp(-pz/H_1) \tag{6a}$$

$$= \beta_m \exp(-pz/H_1) \tag{6b}$$

where β_m refers to h_m and k is the rate of the reaction producing dissociative recombinations.

p = 0 corresponds to uniform distribution of molecules

p = 1 gives perfect mixing of the molecules with atomic oxygen.

p = 2 gives diffusive equilibrium for O_2 which is close to that of N_2.

H_1 = Scale height of atomic oxygen.

D(z) is the coefficient of diffusion of O^+ ions through O. D(z) is mildly dependent on temperature and inversely proportional to the gas density.

$D(z)$ is derived by Dalgarno (1958) as,

$$D(z) = D_m \exp(z/H_1) \quad cm^2/sec \tag{7a}$$

$$\text{where } D_m = 2.3 \times 10^{18} \sin^2 I/N_m(O) \tag{7b}$$

and I is the dip angle at the place. D_m is the diffusion coefficient of O^+ at h_m and $N_m(O)$ is the atomic oxygen concentration at h_m.

The solution of equation (5) has been discussed by Chamberlain (1961e).The general expression for a Chapman electron distribution with $p = 1$ (perfect mixing of molecules with atomic oxygen) is given by,

$$N_e(z) = \text{constant.} \exp(-z/2H_1) \exp\left[-H_1(\beta_m/D_m)^{\frac{1}{2}} \exp(-z/H_1)\right]$$

or (8)

$$N_e(z) = N_{em} \exp\left[H_1(\beta_m/D_m)^{\frac{1}{2}} - z/2H_1 - H_1(\beta_m/D_m)^{\frac{1}{2}} \exp(-z/H_1)\right] \tag{9}$$

where $N_{em} = N_e(z)$ at $z = 0$ $(h = h_m)$.

Here the electron distribution N_e is dependent on the magnetic inclination, through the factor D_m (equation 7b).

Using equations (9) and (6b) and deriving the condition for luminosity maximum we get the difference in the levels of maximum of electron density and of maximum luminosity as

$$h_m - h_{m\epsilon} = H_1 \ln\left[(3/2H_1)(D_m/\beta_m)^{\frac{1}{2}}\right] \tag{10}$$

comparing this equation with equation (4), one notices that the depth of luminosity profile depends on H_1, β_m and D_m. Since the diffusion coefficient depends on the angle of dip I, the depth of maximum luminosity will depend also on the dip of the place. From equation (10) it is evident that for the same h_m the difference in the electron density maximum and the luminosity maximum is larger for the higher dips. As h_m varies with local mean time and with latitude, the factors β_m, D_m and H_1 appearing in (10) are also affected.

When the ambipolar diffusion of ionization is considered along with other factors, it can be shown that the two maxima have a latitude shift also, and that the corresponding points of maximum electron density and maximum luminosity will be connected by a geomagnetic line of force.

To determine this latitude shift in terms of the angle of dip we proceed as follows.

Let us consider a geomagnetic line of force ss' as shown in Fig.5.1. The points E and L are in the ionization maximum and luminosity maximum respectively. Let the radius vector at the point E be r (from the centre of the earth 0) and the geomagnetic latitude be θ. The L and E are connected by magnetic line of force and are displaced radially by dr and latitudinally by an angle dθ. The equation of the line of force ss' is

$$r = K \cos^2\theta \tag{11}$$

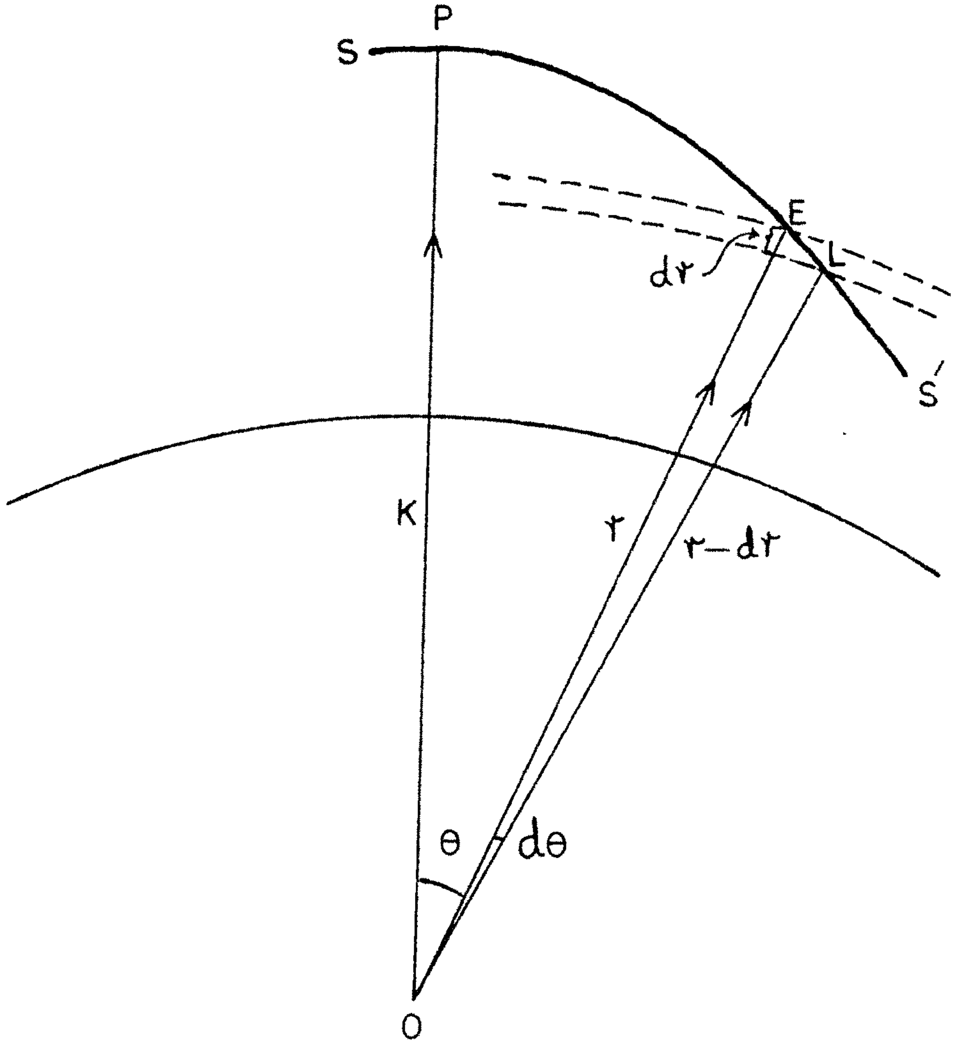

FIG.5.1. Showing the conjugate points, E in ionization maximum and L in 6300 A luminosity maximum on a geomagnetic line of force ss'.

where K is the radius vector of the line of force at the geomagnetic equator. From (11) we get

$$-dr = 2K \cos\theta \,.\, \sin\theta \, d\theta$$

then

$$h_m - h_{m\epsilon} = 2K \cos\theta \sin\theta \, d\theta \qquad (12a)$$

$$= 2r \tan\theta \, d\theta \qquad (12b)$$

comparing (12b) and (10) we get

$$d\theta = (H_1/2r \tan\theta) \ln\left[(3/2H_1)(D_m/\beta_m)^{\frac{1}{2}}\right] \qquad (13a)$$

Using (7b),

$$d\theta = (H_1/2r \tan\theta) \ln\left[2.274\text{x}10^9 \sin I \,/H_1\sqrt{N_m(0)\beta_m}\right] \qquad (13b)$$

$$=(H_1/2r \tan\theta) \ln\left[\left(2.274\text{x}10^9/H_1\sqrt{N_m(0)\beta_m}\right)\sqrt{4 \sin^2\theta/(1+3 \sin\theta)}\right] \qquad (13c)$$

Converting θ in terms of I from the relation 2tanθ = tanI we get,

$$dI = \left\{H_1(3\cos^2 I + 1)/2r \tan I\right\} \ln\left[2.27\text{x}10^9 \sin I/H_1\sqrt{N_m(0)\beta_m}\right] \qquad (14)$$

A sample calculation with solar flux S = 90 appropriate to the year 1962, needed for computing O and N_2 profiles under the square root sign shows that for a typical value of h_m equal to 380 km the displacement of dip angle is 2.3° for a dip angle of 15°.

5.3 Computation of red line intensity over latitudes

The volume emission rate of the red line of atomic oxygen, in the absence of collisional deactivation, is given by the expression (Chamberlain 1961f),

$$\epsilon(z) = F_D . \beta(z) . N_e(z) \tag{15}$$

The factor F_D is the efficiency factor for the formation of ^1D per dissociative recombination.

At night it is necessary to consider $N_e(z)$ according to the recombination diffusion equation. Diffusion continues to bring down ions to lower levels where recombination proceeds throughout the night. For simplicity we use equation (9), with p = 1. The integration of (15), between appropriate limits and taking into account all the recombinations contributing to sky brightness in 6300 Å gives the photon emission in a vertical column. To get the integrated emission Q_{6300} at different latitudes, the dip angle I included in D_m is varied at convenient intervals.

5.4 Procedure and Assumptions

For computing Q_{6300}, one uses the values of $N_m(N_2)$, $N_m(O)$ and H_1. The atmospheric model by Harris and Priester (1962) was adopted for computing these parameters. It was convenient to make the calculations using IBM 1620 computer. In the calculations, the time-dependent temperature profiles of Harris and Priester (1962) were used. The temperature profile which is dependent on the solar activity index S, the 10.7 cm solar radio noise flux, corresponds to an average value S = 90 for the year 1962. This year was chosen with the idea that the final calculations could be compared with the observations made on board the Altanin in the same year (Davis and Smith, 1964).

There is a wide range of variation in 6300 A emission during the post-twilight period and there is also a seasonal difference in the layer sunset times. There can also be large changes of intensity in different latitudes. But one can reasonably assume that the night conditions are well set around midnight. Therefore for simplicity, the computations of 6300 A emission at 0000 LMT only were made.

After the substitution of $\beta(z)$ and $N_e(z)$ from equations (6a) and (9) the integration of (15) appears in the final form as

$$Q_{6300}(\text{Rayleighs}) = (2F_D/3)\,k\,N_m(N_2)\,N_{em}\times 10^{-6}\int_{h_1}^{h_2}\exp(Z)\,dh \qquad (16)$$

where

$$Z = H_1(\beta_m/D_m)^{\frac{1}{2}} - 3(h-h_m)/2H_1 - H_1(\beta_m/D_m)^{\frac{1}{2}}\exp\left(-(h-h_m)/H_1\right)$$

then

$$Q_{6300} = (2F_D/3)(4.96\times10^{-14})\,N_m(N_2)\,(f_oF_2)^2\,\text{SUM} \qquad (17)$$

$$= (2F_D/3)\,C\,(f_oF_2)^2\,\text{SUM} \qquad (18)$$

where the integral of the exponential factor is replaced by SUM. The N_{em} in (16) has been replaced by

$$N_{em} = 1.24 \times 10^4 \, (f_oF_2)^2$$

The rate coefficients k is adopted to be 4×10^{-12} (Nisbet and Quinn 1963). The factor C is constant for a constant height of maximum electron density. The factor, SUM, is dependent on a number of variables, height h, h_m, scale height, $N_m(O)$, temperature and I the angle of dip. The lower limit of the height of the night-time ionospheric F-region has been taken to be around 200 km and the integration has been performed between the limits of 150 km to 550 km, as below 150 km the ionization becomes negligible and above 550 km the recombinations of ions become considerably small.

The computation, for a single dip angle, has been done for different h_m values ranging from 240 km to 450 km at an interval of 10 km. At each value of h_m, the values of β_m, D_m, the scale height of atomic oxygen, the concentration of atomic oxygen and molecular nitrogen have been listed. A sample listing of θ, h_m, β_m, D_m, $N_m(O)$, $N_m(N_2)$ and SUM i.e. integration for two values of θ (15^o and 20^o) is given in Table 5-I and Table 5-II. Then the dip angle is changed and the computations are repeated. Thus, from 5^o dip to 85^o dip the integrations were performed at intervals of 5^o dip. The expression for electron density profile (9), which has been used here becomes indeterminate over the magnetic equator

TABLE 5-I

NUM INTEGRATION OF ELECTRON DENSITY FOR DIFF. ZMAX OVER DIP LATITUDES

S= 90.0

DIP	HM	TEMP	(B)M	(D)M	N(O)	N(N2)	H(O)	SUM
15	240	921.	.200E-02	.143E 09	.897E 09	.502E 09	50.3	.650E 18
15	250	955.	.139E-02	.182E 09	.717E 09	.348E 09	52.2	.300E 15
15	260	988.	.982E-03	.229E 09	.579E 09	.245E 09	54.1	.141E 13
15	270	1019.	.702E-03	.286E 09	.471E 09	.175E 09	55.8	.337E 11
15	280	1048.	.507E-03	.354E 09	.387E 09	.126E 09	57.5	.256E 10
15	290	1076.	.370E-03	.434E 09	.319E 09	.927E 08	59.2	.442E 09
15	300	1103.	.273E-03	.528E 09	.266E 09	.684E 08	60.7	.136E 09
15	310	1129.	.204E-03	.638E 09	.222E 09	.510E 08	62.2	.621E 08
15	320	1153.	.153E-03	.766E 09	.187E 09	.383E 08	63.7	.373E 08
15	330	1176.	.115E-03	.916E 09	.158E 09	.289E 08	65.1	.272E 08
15	340	1199.	.884E-04	.108E 10	.134E 09	.221E 08	66.4	.227E 08
15	350	1220.	.678E-04	.128E 10	.114E 09	.169E 08	67.7	.210E 08
15	360	1240.	.523E-04	.151E 10	.983E 08	.130E 08	68.9	.209E 08
15	370	1259.	.406E-04	.177E 10	.844E 08	.101E 08	70.1	.220E 08
15	380	1278.	.316E-04	.207E 10	.728E 08	.791E 07	71.2	.242E 08
15	390	1296.	.248E-04	.241E 10	.630E 08	.620E 07	72.3	.273E 08
15	400	1313.	.195E-04	.280E 10	.546E 08	.488E 07	73.4	.317E 08
15	410	1329.	.154E-04	.324E 10	.475E 08	.386E 07	74.4	.374E 08
15	420	1344.	.122E-04	.374E 10	.414E 08	.306E 07	75.3	.447E 08
15	430	1359.	.977E-05	.430E 10	.362E 08	.244E 07	76.3	.540E 08
15	440	1373.	.781E-05	.493E 10	.317E 08	.195E 07	77.2	.658E 08

TABLE 5-II

NUM INTEGRATION OF ELECTRON DENSITY FOR DIFF. ZMAX OVER DIP LATITUDES

S= 90.0

DIP	HM	TEMP	(B)M	(D)M	N(O)	N(N2)	H(O)	SUM
20	240	921.	.200E-02	.249E 09	.897E 09	.502E 09	50.3	.490E 15
20	250	955.	.139E-02	.318E 09	.717E 09	.348E 09	52.2	.160E 13
20	260	988.	.982E-03	.401E 09	.579E 09	.245E 09	54.1	.372E 11
20	270	1019.	.702E-03	.500E 09	.471E 09	.175E 09	55.8	.229E 10
20	280	1048.	.507E-03	.618E 09	.387E 09	.126E 09	57.5	.394E 09
20	290	1076.	.370E-03	.758E 09	.319E 09	.927E 08	59.2	.122E 09
20	300	1103.	.273E-03	.922E 09	.266E 09	.684E 08	60.7	.566E 08
20	310	1129.	.204E-03	.111E 10	.222E 09	.510E 08	62.2	.344E 08
20	320	1153.	.153E-03	.133E 10	.187E 09	.383E 08	63.7	.253E 08
20	330	1176.	.115E-03	.159E 10	.158E 09	.289E 08	65.1	.214E 08
20	340	1199.	.884E-04	.190E 10	.134E 09	.221E 08	66.4	.199E 08
20	350	1220.	.678E-04	.224E 10	.114E 09	.169E 08	67.7	.199E 08
20	360	1240.	.523E-04	.264E 10	.983E 08	.130E 08	68.9	.211E 08
20	370	1259.	.406E-04	.310E 10	.844E 08	.101E 08	70.1	.232E 08
20	380	1278.	.316E-04	.362E 10	.728E 08	.791E 07	71.2	.263E 08
20	390	1296.	.248E-04	.422E 10	.630E 08	.620E 07	72.3	.305E 08
20	400	1313.	.195E-04	.489E 10	.546E 08	.488E 07	73.4	.361E 08
20	410	1329.	.154E-04	.566E 10	.475E 08	.386E 07	74.4	.432E 08
20	420	1344.	.122E-04	.653E 10	.414E 08	.306E 07	75.3	.522E 08
20	430	1359.	.977E-05	.751E 10	.362E 08	.244E 07	76.3	.636E 08
20	440	1373.	.781E-05	.862E 10	.317E 08	.195E 07	77.2	.779E 08
20	450	1386.	.626E-05	.987E 10	.278E 08	.156E 07	78.0	.960E 08

(I = 0), hence the integrations were performed starting with 5^{o} dip. The method of integration has been by Gauss's Quadrature method. Three-point integration using this method was quite adequate for the purpose.

Equations (16) and (18) need determination of f_oF_2 profile. This is calculated, from the data published by CRPL and other sources, in the following way.

The monthly median f_oF_2 values at 00 LMT were averaged for the 12 months of 1962 for stations between dip latitude 4.8^{o}N to 90^{o}S. The data are listed in Table 5-III from dip latitude 89^{o}S towards North. These f_oF_2 values at 5^{o} dip interval along with other necessary parameters computed in the programme have been used for computing the latitude profile of the 6300 Å emission. The results are listed in Table 5-IV for six h_m values from 300 km to 450 km.

The intensity associated with 6300 Å line is 2/3 of the total associated with the red doublet. The factor F_D remains uncertain. We therefore take one value of $(2F_D/3)$ arbitrarily for each calculated profile with a single value of h_m to normalise the calculations, such that they can be compared with the Altanin 6300 Å latitude profile. The F_D values so chosen for different profiles are given along with the h_m values in Table 5-IV.

It is expected that there is a latitude shift of Q_{6300} latitude profile with respect to the f_oF_2 latitude

TABLE 5-III

S.No.	Station	Geographic Lat.	Geographic Long.	Geomag. Lat.	Dip.	f_oF_2 Mc/S.
1.	Terre Adelie	66.7 S	110. E	75 S	-89	2.86
2.	Cape Hallett	72.3 S	170.2E	74 S	-84	2. 9
3.	Scott Base	77.8 S	166.8E	78 S	-83	3.13
4.	Cambell Is.	52.5 S	169.2E	57 S	-76	3. 1
5.	Byrd (Antarc)	80.0 S	120 W	70 S	-75	3. 8
6.	Godle Head	43.6 S	172.8E	48 S	-68	4. 2
7.	Halley Bay	75.0 S	26 W	65 S	-65	3.56
8.	Argentine Is.	65.0 S	64 W	53 S	-59	4. 4
9.	Port Lockroy	65.0 S	64 W	53 S	-58	4.64
10.	Brisbane	27.0 S	152 E	35 S	-57	4. 4
11.	Tananarive	18.0 S	47 E	23 S	-52	4. 1
12.	Port Stanley	51.7 S	57.8W	40 S	-48	5. 3
13.	Rarotonga	21.0 S	159 W	20 S	-38	5. 5
14.	Tahiti	17.0 S	149 W	15 S	-29	6. 5
15.	Talara	4.6 S	81.3W	06 N	-13	7. 4
16.	Ibadan	7.0 N	4.0E	10 N	- 3	6. 5
17.	Huancayo	12.0 S	75 W	00 S	1	6.65
18.	Trivandrum	8.5 N	76.5E	0.9S	1	6. 1
19.	Kodaikanal	10.2 N	75.5E	0.7N	3.5	5. 8
20.	Tiruchirapali	10.8 N	78.7E	1.1N	4.8	6. 3

TABLE-5 - IV

DIF	$(f_oF_2)^2$	h_m = 300 km, C=3.390 (-6), F_D=0.030		h_m = 350 km, C=0.838(-6), F_D=0.156		h_m = 370 km, C=0.500 (-6), F_D=0.22		h_m = 380 km, C=0.392 (-6), F_D=0.25		h_m = 400 km, C=0.242 (-6), F_D=0.30	
		SUM	Q_{6300}	SUM	Q_{6300}	SUM	Q_{6300}	SUM	Q_{6300}	SUM	Q_{6300}
5	48.30	.275(13)	9.02(6)	.947(8)	3990.	.284(8)	101.0	.207(8)	65.4	.157(8)	36.7
10	54.02	.114(10)	4178.8	.249(8)	117.3	.206(8)	81.8	.209(8)	74.4	.248(8)	65.1
15	56.25	.136(9)	519.1	.210(8)	103.0	.220(8)	91.0	.242(8)	89.0	.317(8)	86.3
20	51.84	.566(8)	198.8	.199(8)	90.0	.232(8)	88.4	.263(8)	89.1	.316(8)	91.0
25	46.92	.353(8)	83.4	.195(8)	97.8	.240(8)	82.8	.278(8)	85.3	.390(8)	86.6
30	40.96	.263(8)	73.0	.192(8)	68.6	.246(8)	74.1	.288(8)	77.6	.412(8)	81.6
35	34.81	.216(8)	51.0	.191(8)	58.0	.251(8)	64.2	.296(8)	67.4	.427(8)	72.0
40	30.25	.187(8)	38.4	.190(8)	50.1	.254(8)	56.5	.302(8)	59.7	.439(8)	64.2
45	26.52	.168(8)	30.2	.189(8)	44.0	.257(8)	50.1	.306(8)	53.0	.448(8)	57.5
50	23.52	.155(8)	24.7	.189(8)	39.0	.259(8)	44.8	.310(8)	47.7	.456(8)	52.0
55	20.70	.146(8)	20.5	.188(8)	34.0	.260(8)	39.6	.312(8)	42.2	.461(8)	46.2
60	18.49	.139(8)	17.4	.188(8)	30.3	.262(8)	35.6	.315(8)	38.1	.466(8)	41.7
65	16.00	.134(8)	14.5	.188(8)	26.4	.263(8)	31.0	.316(8)	33.0	.470(8)	36.4
70	13.69	.130(8)	12.1	.188(8)	22.4	.264(8)	26.6	.318(8)	28.5	.472(8)	31.4
75	12.25	.127(8)	10.5	.188(8)	20.1	.264(8)	24.0	.319(8)	25.5	.474(8)	28.1
80	10.25	.126(8)	8.7	.188(8)	16.8	.265(8)	20.0	.320(8)	21.4	.476(8)	23.6
85	9.00	.125(8)	7.6	.188(8)	14.7	.265(8)	17.5	.320(8)	19.0	.477(8)	20.8

Note: (i) Q_{6300} in Rayleighs, (ii) 1.33 (8) $\equiv 1.33 \times 10^8$

profile. This is evidenced from Figs.5.2a and 5.2b. The f_oF_2 maximum in the smooth curve is at 15° dip while the Q_{6300} maximum is at 20° dip.

The shift dI, calculated from equation (14) with h_m = 380 km showed that the shift is greater towards lower latitudes and practically disappears towards higher latitudes. Therefore at higher latitudes the electron density profile will correspond to the red line luminosity profile overhead only. In terms of geographic latitude, a distance of 110 km is approximately equivalent to a change of 1° in latitude. Thus for dip latitude 15°, a 250 km shift in the two profiles is expected.

5.5 Comparison of theory and observation

The comparison of the calculated latitude profiles with the observations made by Altanin ship gives very interesting results. The Altanin data are plotted in Fig.5.3a. The Altanin observations show a maximum of intensity at about 20-22° dip. The calculated profiles with h_m = 300 km and h_m = 380 km are also plotted along with this. The curve with h_m = 300 km shows a close fit with the Altanin curve from 85°S to 25°S as shown by the part AB of the calculated curve, while the calculated Q_{6300} curve with h_m = 380 km shows a good resemblance below 25°S dip. Therefore it seems that below 25° dip the higher h_m values of 380 km are favourable and above 25° dip lower values of h_m = 300 km are favourable,

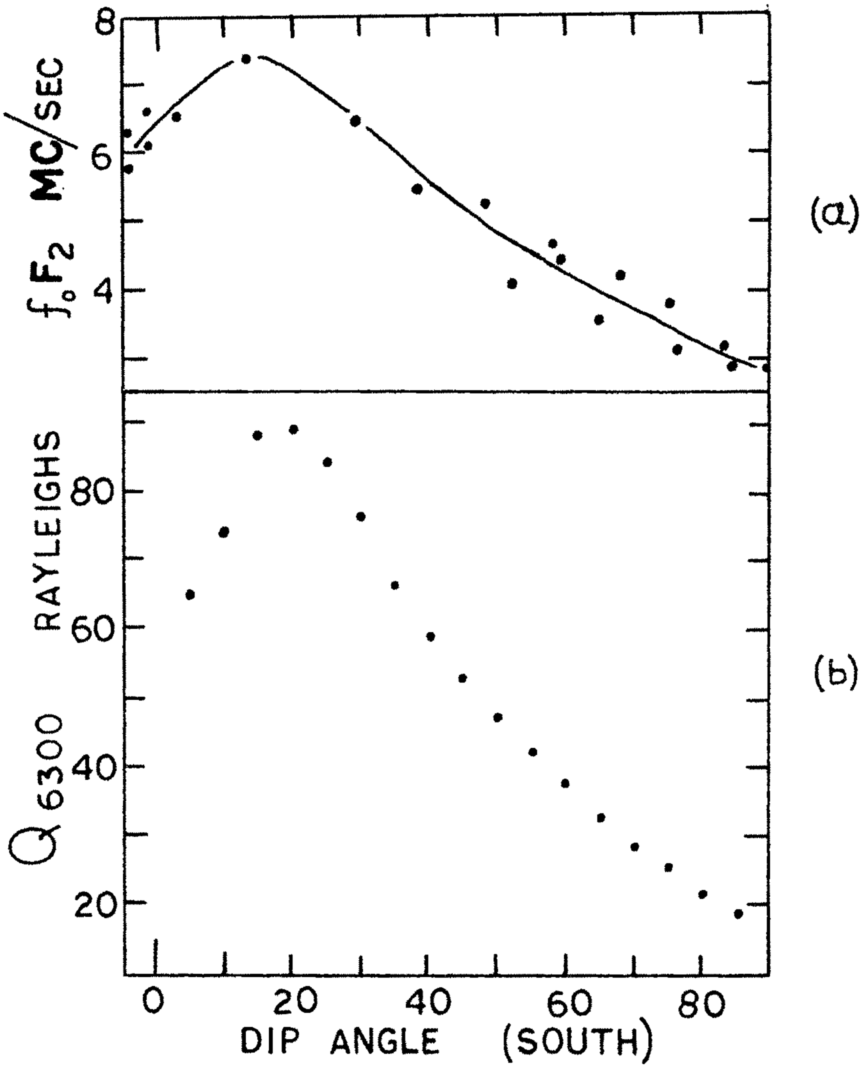

FIG.5.2. (a) The latitude distribution of f_oF_2 at 0000 LMT averaged for 12 months of 1962; (b) the calculated latitude distribution of 6300 A emission for h_m =380 km, normalised with respect to Altanin observation.

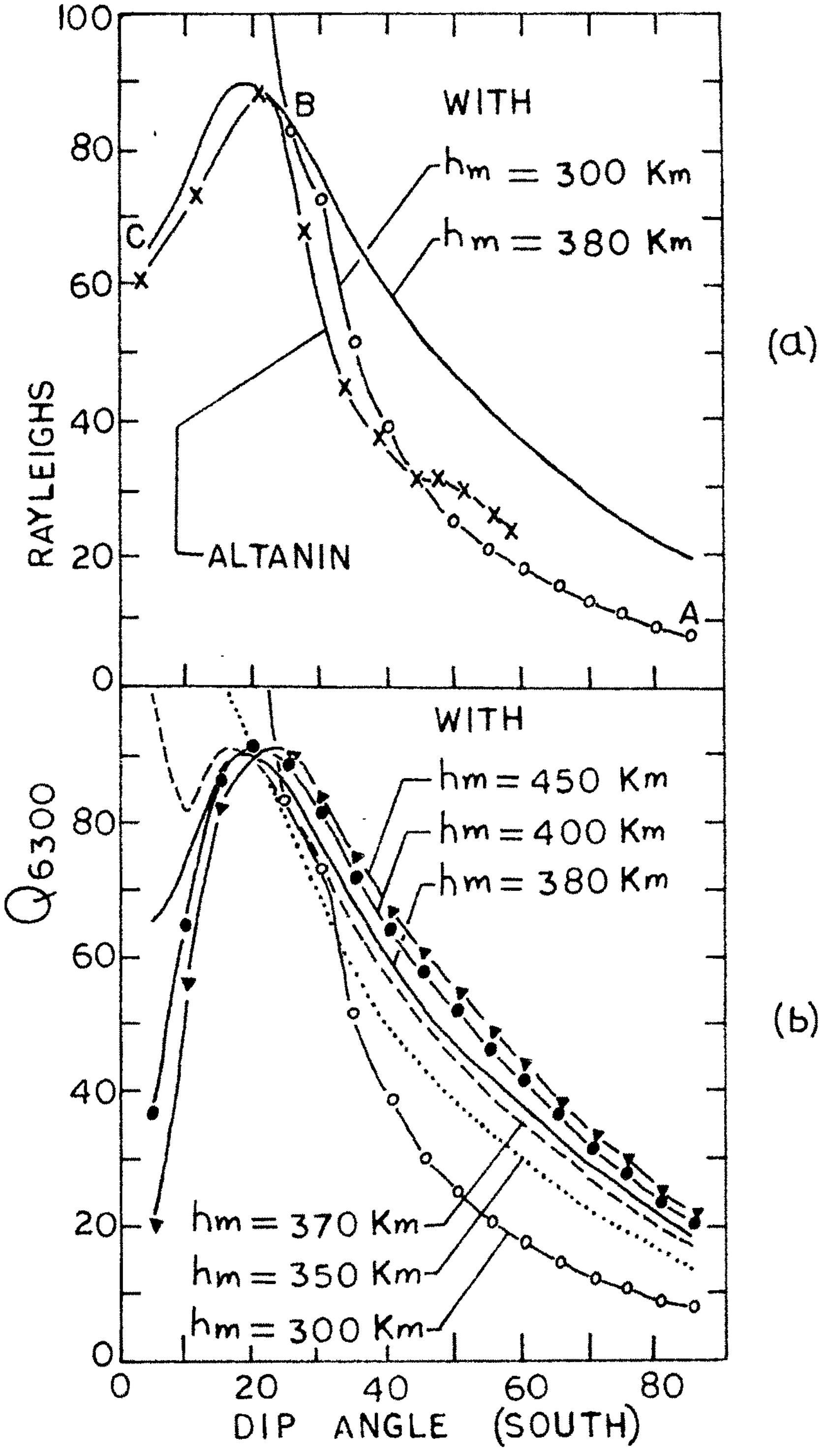

FIG.5.3. (a) The latitude distribution of I_{6300}, observed on board the Altanin (Davis and Smith, 1964) and Q_{6300} calculated; (b) variation of Q_{6300} over latitudes with different h_m values.

such that the combination makes the joint profile ABC to represent the red line emission latitude profile, well fitting to the observed latitude profile.

A small departure in the latitude shift and a lack of close fit of the observed and calculated curves can be due to the following :

(a) The motion of ionization in the F-region is not strictly ambipolar; a more complicated state of affairs is possible.

(b) Altanin data are averaged intensity observations made at different times of the night which depends on the moon's phase while the computations are limited to 00 LMT.

5.6 The effect of variation of h_m on Q_{6300}

At I = 0, the expression (9) becomes indeterminate and in the vicinity of I = 0, i.e. $I \sim 5^o$ to 10^o, Q_{6300} curves with $h_m < 380$ km show anomalous behaviour (Fig.5.3b). With h_m changed from 380 km to 450 km, Q_{6300} latitude profiles are achieved comparable to the observed one. The values of h_m for 450 km and above give abnormally small values of Q_{6300} due to very low recombinations. In the range of h_m values from 380 km to 400 km the normalising factor $(2F_D/3)$ happens to be 1/6 to 1/5. The efficiency of the dissociative recombination reaction in producing ^1D term in fitting the Altanin data to the calculated profile is therefore about 25 % to 30 %.

From the curves of Fig.5.3b, an interesting feature can be seen, namely, that when h_m increases the peak in Q_{6300} profile shifts to higher dip latitudes. This indicated that at high levels the ambipolar diffusion of ionization is important and causes ionization to diffuse to greater distances along geomagnetic lines of force, causing an increase in the shift of Q_{6300} curve. Moreover, high neutral concentration at low levels destroys the ambipolar diffusion soon, presumably by the recombination of ions and the collision effects of the neutral gas.

It may therefore be concluded that 'ambipolar diffusion' plays an important part in determining the 6300 Å vertical emission profile and its distribution over latitudes.

CHAPTER VI

THE OCCASIONAL COVARIATION OF 6300 A AND 5577 A EMISSIONS

CHAPTER VI

THE OCCASIONAL COVARIATION OF 6300 A AND 5577 A EMISSIONS

6.1 Introduction

The airglow observations at Mt.Abu indicate in general an absence of covariation between 6300 A and 5577 A emissions. The 5577 A emission generally shows a peak around midnight, and 6300 A shows a minimum around midnight. The variations on three general nights are presented in Fig.6.1. There are however a few occasions when covariation in the two emissions has been observed. On such nights, both red and green emissions show a general covariation on which is superposed abnormal enhancements lasting for an hour or so.

In Figs.6.2a, b, c pronounced peaks occur around 2100 IST in both 5577 A and 6300 A and are superposed on the dotted curve which may be considered as the 'general variation' of the two radiations. In Figs.6.3a, b, c and 6.4 are represented curves of intensity on a few nights on which there was covariation of the two emissions during March 1967 and December-January-February, 1964-65. Such occasions, having peak to peak covariation in the two emissions are however not very frequent.

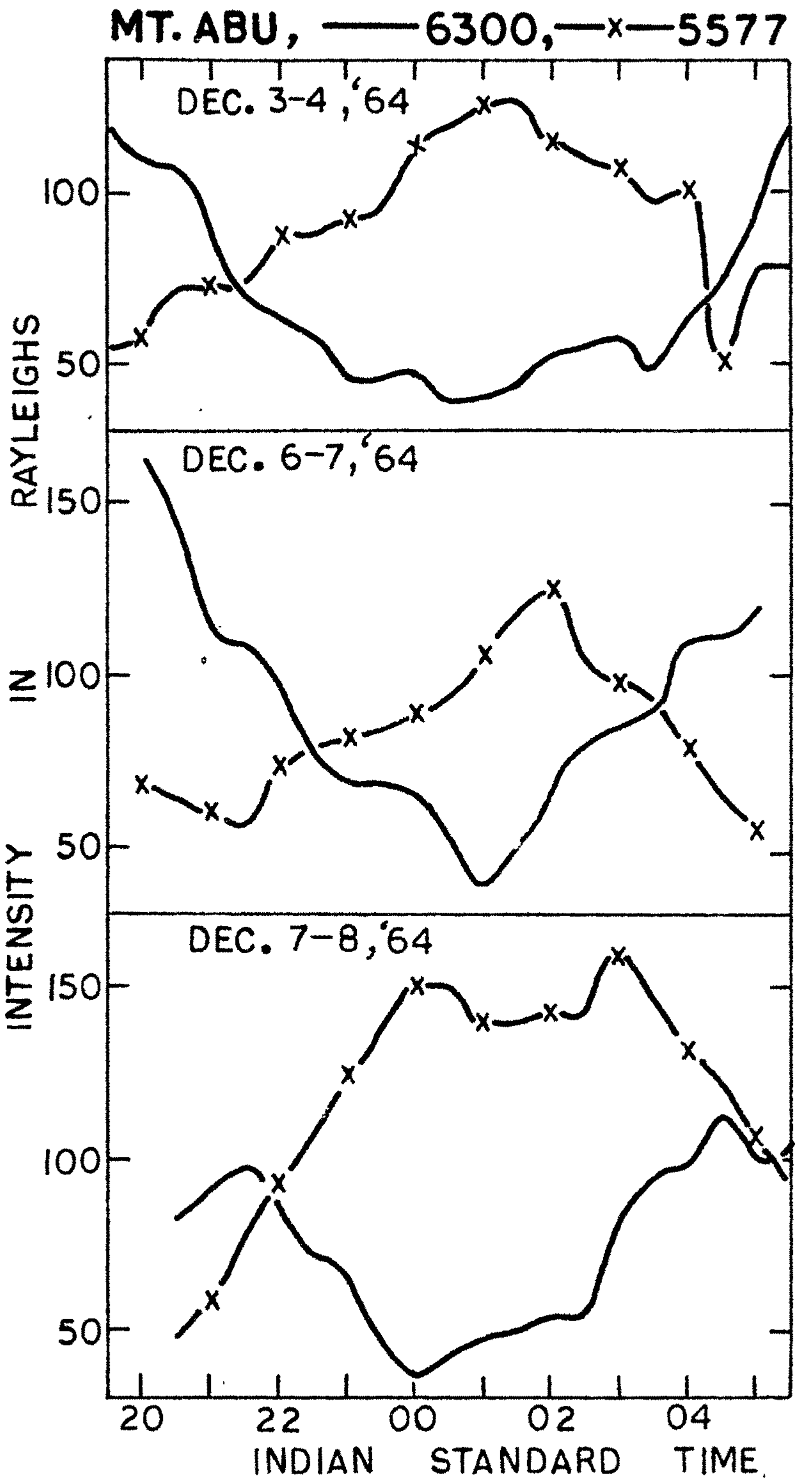

FIG.6.1. Nights showing general nocturnal variation of 6300 A and 5577 A at Mt.Abu.

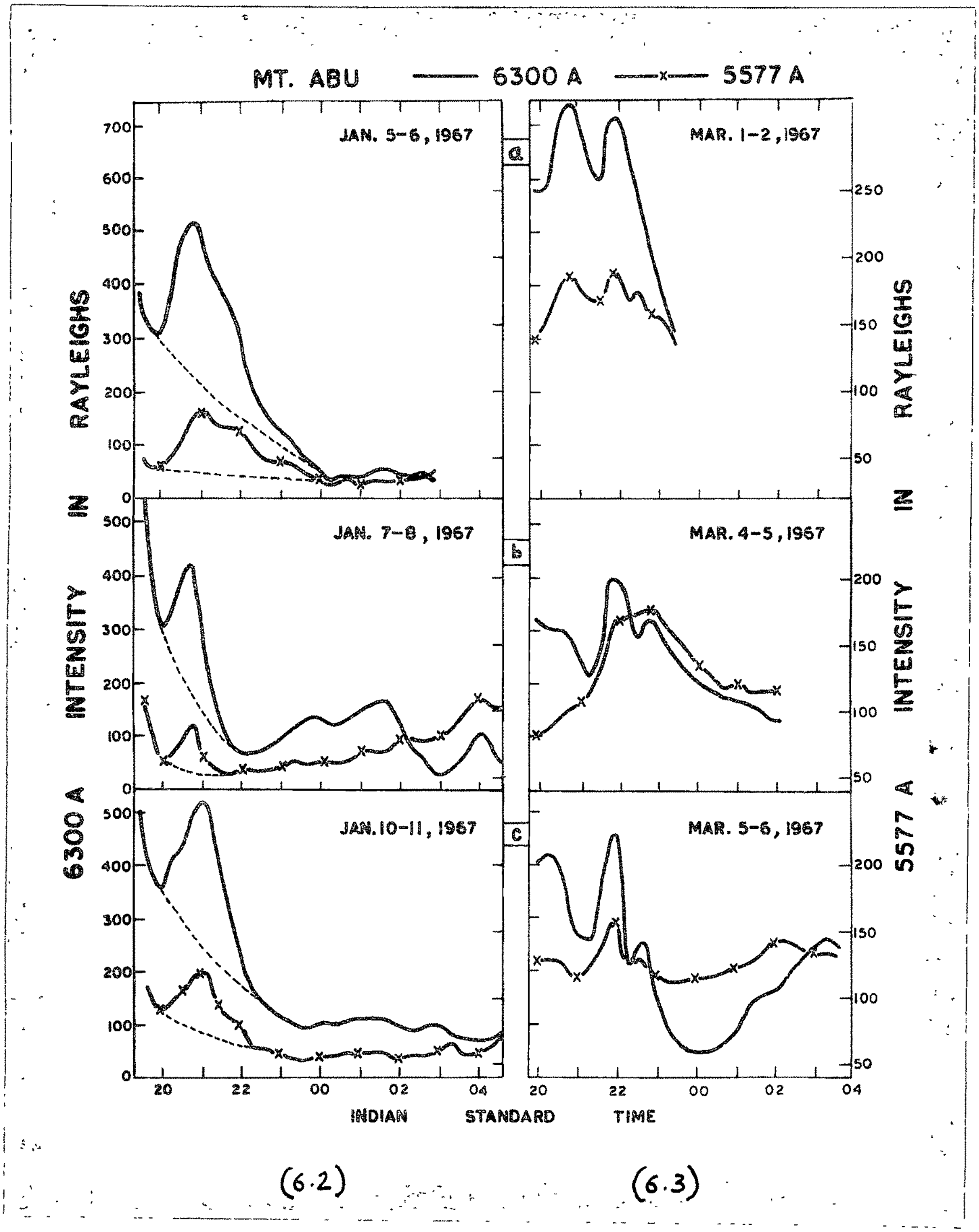

FIGS.6.2.,6.3. Showing occasions when enhancement and covariation in 6300 A and 5577 A emissions were observed.

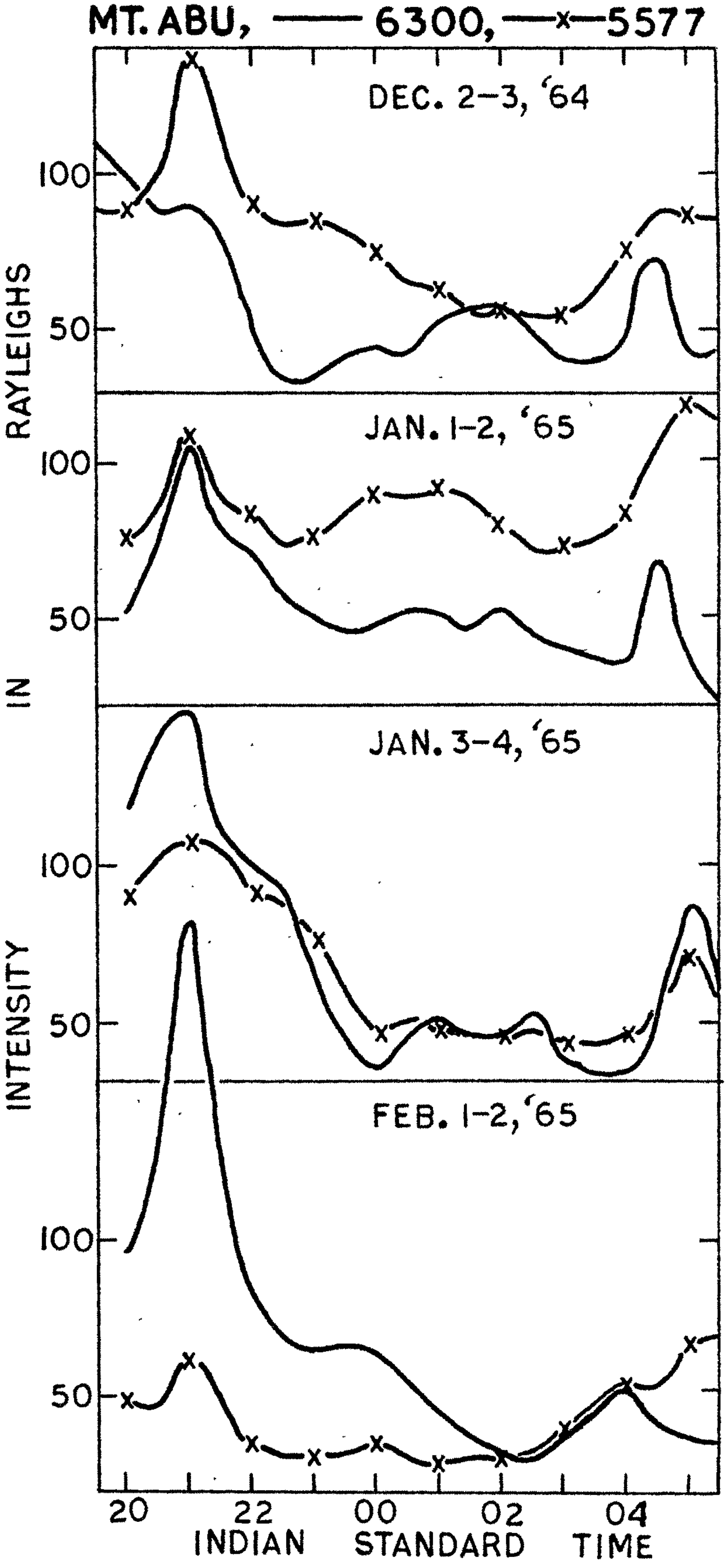

FIG.6.4. The occasions when 6300 A and 5577 A emissions had covariation.

6.2 Photochemical reactions

Normally 5577 Å emission is from the 100 km region of the atmosphere and 6300 Å is from 250-300 km region, which is associated with the ionization of the night time F-layer. The study of the covariation in the two emissions may be expected to elucidate the mechanism of the emissions.

The dissociative recombination reactions in night time F-region, which are important in this respect are the following

$$NO^{+} + e = N^{*} + O^{*} \quad (2.76\ ev) \qquad (1)$$

$$O_2^{+} + e = O^{*} + O^{*} \quad (6.96\ ev) \qquad (2)$$

$^1S_0$ term production is not possible in reaction (1) as an energy 4.17 ev is required for this excitation. Only 6300 Å emission (1.96 ev) is possible. The energy available in the excited oxygen atoms in reaction (2) is sufficient for the production of 5577 Å (4.17 ev) line. Thus the green and red emission covariation may be possible when reaction (2) is operative.

The observations indicate that the covariation in the two emissions are not very frequent and therefore the mechanism of reaction (2) taking place in the F-region may be operative only infrequently. Normally, if reaction (2) were operative like (1), the yield in 5577 Å radiation will be much smaller than in 6300 Å radiation (Peterson et al 1966, referring I_{6300}/I_{5577}). Gulledge et al (1966) showed that the intensity of the green emission from the layer at 250 km was about 0.2 that of the red line. Therefore, for a good and a point-to-point covariation in two emissions, the mechanism (2) must be enhanced or a different mechanism producing $^1S_0$ term should operate.

The OSO-B2 satellite observations (Sparrow et al 1968) showed that this high altitude 5577 Å emission layer could not be detected at middle latitudes but was readily seen within 20° of the equator. The observations at our station (30°N) did not in general show a covariation of the two emissions, and if there was a small component of 5577 emission from 250 km layer, it was masked by the independent and stronger emission of 5577 Å at 100 km region.

The covariation if observed in the two emissions could be interpreted to mean that when there is an enhancement of emission from F-region, the 5577 Å emission could extend occasionally from equator to 30°.

Then it can be conceived that on nights, on which both the emissions are enhanced for a short period and, later covary for a few hours, conditions are favourable for reaction (2). The point-to-point covariations observed in the two emissions on January 5, 7, 10, 1967 and March 1, 4, 5, 1967 (Figs.6.2, 6.3) are interesting examples in this regard.

One can observe a covariation in the two emissions in the pre-midnight period when the phenomenon is very pronounced. It is also seen that in some cases there may or may not be a peak-to-peak covariation in the two emissions, after the initial period of enhancement.

An examination of magnetic index K_p and the total magnetic field recorded at Ahmedabad showed that there was no relation of these enhancements with magnetic activity.

Ionospheric data indicate that such events occurred with h_pF_2 relatively high during the enhancements of 6300 Å and 5577 Å at 2100 IST and that the high value of f_oF_2 with the presence of spread F was the speciality of such events.

Without commenting on the mechanism of enhanced peaks in both the emissions at 2100 IST we proceed to study the nature of both emissions in their 'general background curves' (enhanced peaks excluded over dotted interpolation, Figs.6.2).

6.3 The study of covariation in normal curves on January 5-6 and January 10-11, 1967

It is found in the general background curves that both emissions decay simultaneously. It is our object here to study the variation of red to green intensity ratio during the decay of both emissions. The red to green intensity ratios for these two nights show a definite trend of variation as can be seen from Fig.6.5. This trend of variation is interpreted on the basis of the dissociative recombination theory of forbidden transitions of atomic oxygen (both 5577 A and 6300 A) as put forward by Peterson et al (1966).

The relevent part of the theory and its use in the present context is reproduced below.

In their theory, Peterson et al (1966), considering the contribution of dissociative recombination reactions, have derived the following expression for red to green emission ratio,

$$\epsilon(6300)/\epsilon(5577) = (k_D/k_{S_1}) \quad 0.81/(1 + d_D/A_D) \qquad (3)$$

where k_D is a factor dependent on the efficiency of the reactions, in producing the forbidden terms of atomic oxygen and is weakly height-dependent through the ratio of recombination coefficients. k_{S_1} is the efficiency of reaction (2) in producing $^1S_0$ term per recombination. Its value lies somewhere between the limits zero to one. The collisional deactivation coefficient d_D has a strong height-dependence through the molecular oxygen concentration as it is related to the latter in the form $d_D = S_D(O_2)$, where S_D is the specific reaction rate. $A_D = .0091\ \text{sec}^{-1}$ is the Einstein transition coefficient for the ^1D level. Equation (3) shows therefore that the red-to-green emission ratio is proportional

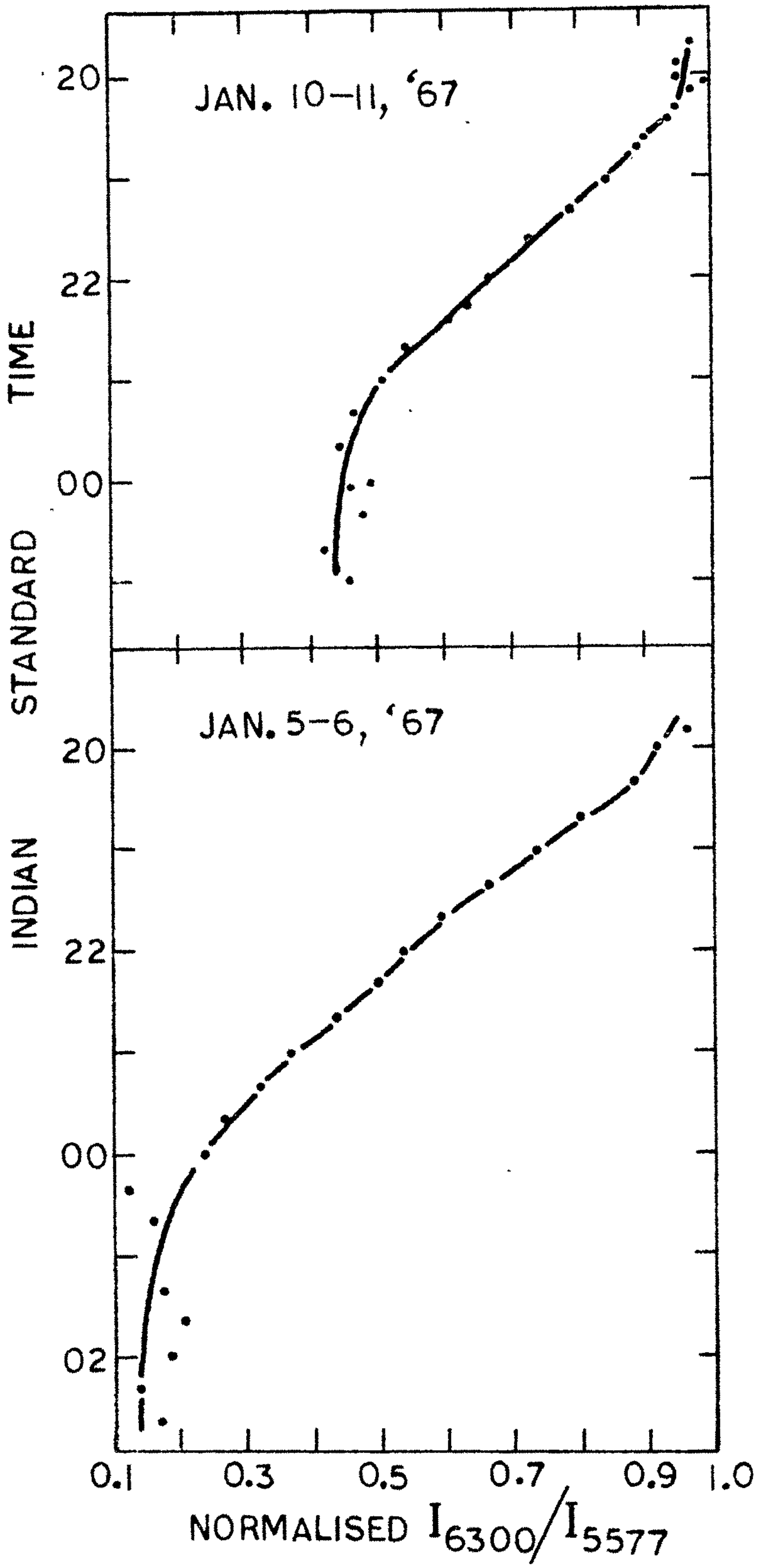

FIG.6.5. The time variation of the intensity ratio of 6300 A to 5577 A observed at Mt.Abu. The ratio is proportional to the factor $1/(1 + d_D/A_D)$.

to the factor $1/(1 + d_D/A_D)$. Peterson and others (1966), assuming three values of the specific reaction rate S_D, have plotted $1/(1 + d_D/A_D)$. Their diagram is shown here as Fig.6.6.

When the reaction (2) which is capable of producing 5577 Å does not remain effective, which may result in no covariation of two emissions, the ratio $\epsilon(6300)/\epsilon(5577)$ losses its significance. But when the covariation continues through a considerable part of the night the ratio $\epsilon(6300)/\epsilon(5577)$ remains proportional to the factor $1/(1 + d_D/A_D)$.

For testing this inference the observed ratio I_{6300}/I_{5577} on the two nights reported, has been computed at intervals of 20 minutes. Now again, it is difficult to locate the height where the emission mechanism is predominently present. Therefore a plot of I_{6300}/I_{5577} versus height could not be obtained. On the other hand, a checking of h_pF_2 values over Ahmedabad indicated that ionization maximum was confined to higher levels in the beginning of these two nights and came down steadily to lower levels as the night progressed. For illustrative purpose therefore, the height scale was replaced by a linear time scale, for plotting I_{6300}/I_{5577} in Fig.6.5.

The observed curves of Fig.6.5 resemble the curves of Fig.6.6. It was not possible to separate from ground based observations, the contribution from the lower green layer at

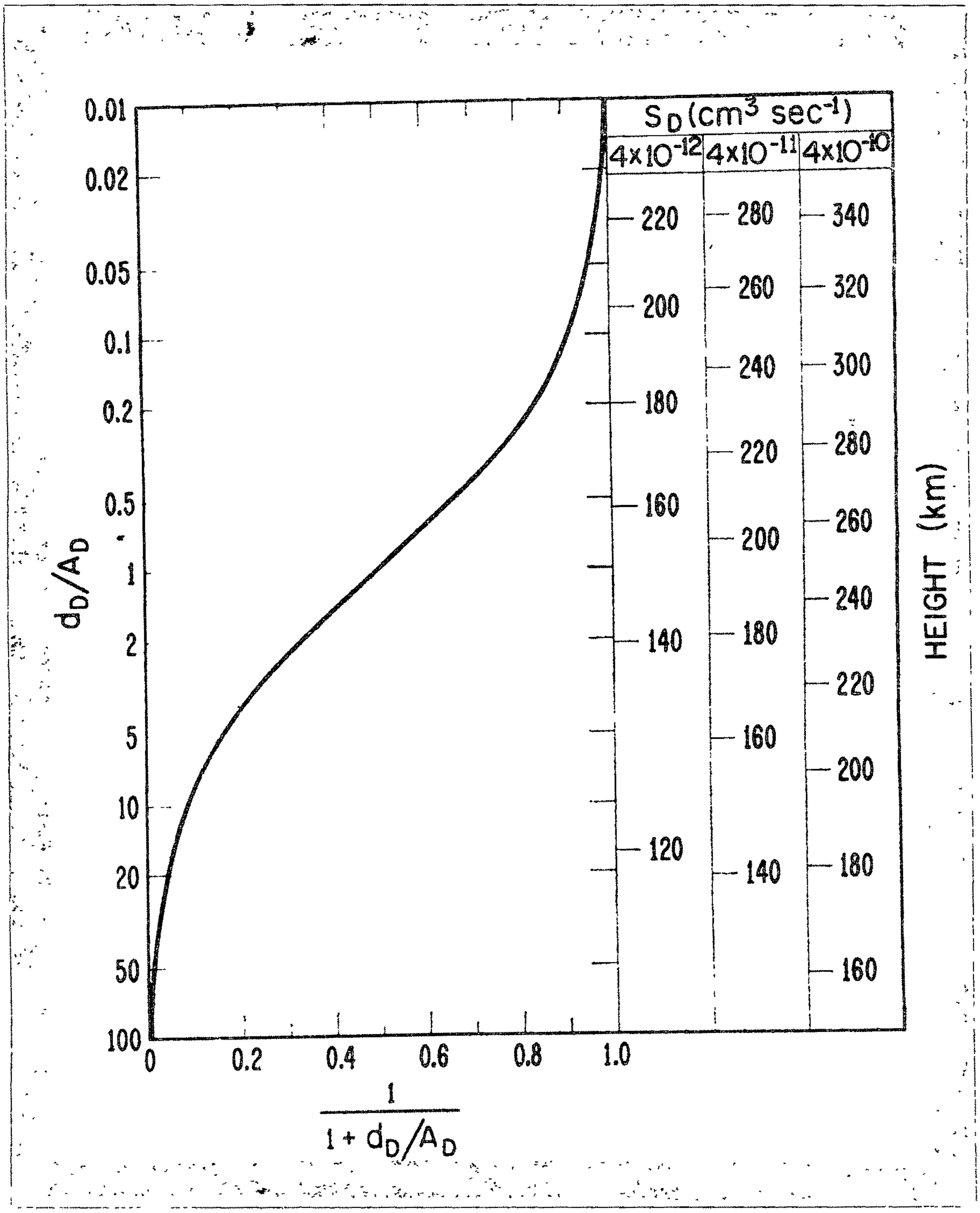

FIG.6.6. The height dependence of the collisional deactivation factor $1/(1 + d_D/A_D)$, (after Peterson et al 1966).

100 km. But as we saw a good covariation in the two 'general background curves' of the two emissions on these two nights, we have assumed that the variation in 5577 Å intensity was mainly due to dissociative recombination processes making the two emissions to covary.

6.4 Conclusion

The resemblance of the calculated curves with the theoretical curve indicates that on the nights studied here, there is a considerable 5577 Å emission produced by dissociative recombination process in the night time F-layer of ionosphere. Further more, the processes are confined at higher levels in the beginning and then descend as the night progresses. Thus a high level confinement of F-layer with higher electron density (as is observed on these occasions) would favour covariation of two emissions.

On such occasions as studied in the present text the occurrence of spread F is a matter of interest and further investigation is needed in this regard.

CHAPTER VII

STUDIES OF 5890-96 A EMISSION IN NIGHTGLOW

CHAPTER VII

STUDIES OF 5890-96 A EMISSION IN NIGHTGLOW

7.1 Seasonal variation of Na-Doublet in nightglow

The seasonal variation of sodium emission in nightglow at Mt.Abu is represented by the curve in Fig.7.1. The following general conclusions can be drawn.

The December-January minimum in sodium doublet emission for the observational period November 1964 to June 1967 confirmed that observed earlier by Dandekar (1961b) during high solar activity period (1957-58-59). A clear October maximum in 1965 and a November maximum in 1966 perhaps corresponded to the November maximum observed by Barbier (1963) at Haute Provence and Tamanrasset.

Another maximum appears in April-May, 1965; April 1966 and April-May 1967 in the three consecutive periods of observations. This secondary maximum of April-May was not conspicuous in earlier observations by Dandekar at Mt.Abu. In the observations at Tamanrasset and Haute Provence (Barbier 1963), a secondary maximum was present in March-April.

The maximum of October 1965 is found to be more intense than that of October-November 1966. While the secondary maximum of April 1966 was associated with smaller intensity than that of May 1967.

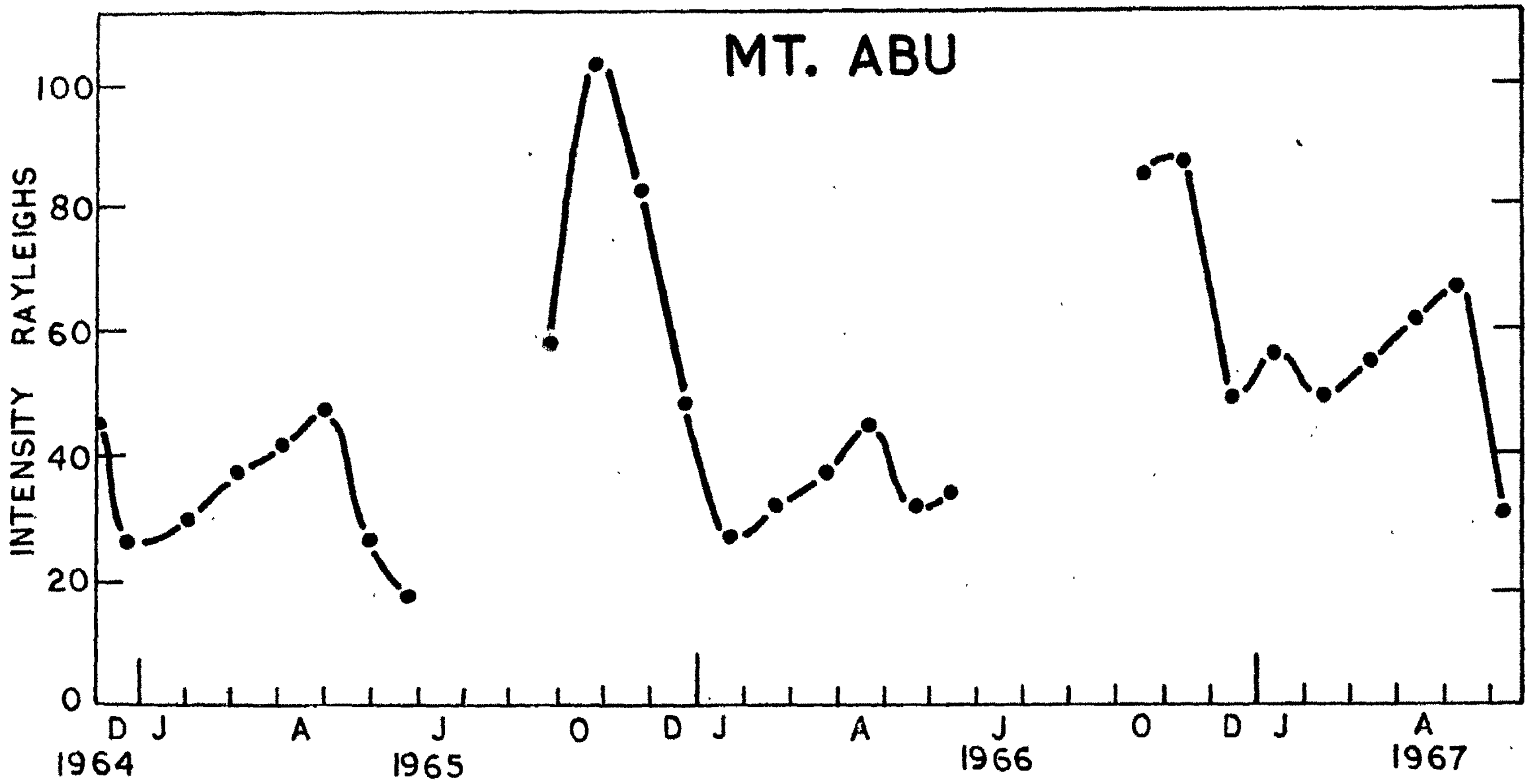

FIG. 7.1. Seasonal Variation of 5893 Å Emission.

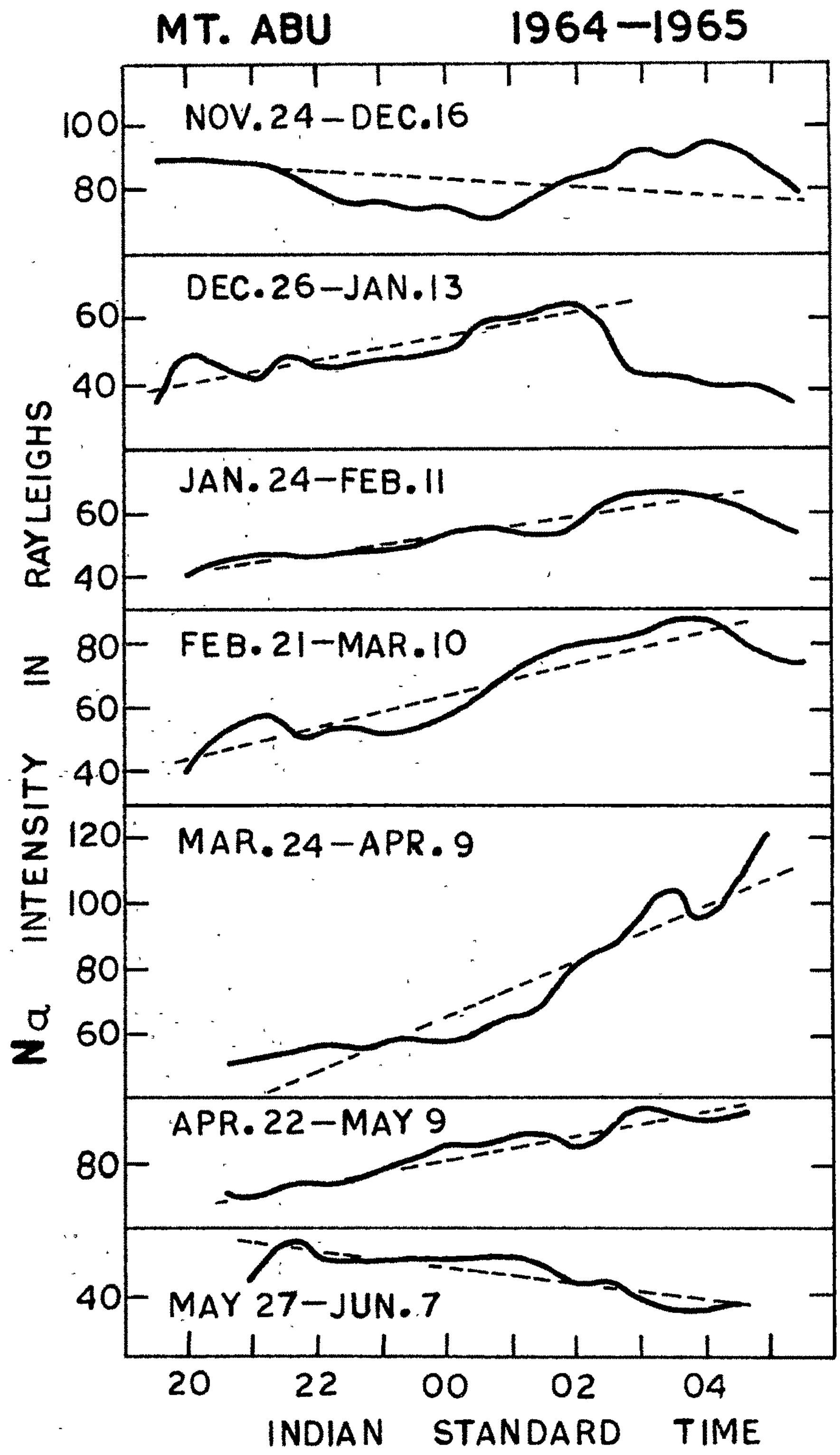

FIG. 7.2. Average nocturnal variation of Na-emission in different lunations.

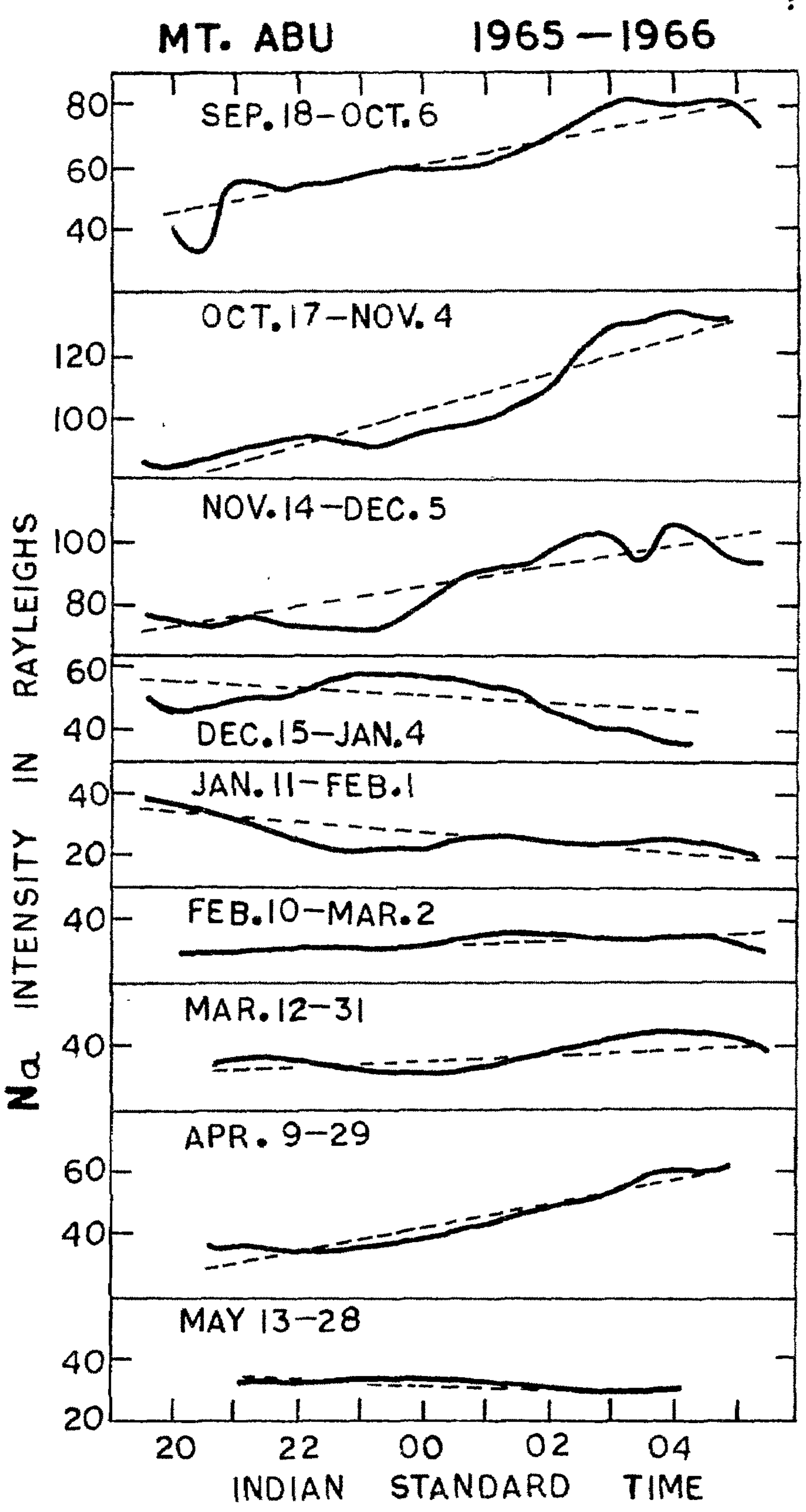

FIG. 7.3. Average nocturnal variation of Na-emission in different lunations.

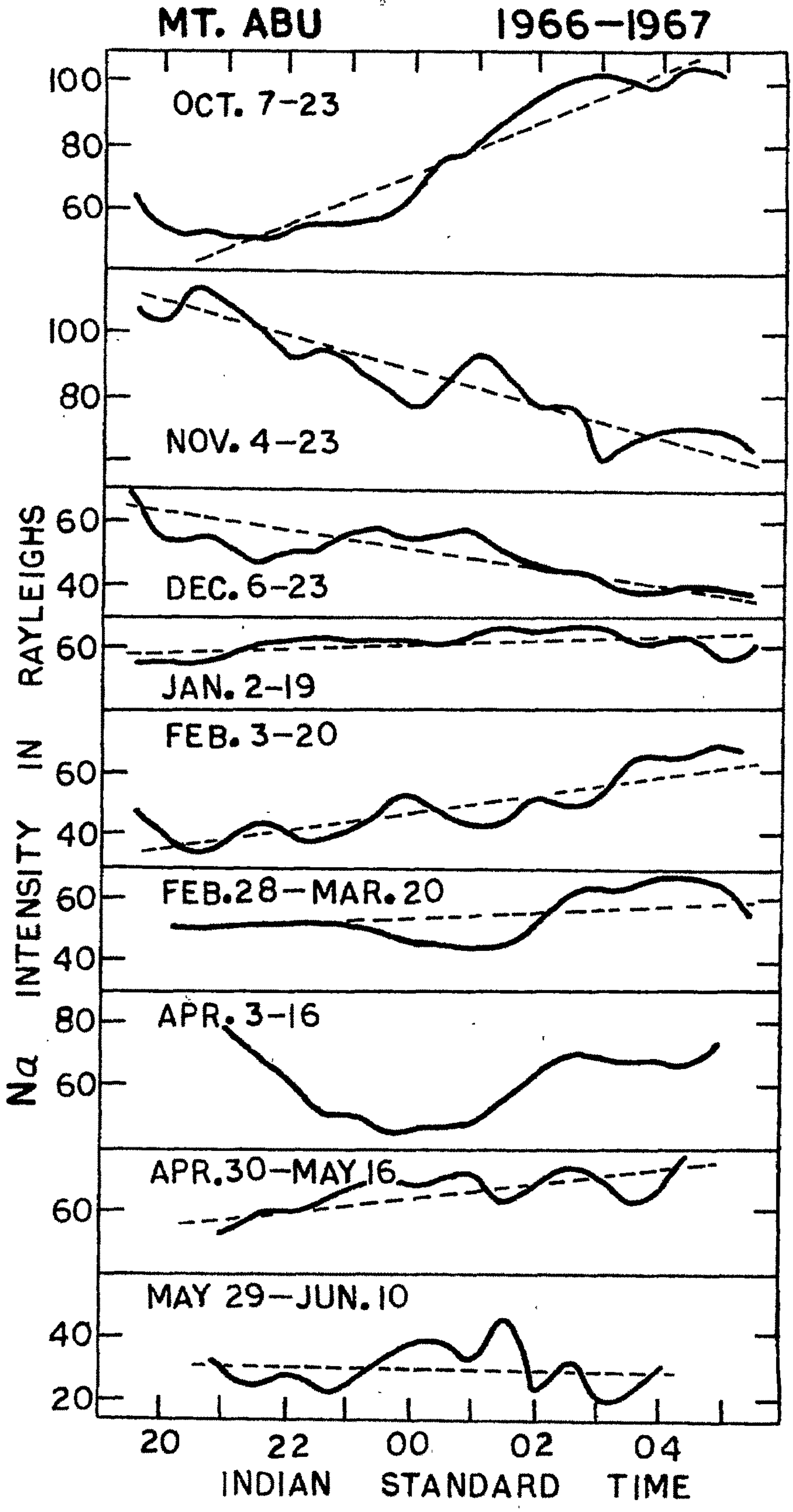

FIG. 7.4. Average nocturnal variation of Na-emission in different lunations.

general trend, however remains as stated above. The general nocturnal variation of sodium at other stations also show similar results. (Dufay and Tcheng 1946, Roach 1955, Steiger 1967).

Ballif and Venkteswaran (1962) have suggested that the sodium excitation in nightglow is governed by ozone concentration at the height of Na-emission. Other workers (Bates and Nicolet 1950, Wallace 1962) having given the theoretical estimates of $n(O_3)$ by taking pure-oxygen and oxygen-hydrogen atmosphere at the appropriate heights, showed that the ozone concentration increases after sunset seeking to attain its equilibrium concentration towards morning. Then increase of $n(O_3)$ during night will increase sodium emission likewise.

The increase of Na-emission during night, as observed at Mt.Abu station would therefore support the ozone hypothesis for sodium emission. From November 1964 to June 1967, only three to four monthly average curves show fall of intensity during the course of night. The curves of November 1966 and December 1966 are good examples of this kind (Fig.7.4). This was opposite to the above mentioned theoretical deduction.

7.3 Comparison of monthly mean curves

The comparison of different monthly curves of similar periods of observations over three years, is furnished by the

Fig.7.5. It is shown by the curves of October 1965 and October 1966 that the intensity rises towards morning in both lunations and the intensity variation is considerable in this period. The trend of variation is more or less the same in both curves. Curves of the period from November 1964 to June 1965 have not been considered because the observations fall into two months and can not be compared with the curves of the following periods. The curves of November-December 1965 and 1966 have no resemblance as the former rises upto 3 am and then falls while the later shows a continuous decrease of intensity towards morning. However a comparison of November 1965 and November-December 1967 curves show some similarity.

It is very interesting to note that the curves of December 1965 and 1966 have exactly similar variations. The curves of March 1966 and 1967 also show simultanity with 1967 curve showing higher intensity than that of 1966. In February 1967 more fluctuations of intensity are seen than those in February 1966.

7.4 Two features of Na-emission

From the observed curves of Figs.7.2, 7.3, 7.4 and other individual nocturnal variations, the following two features can be noted.

(1) Nocturnal variation of sodium intensity can be looked upon as a linear variation, with a certain slope, which to the

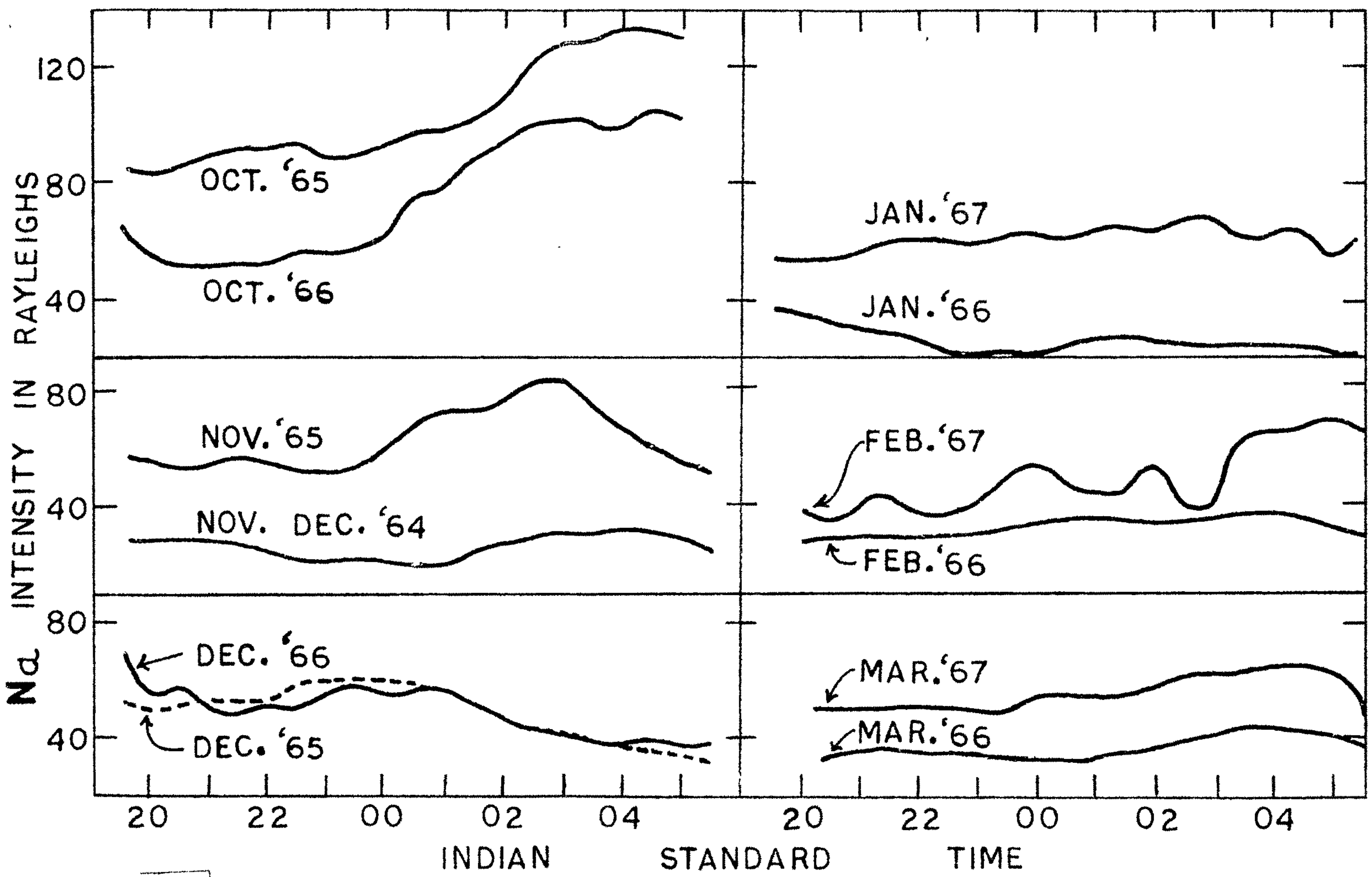

FIG. 7.5. Comparision of nocturnal variations in similar season curves.

first apoproximation remains constant during the night. Different value slopes, from positive to negative are present in the observations made, but in general one value of slope can be associated for one night. Departures from a single slope value are of course present in some cases. Fig.7.6 showing nocturnal variation on individual nights shows the above mentioned features. The generating line is represented by the dotted line.

(2) Whether the intensity rises, or falls or remains constant during a night, intensity fluctuations are present in the nocturnal variations of Na-emission. The fluctuations can be visualized better in individual nocturnal curves than in the monthly curves where the fluctuations are smoothed out due to averaging. When such fluctuations are present, a periodicity of the order of one to two hours is observed. This periodicity is seen to be present for a considerable part of the night. The consecutive nights represented in Fig.7.6 examplify the fluctuating nature of sodium intensity.

The genuineness of these fluctuations is felt when the simultaneous recording, of 5577 A and 6300 A emissions reduced with the common calibration, does not show such fluctuations. The observations at Poona (Chiplonkar and Agashe 1961, Fig.7.7a), Barbier's observations (1954b) at Haute Provence (Fig.7.7b), at Haute Provence and Tamanrasset (1963) (Fig.7.7c) and the observations at Haleakala (Steiger 1967, Fig.7.7d) show the fluctuations in sodium intensity curves.

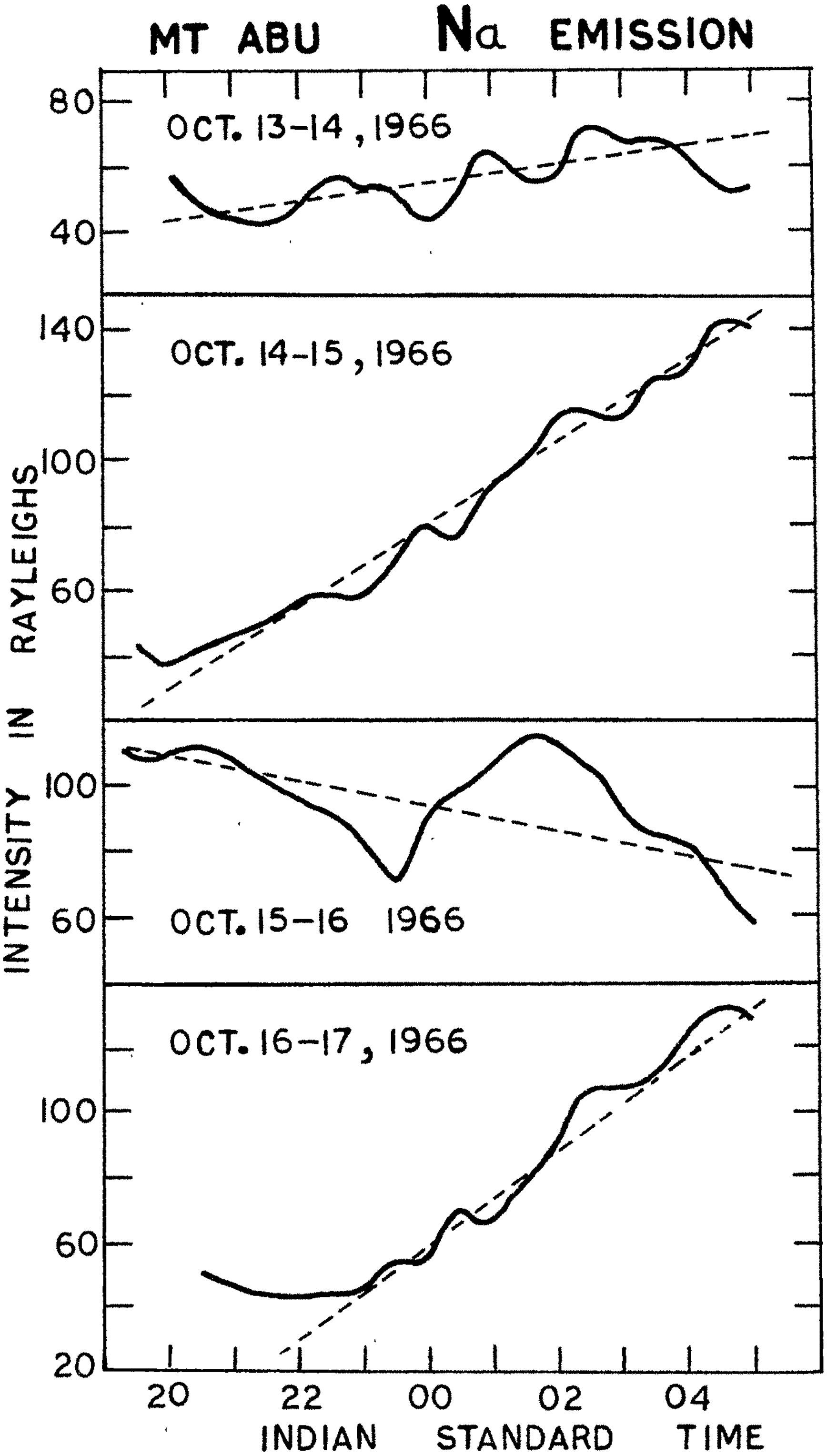

FIG. 7.6. Typical Nocturnal Variation of Na-emission on consecutive nights.

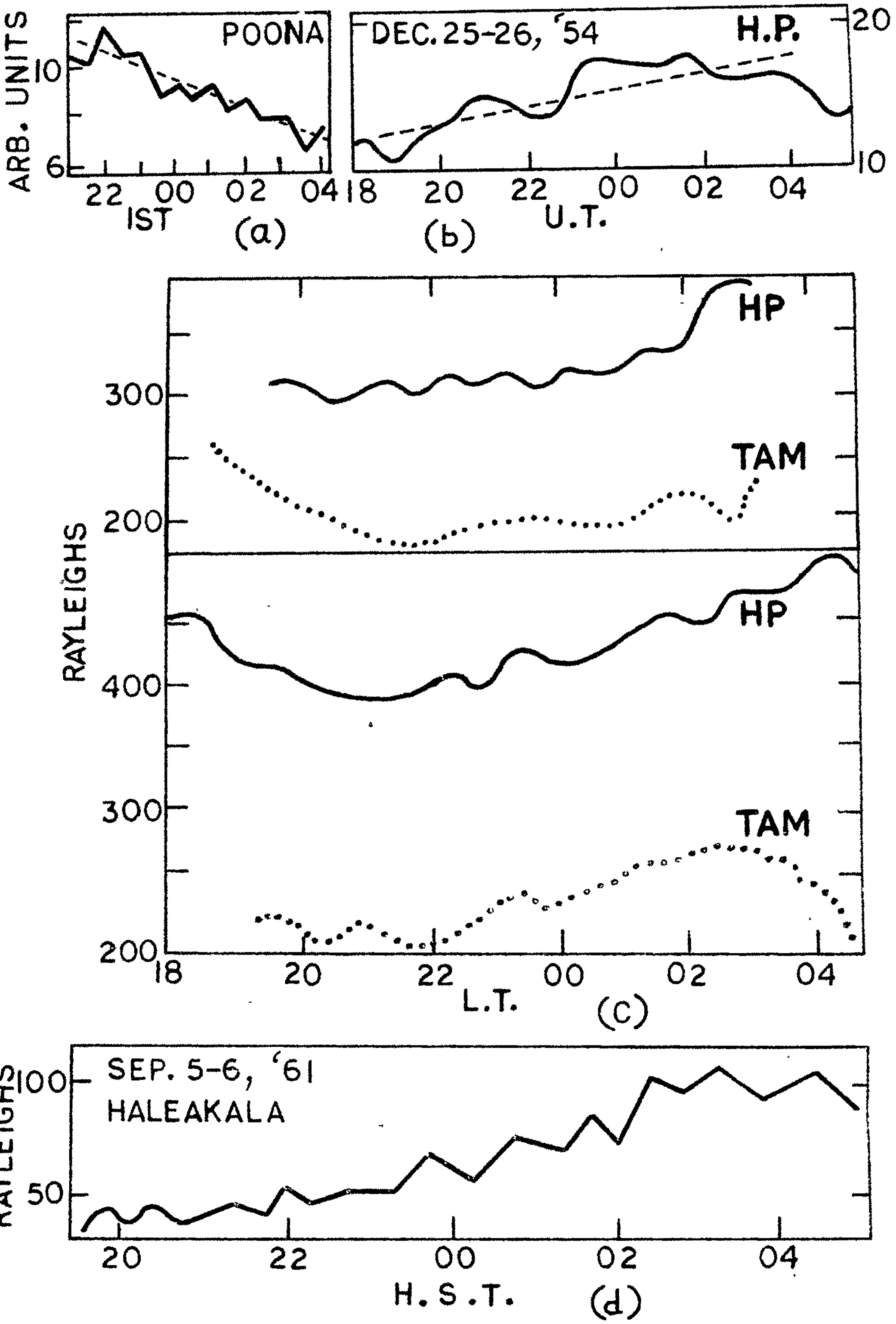

FIG. 7.7. The curves showing fluctuations in the nocturnal variation of Na-emission on typical nights presented by other authors at (a) Poona(Chiplonkar & Agashe), (b) Haute-Provence(HP)(Barbier), (c) Haute-Provence & Tamanrasset(TAM)(Barbier) & (d) Haleakala(Steiger).

The interpretation of the observed curves has been tried in a theoretical background which will be published elsewhere. A possible explanation of the fluctuating nature of the glow has also been included in the same treatment.

7.5 Isophote-study of night time sodium emission

The isophote study of sodium light in the dome of the sky over Mt.Abu has been made on a few nights in 1967. Here attention is directed to the observations on the nights of April 12-13, 1967 and May 8-9, 1967. Calculations showed that a relative variation of 2 Rayleighs was significant and therefore isophote lines have been drawn at an intensity difference of 10 Rayleighs. The isophotes for April 12-13, 1967 are presented in Fig.7.8.

7.51 Discussion

On April 12-13, 1968 upto 2330 IST the dome remained nearly uniformly bright with intensity lying between 30-40 Rayleighs (R), without showing any particular cell structures of intensity. At 0000 IST the dome seemed to be nearly uniformly bright with 40 R intensity at zenith and extending to 70°zenith angle towards south. On the periphery of the dome a 30 R isophote line was visible towards E and N-E. This line disappeared after half an hour and the 40 R isophote seemed to expand covering a large area of the sky. The increased intensity was aligned along North-West to South-East. A small

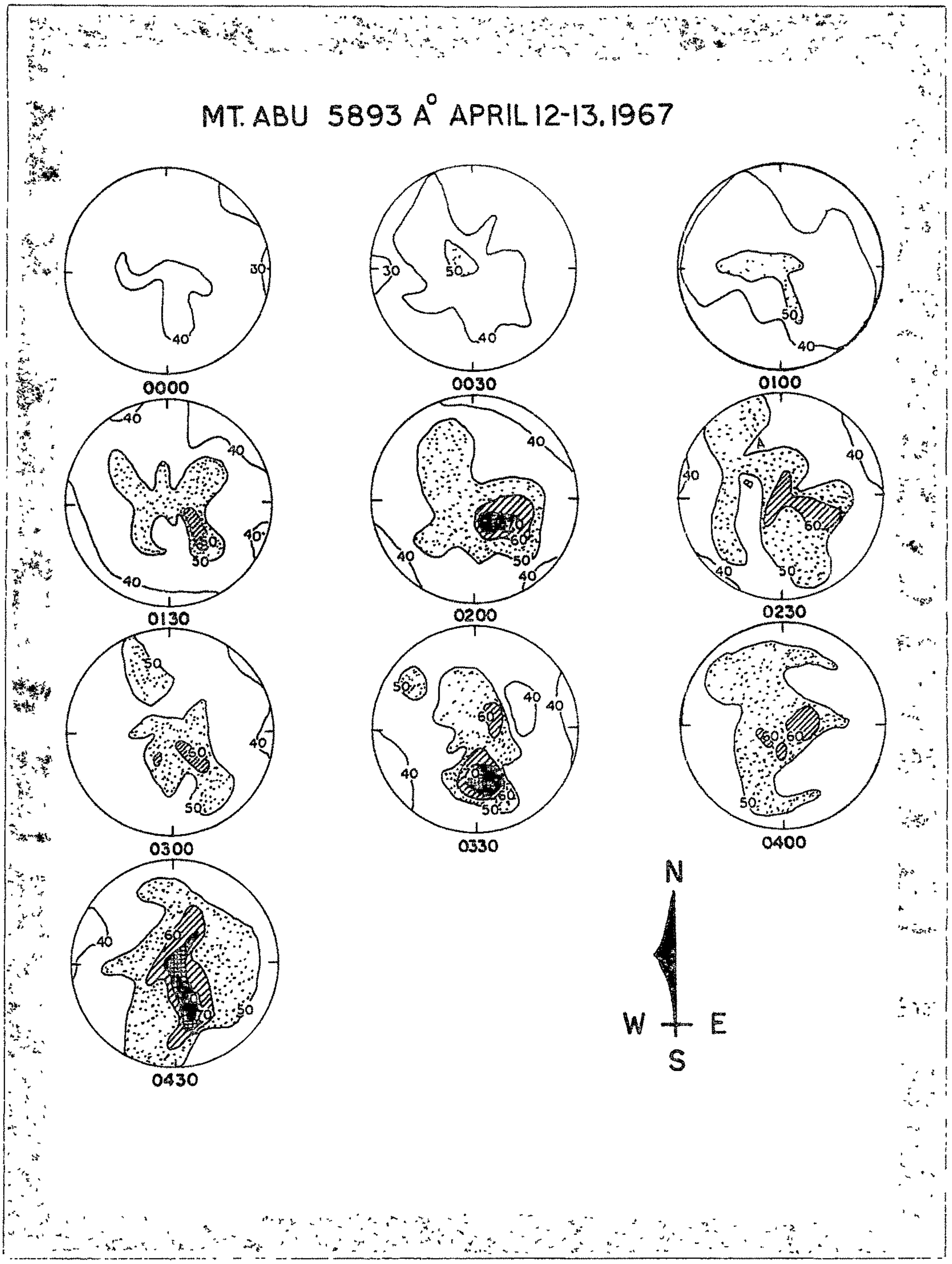

FIG.7.8. Isophote-maps of Na-intensity showing development and dissipation of airglow cells.

cell of 50 R also developed at 60^{o} zenith angle along the same alignment. At 0100 IST, 50 R cell expanded extending to about 70^{o} zenith angle South. The 40 R isophote expanded still further covering almost all the dome. After half an hour 40 R isophote went out of sight in the N, N-W, E and S-E periphery. The 50 R cell expanded still further S-ward and E-ward with a new development of 60 R cell at 40^{o} to 65^{o} zenith angle towards S-E direction.

The 50 R cell expanded at 0200 IST in the same way as the 40 R cell at 0030 IST. With the expansion of 50 R cell a new development of 60 R and 70 R in 60 R cell was also observed. At this hour the region of 40^{o} to 60^{o} zenith angle in S-E direction was active.

The new development of 70 R cell at 0200 IST seemed dissipated at 0230 IST with a shaping in 60 R cell and the 50 R cell receded South ward while taking a peculiar shape.

The 50 R cell, it was felt, would break at the points A B and it did break at 0300 IST in two 50 R cells. The 60 R cell dissipated further.

At 0330, the smaller 50 R cell was reduced in size with a change of place and the other 50 R cell expanded with a N-S alignment and with new development of 60 R, 70 R and 80 R cells being located at 65^{o} to 70^{o} zenith angle in the S-direction. Then at 0400 IST 50 R cell expanded with a disappearance of 70 R and 80 R cell in it. After half an hour (0430 IST) again 60 R, 70 R and 80 R cells were observed with nearly N-S alignment. The sky was active in Na-emission between 40-60° zenith angle South at this time.

Another night which is typical and rather active has been presented. On May 8-9, 1967 the variation of Na-emission was somewhat similar to the night studied above. For a part of the night the expansion of cells was observed and development of active regions and their dissipation was observed in the other part of the night (Fig.7.9).

From 2130 IST to 2200 IST the 90 R and 100 R isophotes expanded while the latter continued expanding till 2230 IST. At 2300 IST there was a new development of 130 R isophote at about 60°N. The new development dissipated at 2330 IST leaving a small patch at 40°N-W zenith angle.

Then 80 R and 90 R isophotes still expanded at 0000 IST. At 0030 IST, 90 R isophote divided into two with the smaller cell towards S-W and the bigger one towards N-E.

Around zenith new developments at 0100 IST started which reached to 40° zenith angle towards S-E along with an expansion of 100 R cell. The activity of sodium glow seemed to increase after 0100 IST when the sky remained quite active from zenith to 70° zenith angle. At 0330 the activity dissipated and at 0400 IST, the 100 R cell was found to break in pieces.

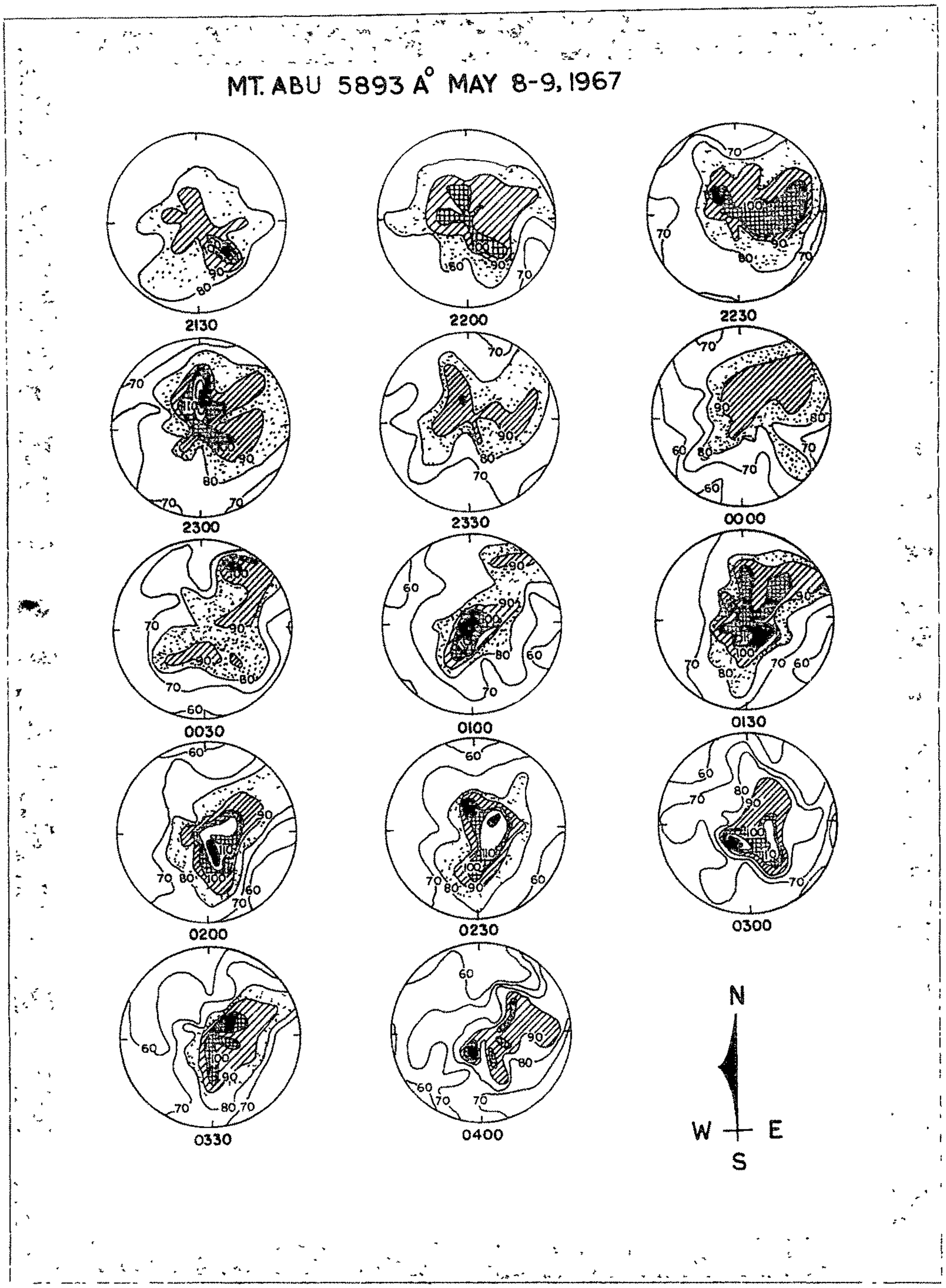

FIG.7.9. Isophote-maps of Na-intensity showing development and dissipation of airglow cells.

7.52 Conclusion

The variation of Na intensity on the dome of the sky as seen in the isophote-maps shows the activity of Na intensity patterns. The regions became active within half an hour and the newly developed cells expanded and dissipated. This behaviour causes a fluctuating pattern of sodium emission. Thus the observed intensity in a direction would consequently indicate the <u>fluctuations</u> in Na-emission which are also observed in the pole-photometer data.

The region of atmosphere at about 80-85 km from where most of the 5893 Å is emitted appears to be quite active at times and shows considerable intensity changes in a few minutes.

CHAPTER VIII

RESULTS FROM THE ISOPHOTE-STUDIES OF THE NIGHT-SKY

CHAPTER VIII

RESULTS FROM THE ISOPHOTE-STUDIES OF THE NIGHT-SKY

8.1 Introduction

The all-sky scanning photometer has been operated on a number of very clear nights. The instrument was calibrated 2 to 3 times in a night and the observations were reduced to absolute units of Rayleighs taking into consideration scattering and extinction by the atmosphere. All the observations have been reduced to local zenith intensities assuming appropriate layer heights. The intensity distribution in nightglow has been studied by plotting isophote-maps for the dome of the sky within 75° zenith angle from the zenith of Mt.Abu. Some of the interesting points observed in the maps are described below.

8.2 Localisation of airglow activity

The red line intensity has been studied at all hours of the night along the meridian passing over Mt.Abu. The magnetic meridian is 1° west of the geographic meridian. The three nights under this study are:

April 12-13, 1967
April 13-14, 1967
May 10-11, 1967

and the results of the observations made at different hours of the night in the meridian are represented in Figs.8.1, 8.2 and 8.3 respectively. In these figures the Y-axis represents zenith angle in degrees from the zenith of Mt.Abu and the X-axis represents the time from the beginning to the end of the night.

8.21 Discussion

These three nights have been selected for this study to show a common feature of intensity development at a particular time of the night in the particular region of the night-sky.

On April 12-13, 1967 (Fig.8.1), in the beginning of the night, the southern sky was brighter from 2200 to 2330 IST and afterwards till 0100 IST the sky remained nearly uniformly illuminated with low intensity. On the night of May 10-11, 1967 (Fig.8.3) the sky remained practically of uniform brightness upto 0030 IST. The night-glow of April 13-14, 1967 was much more intense than on the night of April 12-13, 1967 and of May 10-11. In the hours 0000 to 0130 IST of April 13-14, 1967 the sky showed higher intensity near zenith than at other zenith angles.

At about 0230 IST on all the three nights there was higher intensity at about 40^{o}S-zenith angle. The intensity associated with the 40^{o}S-zenith angle region of the sky on April 13-14, 1967 (Fig.8.2) was about double the intensity

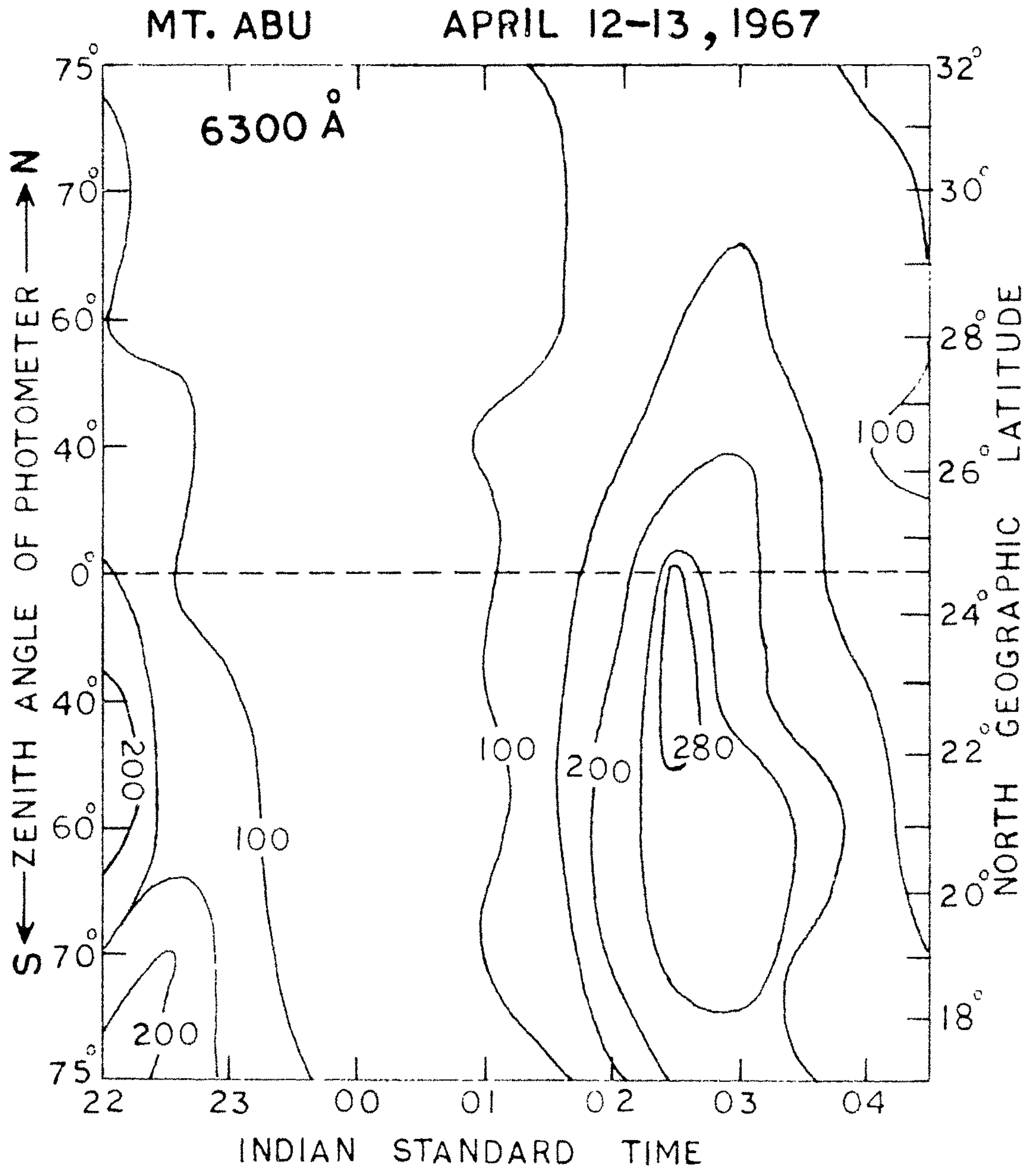

FIG. 8.1. Nocturnal Variation of 6300 Å intensity along the North - South meridian.

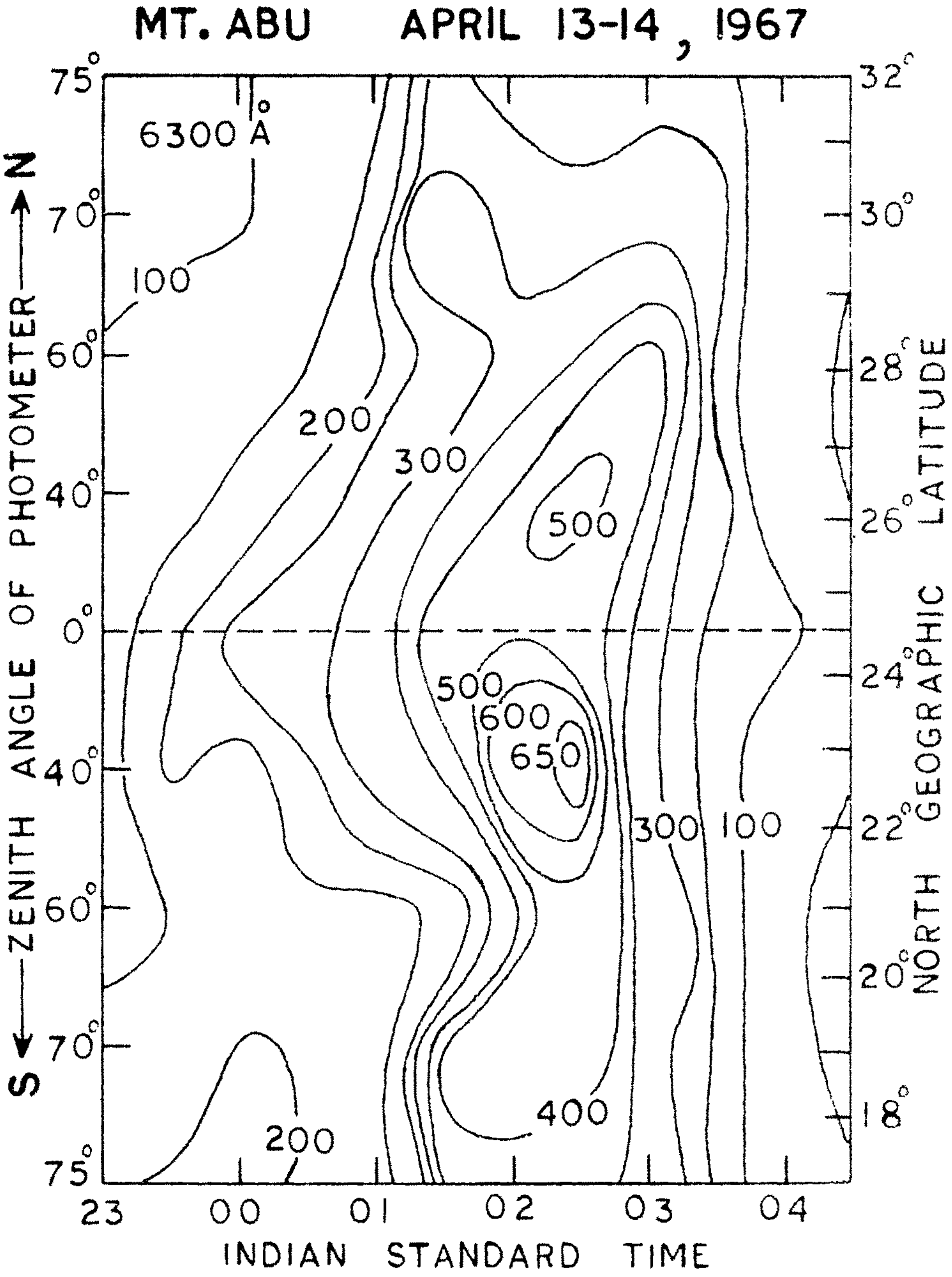

FIG. 8.2. Nocturnal Variation of 6300 Å intensity along the North - South meridian.

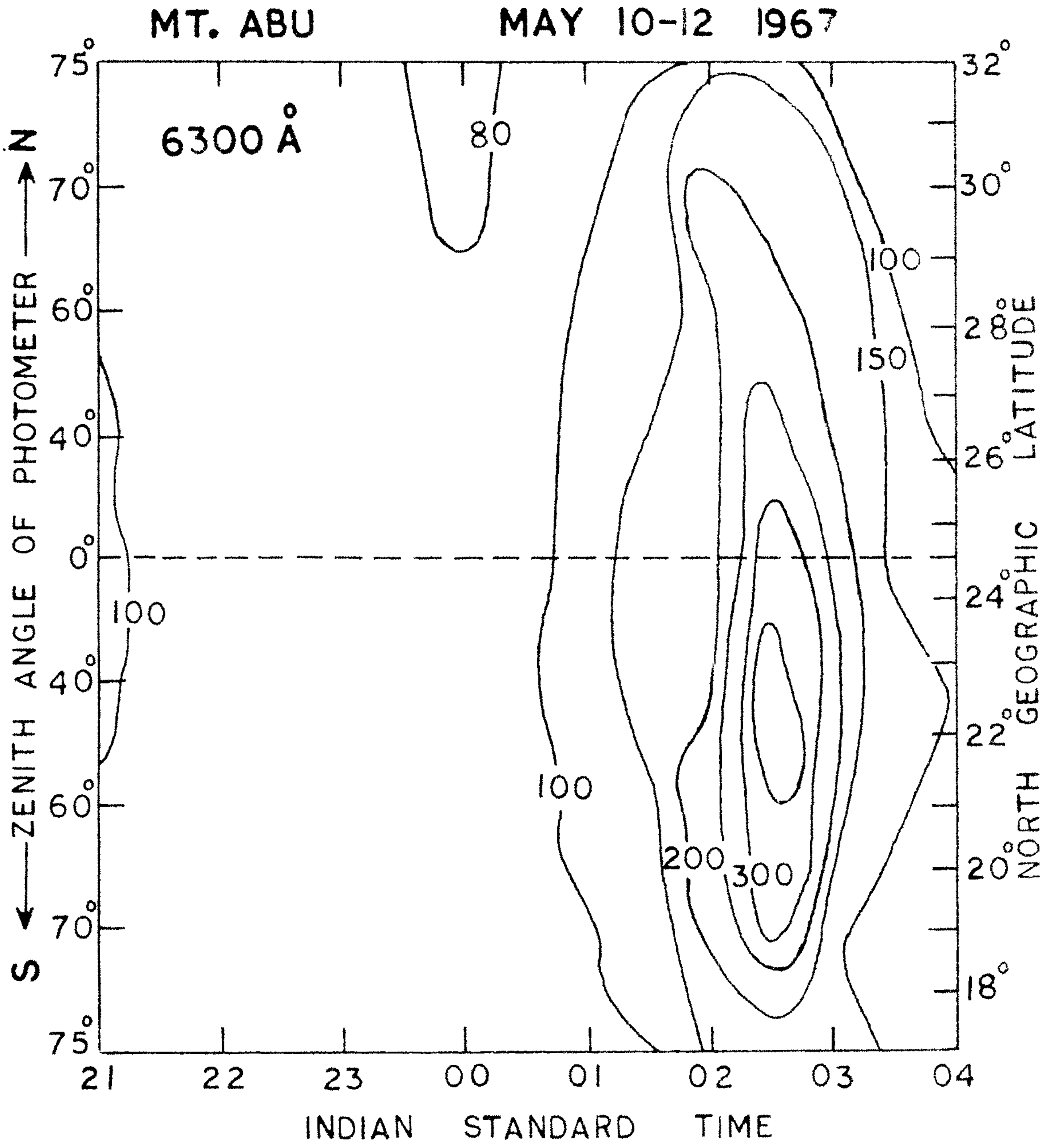

FIG. 8.3. Nocturnal Variation of 6300 Å intensity along the North - South meridian.

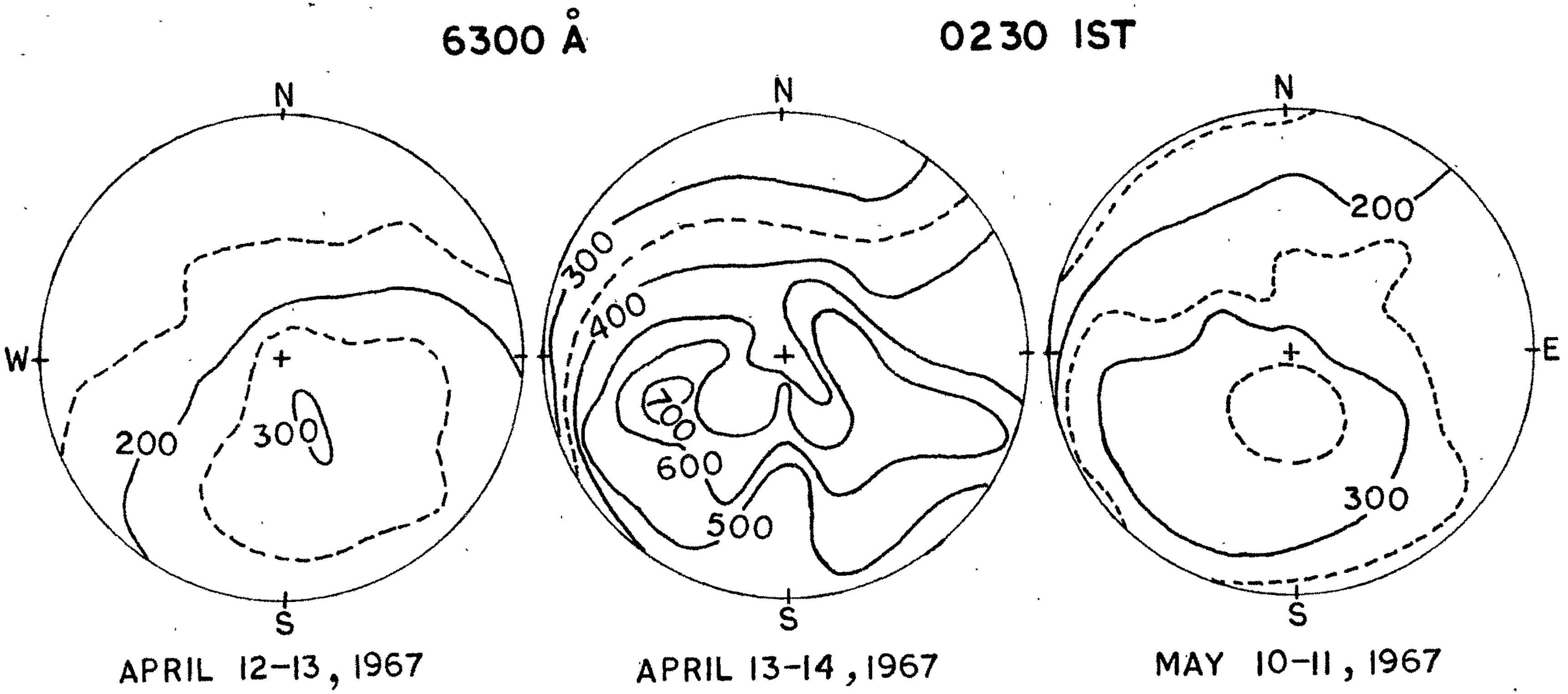

FIG. 8.4. Isophote maps of the dome of sky over Mt. Abu at 0230 IST when sky was active in 6300 Å radiation.

associated with the same zenith angle region on the other two nights. The 40°S zenith angle intercepting the 300 km layer corresponds to a geographic latitude of about 22.5°N.

On these nights the activity faded away gradually as we approached dawn conditions.

Fig.8.4 presents a view of the whole dome of the sky at 0230 IST, on each of these three nights.

8.3 Comparison of isophote-maps of 6300 Å and 5577 Å emissions

The isophote-maps have been studied when the zenith intensity at Mt.Abu showed short lived peaks (or enhancements) simultaneously in 6300 Å as well as in 5577 Å emissions as shown in Fig.8.5. With the idea that covariation in both the emissions may be present when significant increased emission in 5577 Å takes place from F-region, a study of the intensity patterns in both emissions, was made. From the same figure it may be seen that on May 10-11, 1967 a strong peak was observed at 0230 IST in the nocturnal variation of 6300 Å intensity at the Mt.Abu zenith. In the 5577 Å emission also, a small peak is observed at the same time (Fig.8.5). The isophote-maps of May 10-11, 1967 for both emissions have been compared in Fig.8.6 at 0200, 0230 and 0300 IST. The isophote-maps of the two radiations at 0200 and 0300 IST are not similar. However, there is much similarity in green and red isophotes at 0230 IST. This may be due to the fact that at this time major part of 5577 Å may be from the F-layer.

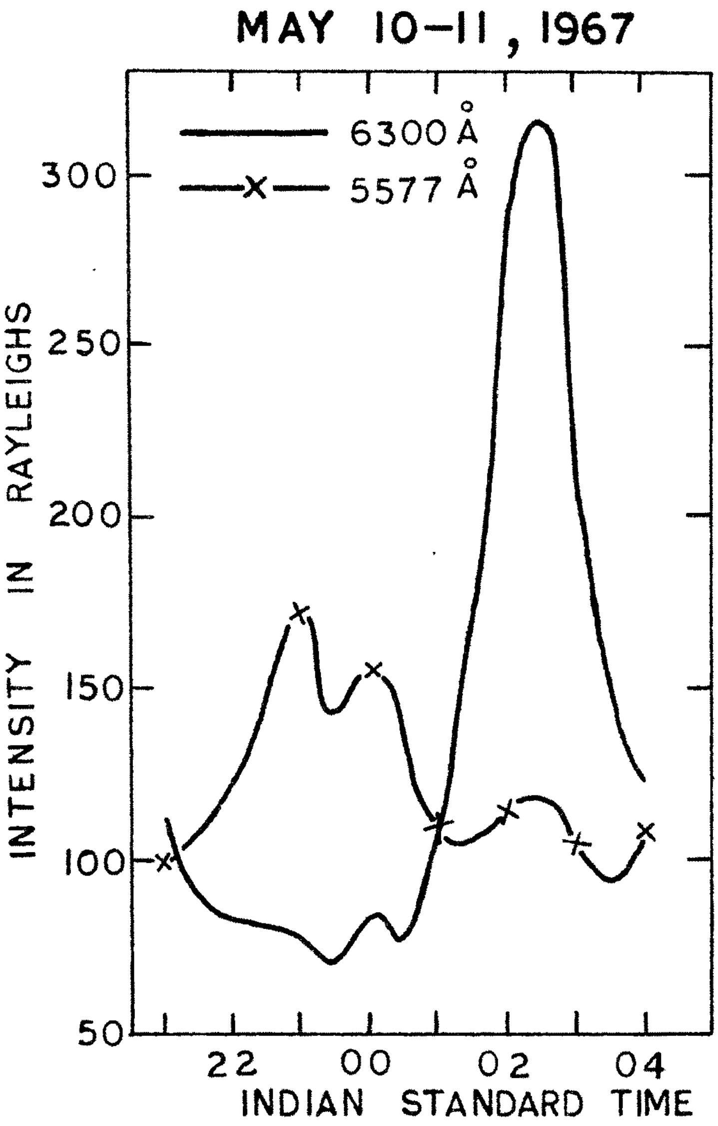

FIG. 8.5. Nocturnal variation of 5577 Å and 6300 Å intensity at Mt. Abu zenith.

In Fig.8.5 a small intensity increase, common to both the emissions, is seen on the same night at 0000 IST. Fig.8.7 represents the isophote-maps at 2330, 0000 and 0030 hrs on the same night.

Another night under consideration was April 13-14, 1967. On this night, the activity was more than on May 10-11, 1967. Here also a common intensity increase at 0200 is observed as shown in Fig.8.8.

8.31 Conclusion

This short study shows that occasionally, common variations are present in the two emissions. The F-layer also probably contributes to 5577 Å emission on such occasions. A considerable common area of the sky shows this tendency of increased intensity of 5577 Å together with that of 6300 Å.

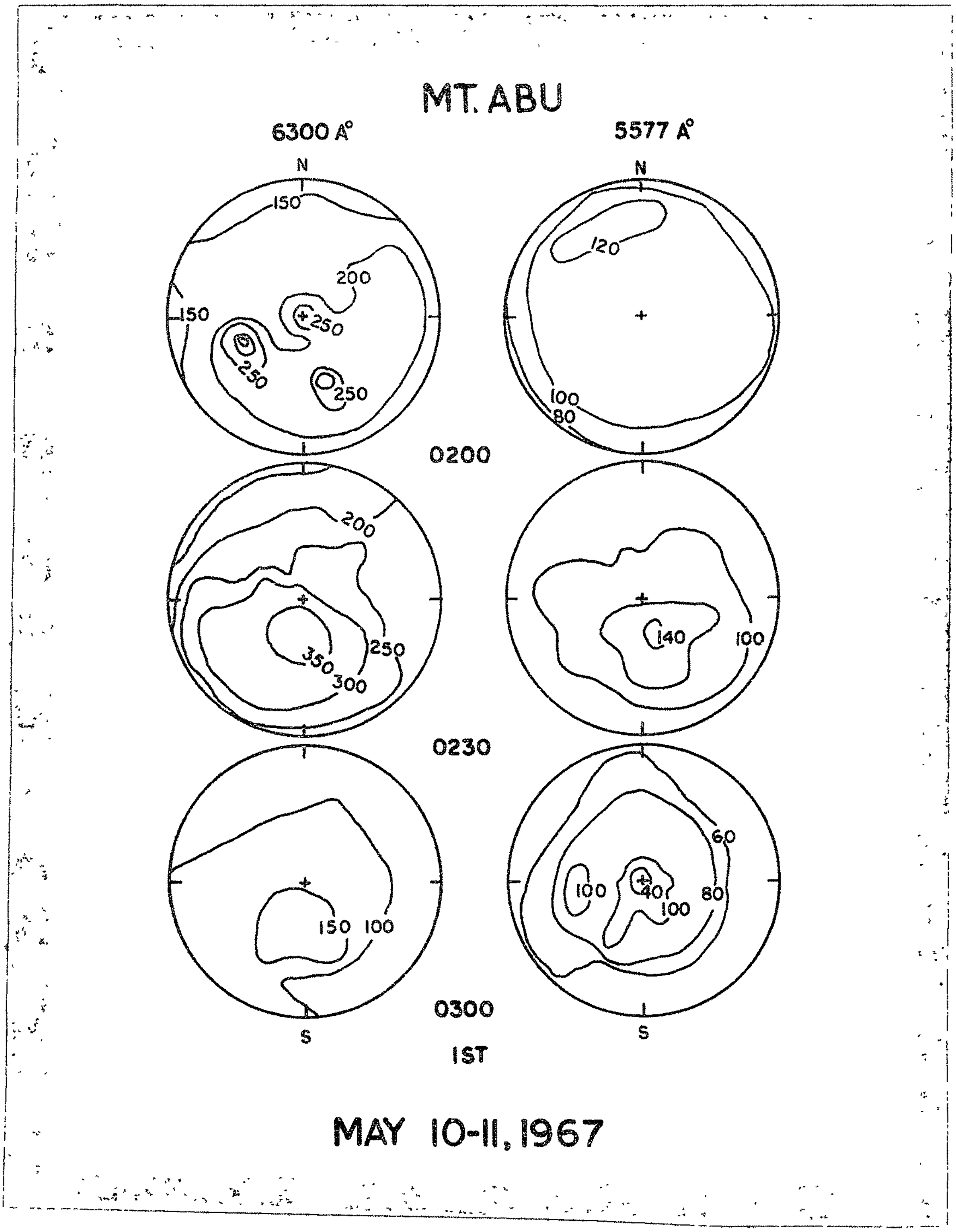

FIG.8.6. Comparision of the isophote-maps when a common enhancement in 6300 A and 5577 A was observed.

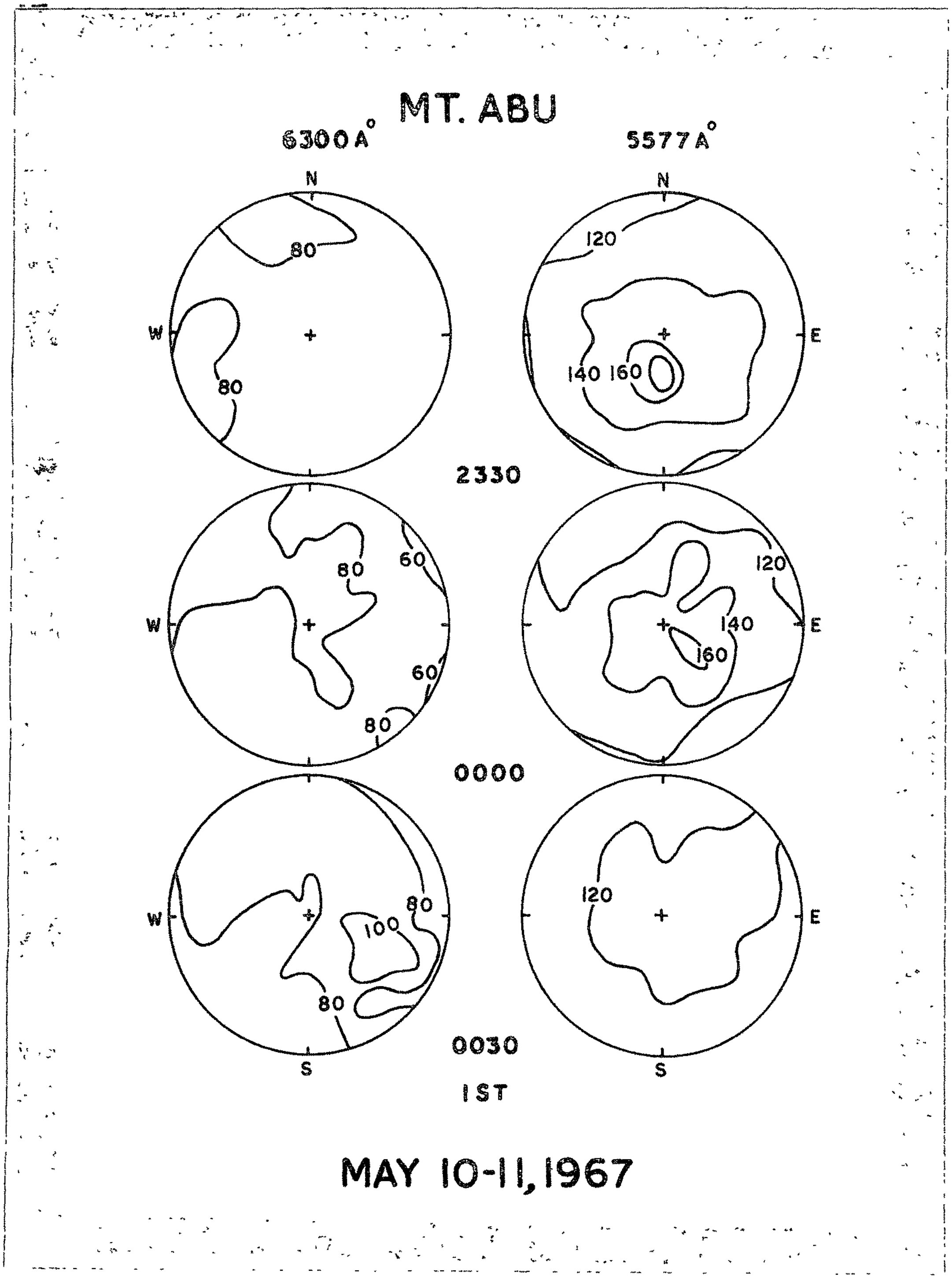

FIG.8.7. Comparision of the isophote-maps when a common enhancement in 6300 A and 5577 A was observed.

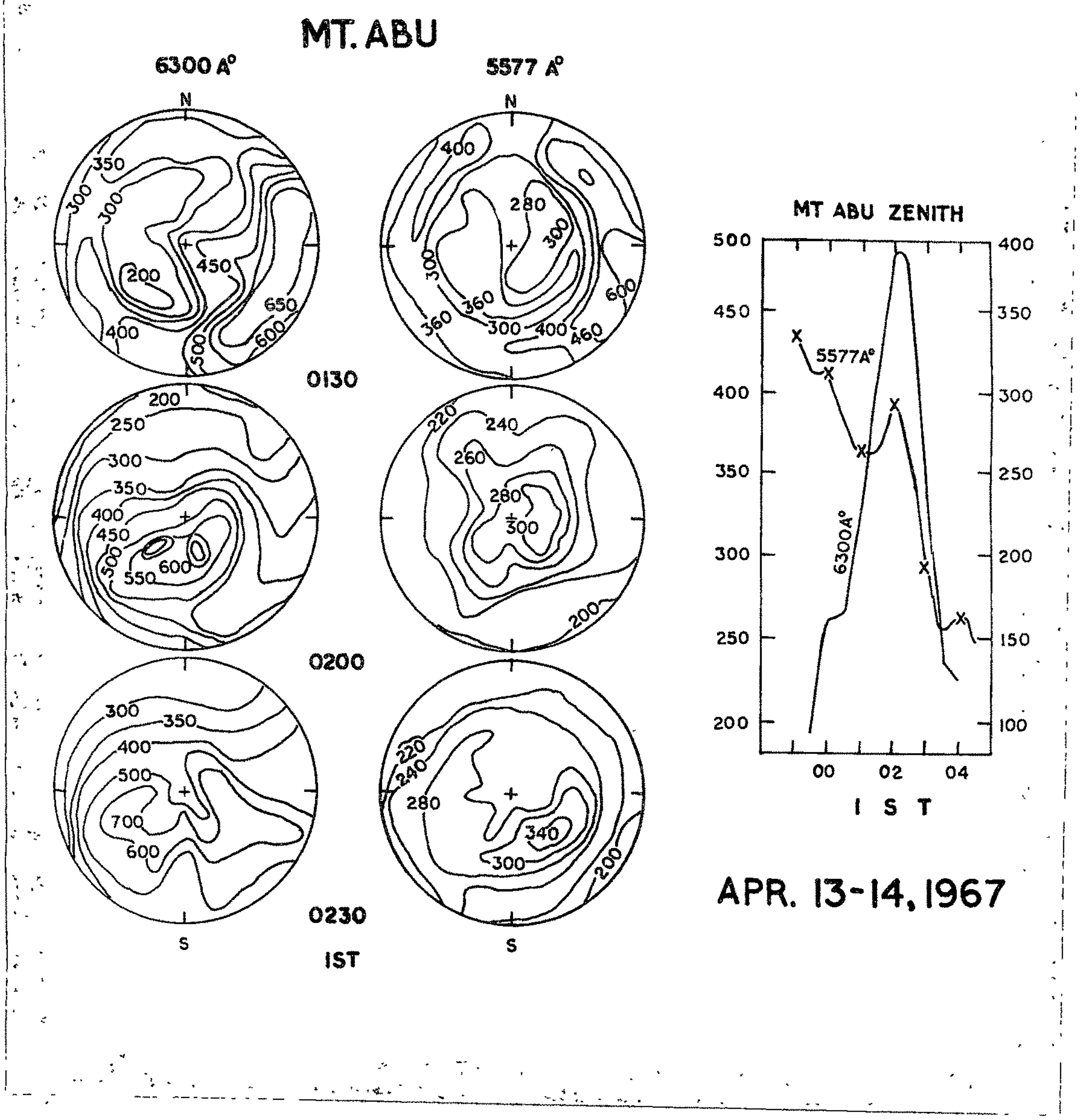

FIG.8.8. Comparision of the isopote-maps when a common enhancement in 6300 A and 5577 A was observed.

REFERENCES

Angreji, P.D.	1961	Proc.I.G.Y.Symp., V.II Feb.1961, New Delhi, pp.112-118.
Angreji, P.D.	1967	Ph.D.Thesis, Gujarat Univ., Ahmedabad (India), pp.162-174.
Armstrong, E.B.	1956	'The Airglow and Aurora' (E.B.Armstrong and A.Dalgarno, eds.) pp.63-66, Pergamon Press, London.
Babcock, H.W.	1923	Astrophys.J., 57, 209.
Ballif, J.R. and Venkateswaran, S.V.	1962	J.Atmos.Sci., 19, 426.
Barbier, D.	1953	Ann.Astrophys., 16, 96.
Barbier, D.	1954a	Compt.Rend., 234, 770.
Barbier, D.	1954b	Airglow and Aurora (E.B.Armstrong and A.Dalgarno, eds.) pp.42, Pergamon Press, London.
Barbier D.	1956	'The Airglow and Aurora' (E.B.Armstrong and A.Dalgarno, eds.) pp.38-59, Pergamon Press, London.
Barbier, D.	1957a	Compt.Rend., 245, 1559.
Barbier, D.	1957b	Compt.Rend., 244, 1809.
Barbier, D.	1958a	Ann.Geophys., 14, 334.
Barbier, D.	1958b	Compt.Rend., 246, 2780.
Barbier, D.	1959a	Ann.Geophys., 15, 179.
Barbier, D.	1959b	Ann.Geophys., 15, 412.
Barbier, D.	1963	Geophysics, The Earth's Environment (C.Dewitt, J.Hieblot and A.Lebeau, eds.) New York: Gordon and Breach.
Barbier, D.	1965	Ann.Geophys., 21, 265.

Barbier, D. and Glaume, J.	1959	Ann.Geophys., 15, 266.
Barbier, D. and Glaume, J.	1962	Planet.Space Sci., 9, 133.
Bates, D.R. and Nicolet, M.	1950	J.Geophys.Res., 55, 301.
Bates, D.R. and Dalgarno, A.	1953	J.Atmos.Terr.Phys., 4, 112.
Berthier, P.	1955	Compt.Rend., 240, 1919.
Berthier, P.	1956	Ann.Geophys., 12, 113.
Cabannes, J.	1934	Compt.Rend., 198, 2132.
Cabannes, J.	1935	Compt.Rend., 200, 1905.
Cabannes, J., Dufay, J. and Dufay, M.	1950	Compt.Rend., 230, 1233.
Chamberlain, J.W.	1958	Astrophys.J., 127, 54.
Chamberlain, J.W.	1961a	Physics of the Aurora and Airglow, Academic Press, New York.
Chamberlain, J.W.	1961b	Physics of the Aurora and Airglow, Academic Press, New York, p.513.
Chamberlain, J.W.	1961c	Physics of Aurora and Airglow, Academic Press, New York, p.524.
Chamberlain, J.W.	1961d	Physics of the Aurora and Airglow, Academic Press, New York, p.525.
Chamberlain, J.W.	1961e	Physics of the Aurora and Airglow, Academic Press, New York, pp.524-530.
Chamberlain, J.W.	1961f	Physics of the Aurora and Airglow, Academic Press, New York, p.530.
Chiplonkar, M.W. and Agashe, V.V.	1961	Ann.Geophys., 17, 232.
Christophe-Glaume, J.	1963	C.R.Acad.Sci., 256, (4), 988.
Chvostikov, I. and Lebedev, A.	1935	Compt.Rend. (U.S.S.R.), 1, 118.

Dalgarno, A.	1958	J.Atmos.Terr.Phys., 12, 219.
Dalgarno, A. and Walker, J.C.G.	1964	J.Atmos.Sci., 21, 463.
Dandekar, B.S.	1961a	Proc.I.G.Y.Symp.Vol.II, Feb.1961. New Delhi, pp.88-97.
Dandekar, B.S.	1961b	Ph.D.Thesis, Gujarat Univ., Ahmedabad (India).
Dandekar, B.S., Bhonsle, R.V. and Ramanathan, K.R.	1961	Ann.I.G.Y., 11, 123.
Dandekar, B.S. and Silverman, S.M.	1964	Planet.Space Sci., 12, 867.
Davis, T.N. and Smith, L.L.	1964	Geophys.Res.Report No.10.
Dejardin, G.	1936	Rev.Mod.Phys., 8, 1.
Dobrotin, N., Frank I. and Cerenkov, P.	1935	Compt.Rend. (U.S.S.R.), 1, 110.
Dufay, J.	1931	Compt.Rend., 193, 1106.
Dufay, J. and Dufay, M.	1951	Compt.Rend., 232, 426.
Dufay, J. and Tcheng Mao-Lin.	1942	Chiers Phys. No.8, 51.
Dufay, J. and Tcheng Mao-Lin.	1946	Ann.Geophys., 2, 189.
Dufay, J. and Tcheng Mao-Lin.	1947	Ann.Geophys., 3, 153.
Duncan, R.A.	1959	Austral.J.Phys., 12, 197.
Elsasser, H. and Siedentopf, H.	1956	J.Atmos.Terr.Phys., 8, 222.
Elvey, C.T.	1943	Astrophys.J., 97, 65.
Elvey, C.T. and Farnsworth, A.H.	1942	Astrophys.J., 96, 451.

Ferraro, V.C.A.	1945	Terr.Magn., 50, 215.
Frerichs, R.	1930	Phys.Rev., 36, 398.
Gulledge, I.S., Packer, D.M. and Tilford, S.G.	1966	Trans.Am.Geophys.Union, 47, 74.
Harris, I. and Priester, W.	1962	(a) J.Atmos.Sci., 19, 286. (b) NASA TN-D 1444.
Heppner, J.P. and Meredith, L.H.	1958	J.Geophys.Res., 63, 51.
Hernandez, G.J. and Silverman, S.M.	1964	Planet.Space Sci., 12, 97.
Hertzberg, M.	1958	J.Geophys.Res., 63, 856.
Huruhata, M.	1950	Rep.Ionosph.Res.Japan, 4, 137.
Huruhata, M.	1953	Ann.Tokyo Ast.Obs., 3, 165.
Huruhata, M.	1965	Proc.II Int.Sympo.Space Tech. and Sci., (Tokyo), p.733.
Johnson, C.Y., Meadows, E.B. and Holmes, J.E.	1958	J.Geophys.Res., 63, 443.
Koomen, M., Scolnik, R. and Tousey, R.	1956	J.Geophys.Res., 61, 304.
Krassovsky, V.I.	1963	NASA, TTF-204.
Kulkarni, P.V.	1965	Ann.Geophys., 21, 58.
Kulkarni, P.V. and Steiger, W.R.	1967	Ann.Geophys., 23, 125.
Lagos, P., Bellew, W. and Silverman, S.M.	1963	J.Atmos.Terr.Phys., 25, 581.
McLennan, J.C. and Shrum, G.M.	1924	Proc.Roy.Soc., A, 106, 138.
McLennan, J.C., McLeod, J.H. and Ireton, H.	1928	Transact.Roy.Soc.Canada, Sec.III, 22, 397.

Meinel, A.B.	1950a	Astrophys.J., 111, 207.
Meinel, A.B.	1950b	Astrophys.J., 111, 433.
Nicolet, M.	1954	Phys.Rev., 93, 633.
Nisbet, J.S. and Quinn, T.P.	1963	J.Geophys.Res., 68, 1031.
Norton, R.B., VanZandt, T.E. and Denison, J.A.	1963	Proc.Inter.Conf.Ionosphere, (Strickland, A.C. ed.) pp.26-34, Institute of Physics and the Physical Society, London.
Packer, D.M.	1961	Ann.Geophys., 17, 67.
Peterson, V.L., VanZandt, T.E. and Norton, R.B.	1966	J.Geophys.Res., 71, 2255.
Ramanathan, K.R.	1932	Ind.J.Phys., 7, 405.
Rayleigh, Lord	1932	Proc.Roy.Soc. A100, 367.
Rayleigh, Lord	1929	Proc.Roy.Soc. A124, 395.
Rayleigh, Lord and Spancer Jones, H.	1935	Proc.Roy.Soc. A151, 22.
Roach, F.E.	1955	Ann.Geophys., 11, 214.
Roach, F.E.	1959	Proc.Inst.Radio Engrs., 47, 267.
Roach, F.E. and Pettit, H.B.	1951	Ann.Astrophys., 14, 392.
Roach, F.E. and Meinel, A.B.	1955	Astrophys.J., 122, 530.
Roach, F.E. and Marovich, E.	1959	J.Res.Nat.Bur.Stan., 63D (3), 297.
Roach, F.E., Megill, L.R., Rees, M.H. and Marovich, E.	1958	J.Atmos.Terr.Phys., 12, 171.
Roach, F.E. and Roach, J.R.	1963	Planet.Space Sci., 11, 523.